SYNTHETIC AGENTS FOR THE DERIVATIZATION OF *N*-ACYL HOMOSERINE
LACTONES

Michael A. Bertucci

A dissertation submitted to the faculty of the University of North Carolina at Chapel Hill in
partial fulfillment of the requirements for the degree of Doctor of Philosophy in the
Department of Chemistry

Chapel Hill
2014

Approved by:

Michel R. Gagné

Marcey L. Waters

Eric M. Brustad

David S. Lawrence

Joseph L. Templeton

ABSTRACT

Michael A. Bertucci: Synthetic Agents for the Derivatization of *N*-Acyl Homoserine
Lactones
(Under the direction of Michel R. Gagné, PhD)

Quorum sensing is a process of chemical communication in bacteria that enables
bacteria to coordinate group function, including unified gene expression. As the quorum
sensing mechanism is in part responsible for the virulent activity of many bacteria, inhibiting
the communication pathway has the potential to lead to the development of novel antibiotics.
The central focus of this dissertation is the investigation of strategies for chemically
activating and modifying *N*-acyl homoserine lactones (AHLs), the agent of chemical
communication in gram-negative bacteria. Probing the inherent reactivity of the AHLs is
critical to understanding their evolved function while uncovering novel modes of inhibition
and tools for chemical biology.

Initial studies began by utilizing small molecule thiourea and guanidine-based
catalysts for accelerating ring-opening reactions of the AHL by amines. The supramolecular
catalysts achieved ten and sixty-five fold increases in reaction rate, respectively, for the
addition of piperidine to the characteristic α-amino-γ-butyrolactone moiety. This
demonstrated the susceptibility of the chemical messengers to be activated for nucleophilic
attack through appropriate arrangement of hydrogen bond donors and acceptors.

Further studies on the derivatization of the AHLs continued with the development of
a hydrazine-mediated transamidation reaction under aqueous conditions. Experimental
evidence supports the progression of the reaction via a condensation at the β-carbon of the

chemical messenger, followed by an intramolecular cyclization to cleave the AHL at the amide bond. The reaction is operable at physiological pH and is specific for the 3-oxo-AHL in the presence of other AHLs.

To rapidly identify a scaffold of non-covalent interactions to increase rate of the transamidation reaction, a reactive tagging assay was developed for high-throughput screening of hydrazine-containing peptide libraries. Combinatorial libraries were synthesized with designer Boc-protected hydrazines and screened against the AHL. Colorimetric hit development was achieved through a strained-cyclooctyne functionalized dye selecting peptides that react most readily with the chemical messenger. First generation library hits were resynthesized and screened for biofilm and quorum sensing inhibition. Further library development and screening holds the potential to identify peptides sequences and structures with the greatest propensity for rapidly functionalizing the 3-oxo-AHL.

To my family, I am so thankful for you and for being a constant voice of encouragement during my time at Chapel Hill. To Kristen, Brian, Joseph, and Lauren, as we grow older, we only grow closer and I am so happy we have each other. Mom and Dad, from the small tokens of encouragement to the long phone calls, you're the best parents anyone could ask for. Thank you for all of your love and support.

TABLE OF CONTENTS

LIST OF TABLES

LIST OF FIGURES

LIST OF SCHEMES

LIST OF ABBREVIATIONS

% v/v	Percent volume per volume
°C	Degrees Celsius
2-Nal	2-naphthylalanine
3,5-diFPhe	3,5-difluorophenylalanine
3-NO$_2$Phe	3-nitrophenylalanine
A	Alanine
Ac$_2$O	Acetic anhydride
AHL	N-acyl homoserine lactone
AIB	α-aminoisobutyric acid
Ala	Alanine
Arg	Arginine
Asn	Asparagine
Boc	t-Butyloxycarbonyl
BODIPY	Boron-dipyrromethene
br	Broad
C	Cysteine
Cha	Cyclohexylalanine
Cit	Citrulline
COMU	(1-Cyano-2-ethoxy-2-oxoethylidenaminooxy)dimethylamino-morpholino-carbenium hexafluorophosphate
d	Doublet
DAB	2,4 diaminobutyric acid
DAP	2,3-diaminopropionic acid

DBU	1,8-Diazabicyclo[5.4.0]undec-7-ene
DCM	Dichloromethane
dd	Doublet of doublets
DFT	Density functional theory
DIEA	N,N-Diisopropylethylamine
DMF	*N,N*-Dimethylformamide
DMF-d$_7$	Deuterated *N,N*-dimethylformamide
DMSO	Dimethylsulfoxide
DMSO-d$_6$	Deuterated dimethylsulfoxide
DNA	Deoxyribonucleic acid
dP	d-Proline
dPro	d-Proline
dt	Doublet of triplets
E	Glutamic acid
ee	Enantiomeric excess
eq	Equivalent
ESI	Electrospray ionization
Et$_2$O	Diethyl ether
EtOAc	Ethyl acetate
F	Phenylalanine
Fmoc	9-Fluorenylmethyloxycarbonyl
G	Glycine
g	Grams

GFP	Green fluorescent protein
Glu	Glutamic acid
Gly	Glycine
h	Hours
HBTU	O-(Benzotriazol-1-yl)-N,N,N',N'-tetramethyluronium hexafluorophosphate
His	Histidine
HOBt	Hydroxybenzotriazole
HPLC	High performance liquid chromatography
Ile	Isoleucine
ivDde	1-(4,4-Dimethyl-2,6-dioxocyclohexylidene)-3-methylbutyl
J	Coupling constant
K	Lysine
k	Rate constant
k_{app}	Apparent rate constant
k_{rel}	Relative rate
L	Leucine
LB	Luria-Bertani
LC-MS	Liquid chromatrography-mass spectrometry
LC-TOF	Liquid chromatography time of flight
Leu	Leucine
LG	Leaving group
LUMO	Lowest unoccupied molecular orbital
Lys	Lysine

M	Molar
m	Multiplet
m/z	Mass to charge ratio
MALDI-MS	Matrix-assisted laser desorption/ionization mass spectrometry
MeCN	Acetonitrile
MeOH	Methanol
MeOH-d_4	Deuterated methanol
MHz	Megahertz
MIC	Minimum inhibitory concentration
mL	Milliliter
mM	Millimolar
mmol	Millimoles
mol %	Mole percent
mol	Mole
MS	Mass spectrometry
NMR	Nuclear magnetic resonance
O	Ornithine
OBOC	One-bead-one-compound
OD	Optical density
Orn	Ornithine
p	Pentet
P	Proline
PBS	Phosphate buffer solution

Phe	Phenylalanine
Phg	Phenylglycine
ppm	Parts per million
Pro	Proline
q	Quartet
QS	Quorum sensing
RB	Round bottom
ROH	An alcohol
RT	Room temperature
s	Seconds or singlet (when related to NMR)
Ser	Serine
SPPS	Solid phase peptide synthesis
T	Threonine
t	Time or triplet (when related to NMR)
$t_{50\%}$	Time to 50% conversion
TFA	Trifluoroacetic acid
TFE-d_3	Deuterated trifluoroacetic acid
THF	Tetrahydrofuran
THQPO	1,2,3,4-tetrahydro-6H-pyrimido[2,1-b]quinazolin-6-one
TLC	Thin layer chromatography
tRNA	Transfer ribonucleic acid
Trp	Tryptophan
TS	Transition state

Tyr	Tyrosine
U	α-aminoisobutyric acid
UV	Ultraviolet
V	Volts or valine (when related to amino acids)
Val	Valine
VEGF	Vascular endothelial growth factor
Vis	Visible
W	Tryptophan
Y	Tyrosine
δ	Chemical shift
μL	Microliters
μM	Micromolar

CHAPTER I: INTRODUCTION

A. Bacterial Quorum Sensing: Background and Significance

It was in the 1970s, while studying the bioluminescence of marine microbe *V.fischeri*, that Nealson and Hastings described an "adaptive function" of the bacteria that enabled it to regulate its luminescence at the colony level. In other words, an observed small colony of *V.fischeri* would not illuminate on a cell by cell basis, but rather simultaneously as a unit.[1] These observations by Nealson and Hastings laid the framework for understand a regulatory mechanism present in a wide-range of bacterial species that allows the organisms to participate in a process of unified gene expression. This process in now known as quorum sensing (QS).[2,3]
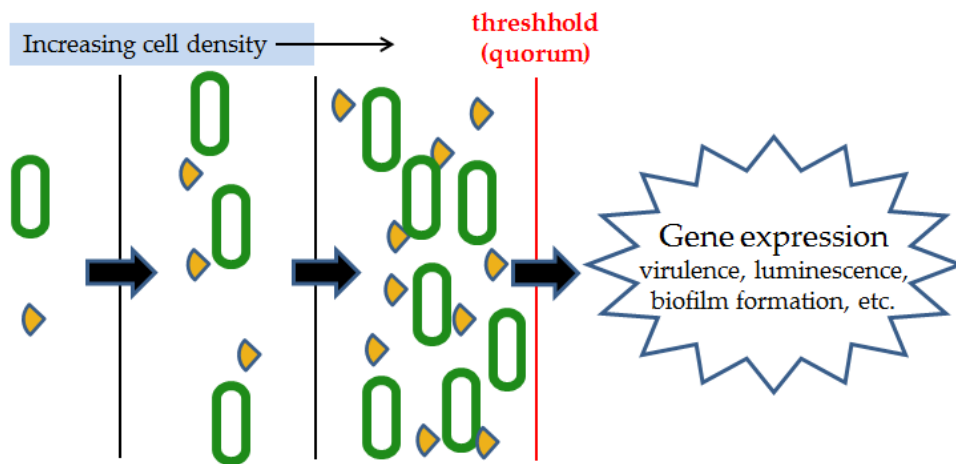
Figure 1.1. Density-dependent regulation of gene expression in bacterial quorum sensing. The bacteria (green ovals) produce small molecule autoinducers (yellow triangles) to promote cell localization until the necessary quorate is reached to initiate gene transcription.

The ability of bacteria to undergo unified gene expression through quorum sensing is dependent on the relative density of bacteria in a given environment. The bacteria must

1

reach a "quorum" or threshold concentration of cells in order to support the phenotype the colony seeks to express given its surroundings (Figure 1.1). Thus, the bacteria have evolved to develop a chemical communication mechanism to ensure that the necessary quorum can be met. The chemical signals, or autoinducers, that serve as this means of communication are continuously synthesized and released into the extracellular environment to be incorporated and recognized by a nearby bacterium of the same species. The increased dispersal of autoinducers enables more bacteria to "sense" the location of the forming consortia, cueing the individual cells to colonize. Upon binding to its cognate receptor, the signal-receptor complex initiates transcription of the gene encoded for the synthase of the signaling molecule. Through this autoinduction mechanism, the cell is directed to produce more of the same chemical signal to be released into the extracellular space. The bacteria gather until a threshold concentration is reached, enabling successful execution of a colony-wide event.

The chemical signal, mechanism of signal transduction, and resultant genes expressed via quorum sensing vary from species to species. Likewise, the density-dependent mechanism has been determined as the driving force for a wide variety of bacterial processes including bioluminescence, motility, conjugation, and virulence, each with the potential to benefit or harm its host.[4] As noted above, the bioluminescence of *V.fischeri* illuminates the surrounding area for its host, the Hawaiian bobtailed squid, enabling it to traverse its marine landscape. In contrast, quorum sensing is the mechanism for the production of virulence factors in prevalent human pathogens such as *P.aeruginosa* and *S.aureus*. The ability of bacteria to regulate group function by these means has been demonstrated to have major impacts in agriculture, manufacturing, and human health.[5] Specifically, quorum sensing has been demonstrated to serve as a precursor to biofilm formation, an extracellular polymeric

substance secreted by bacteria that enhances their resistance to bactericidal treatments. Creation of this protective barrier of DNA, polysaccharide, and protein fragments is the source of pathogenicity in over 80% of bacterial infections.[6,7] The study of bacterial quorum sensing has consequently expanded to not only understanding the molecular underpinnings of its regulation, but also to developing strategies to inhibit the pathway to prevent its virulent impact.

Further, inhibiting quorum sensing poses a unique benefit for the development of new antibiotics. Traditional antibiotics, such as vancomycin or linezolid, generally impede the proliferation of bacteria through inhibiting cell wall biosynthesis, transcription and translations mechanisms, or cellular metabolism.[8] Each of these processes is required for cell survival, imposing an evolutionary pressure on the bacteria and encouraging the formation of resistance to such treatments over time. Though the quorum sensing pathway governs many of the bacteria's infectious capabilities, prohibiting chemical communication between cells does not pose a direct threat to individual cell survival. Hence, therapies that efficiently quench the quorum sensing pathway have the potential to treat bacterial infections without rapidly promoting the development of bacterial resistance.[9,10]

B. *N*-Acyl Homoserine Lactones (AHLs) in Quorum Sensing (QS)

The identity and structure of the chemical signals responsible for regulating quorum sensing vary from autoinducing peptides (AIPs) in *S. aureus,*[11] to diffusible fatty acids (DSFs) in *B.cenocepacia.*[12] In the majority of gram-negative bacteria, small molecules known as *N*-acyl homoserine lactones (AHLs) are the agents of communication (Figure 1.2). AHLs have been identified as critical messengers in greater than fifty species of bacteria.[4] Each member of the AHL family contains several structural similarities, including a

lipophilic hydrocarbon tail terminated with a characteristic α-amino-γ-butyrolactone. These similarities are matched by select sites of structural variability necessary for signal differentiation, including the presence of a β-hydroxyl (3-OH-AHL) or β-keto moiety (3-oxo-AHL) adjacent to the *N*-acyl functionality. As described further in Section IC and ID, the structural similarities and differences amongst AHLs has inspired the development of synthetic analogs to inhibit and study QS systems.

3-hydroxy-AHL	3-oxo-AHL	AHL
R = CH$_3$, C$_3$H$_7$, C$_{11}$H$_{21}$	R = CH$_3$, C$_3$H$_7$, C$_5$H$_{11}$, C$_7$H$_{15}$	R = CH$_3$, C$_3$H$_7$, C$_5$H$_{11}$
	1	**2**
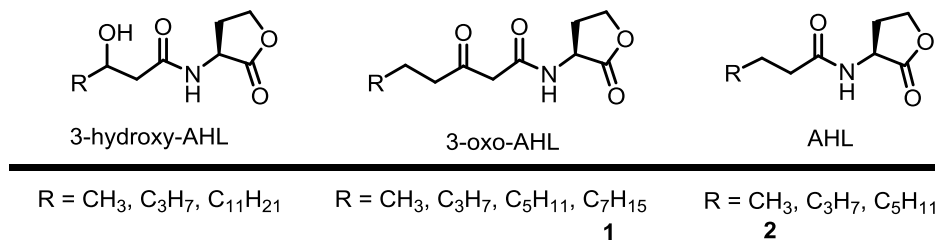
Figure 1.2. Structural subfamilies of the known *N*-acyl-homoserine lactone autoinducers.

Many species of bacteria employ multiple AHLs to regulate different facets of their gene expression profile.[10,13] In *P. aeruginosa*, the 3-oxo-C$_{12}$-AHL (**1**) and its resultant binding to LasR stimulates the production of a series of virulence factors in addition to the transcription of the RhlR receptor for recognition of the C$_4$-AHL (**2**) (Figure 1.3). Subsequent binding of the C$_4$-AHL leads to production of a distinct set of virulence factors promoting *P. aeruginosa* pathogenicity.[14] The collection of AHLs is unique to each species of bacteria, however multiple species employ the same individual autoinducer. This forwards the potential for crosstalk between gram-negative bacteria, adding an additional layer of complexity to the role of AHLs in the organism's social behavior.[15,16]
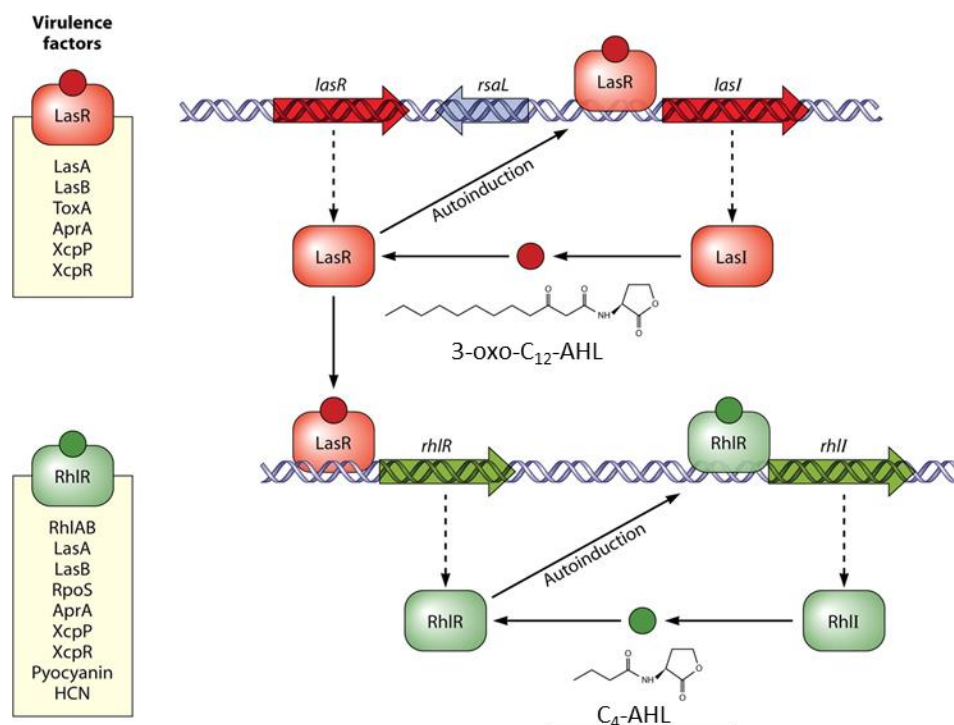
Figure 1.3. The hierarchal QS signaling pathway in *Pseudomonas aeruginosa*. The 3-oxo-C_{12}-AHL binds to its cognate receptor *LasR* to stimulate transcription of the 3-oxo-C_{12}-AHL synthase *LasI* and the receptor for the RhlR/Rh1I pathway, mediated by the C_4-AHL. The corresponding signal-receptor complexes of both autoinducers encode for virulence factors responsible for the pathogenicity of the species. Adapted from Jimenez, et al.[14]

Despite the commonality of *N*-acyl homoserine lactones in gram-negative quorum sensing, few details exist about the reactivity of this family of molecules. Yates and co-workers were the first to fully characterize the susceptibility of the AHLs to lactone hydrolysis in conditions of variable pH.[17] Hydrolysis rates increased with elevated media alkalinity in addition to decreasing length of the AHL hydrocarbon tail, alluding to the function of the lipophilic moiety in stabilizing the parent AHL structure during extracellular transport (Scheme 1.1; Path A). Later, Janda and colleagues detected tetramic acids as a secondary product in 3-oxo-AHLs degradation pending media at or above pH 7.4. (Scheme 1.1; Path B) The corresponding acid derivatives were isolated, characterized, and demonstrated to possess bactericidal activity against a variety of gram-positive bacteria, thus

presenting an alternative role of the AHL as mode of chemical defense.[18] These studies

exemplify how understanding the innate reactivity of the AHLs can provide greater insight

into their evolutionarily determined function.
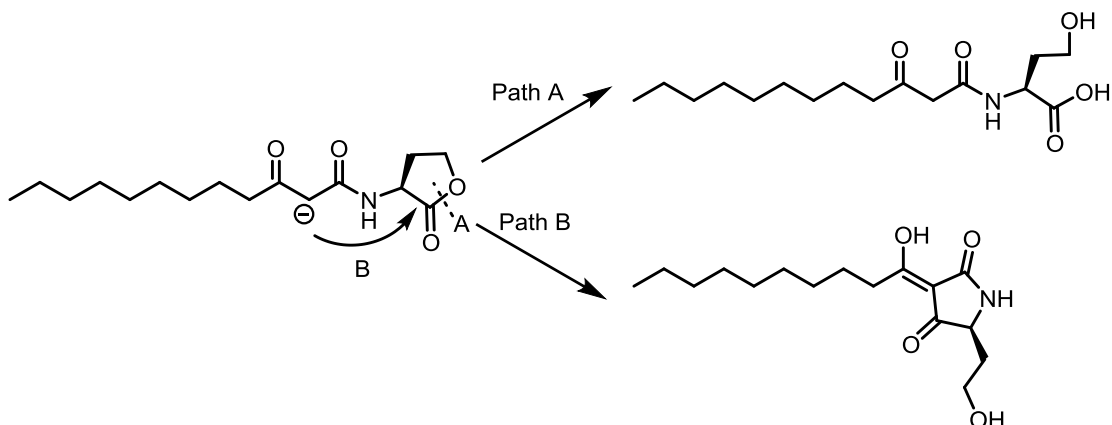
Scheme 1.1. Degradation pathways of the 3-oxo-AHLs under physiological conditions.
Products corresponding to the hydrolysis of the lactone (Path A) detected in all AHLs while
an intramolecular rearrangement to the tetramic acid (Path B) is only detected in the 3-oxo-
AHLs.[18]

Further understanding of AHL reactivity has been gained through the identification of

quorum quenching enzymes in both bacteria and eukaryotes, divulging the chemical basis for

natural defense against the *N*-acyl homoserine lactones. The majority of identified enzymes

function either as lactonases, hydrolyzing the AHL lactone, or acylases, hydrolyzing the

amide bond.[19]   The lactonase AiiA, originally isolated from *Bacillus*, is a dimeric zinc

metalloenzyme determined to promote lactone hydrolysis via activation of a single water

molecule after metal binding to a conserved protein sequence consisting of mostly histidine

and aspartic acid residues.[20]   Multiple enzymes with similar conserved sequences have since

been identified highlighting a commonality for the mechanism of AHL hydrolysis across

multiple bacterial species. The promiscuous family of hydrolytic enzymes in eukaryotes

known as paraoxonases (PON), characterized by a Ca^+-His-His catalytic active site also

demonstrated AHL lactonase activity.[21]   A large number of AHL acylases have also been
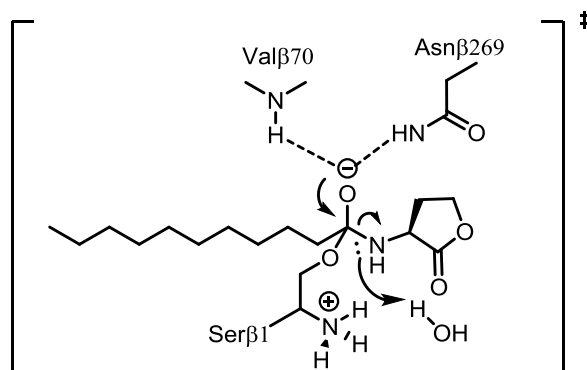
Figure 1.4. Transition state interactions in the AHL acylase PvdQ in *P. aeruginosa*. Stabilization through hydrogen bond donation promotes the terminating scission of the amide bond.[22]

identified[23,24] with PvdQ from *P.aeruginosa* being well understood due to the recent

publication of a substrate-bound crystal structure. Degradation of the AHL proceeds via

activation and attack of a nucleophilic serine reside at the amide with surrounding valine and

asparagine residues to stabilize the developing negative charge in a oxyanion hole fashion

(Figure 1.4).[22] The study of quorum quenching enzymes has aided in the identified

reasonable sites for non-enzymatic chemical modification to the AHLs as well as the types of

non-covalent interactions that enable such a modification. These examples largely

influenced our approach for developing peptide-based enzyme mimics for AHL degradation

(see Chapter IV).

C. Derivatizing AHL Autoinducers for QS Inhibition

Since the discovery and characterization of the AHLs, the family of autoinducers has

served as a scaffold for the development of QS inhibitors. The largest effort over the last

twenty years has focused on the creation of small molecules capable of inhibition through

competitive receptor binding. Thousands of compounds have been synthesized in library

format and screened to offer valuable structure-activity relationships for signal-receptor

affinities. Modifications to the AHL framework include heteroatom substitutions at the 3-

oxo position and lactone,[25,26] alteration of the lactone structure and size,[27–29] and arylation of the hydrophobic tail.[4,30,31] (Figure 1.5a). Amongst the array of analogs synthesized, several displayed notable antagonism and agonism of the QS pathway at low micromolar potencies in species that employ the native AHLs for communication, including *P. aeruginosa, A.tumefaciens,* and *V. fischeri*. The aggregate data from these screens has led to the establishment of structural guidelines for receptor specific and cross-species analog affinity, forwarding a better understanding of messenger-receptor binding and the creation of more potent analogs.[13]

a)

Smith et al., 2003.
$IC_{50} = 10 \ \mu M$

Geske et al., 2005.
$IC_{50} = 100 \ nm$

b)

AHL-cyclodextrin complex
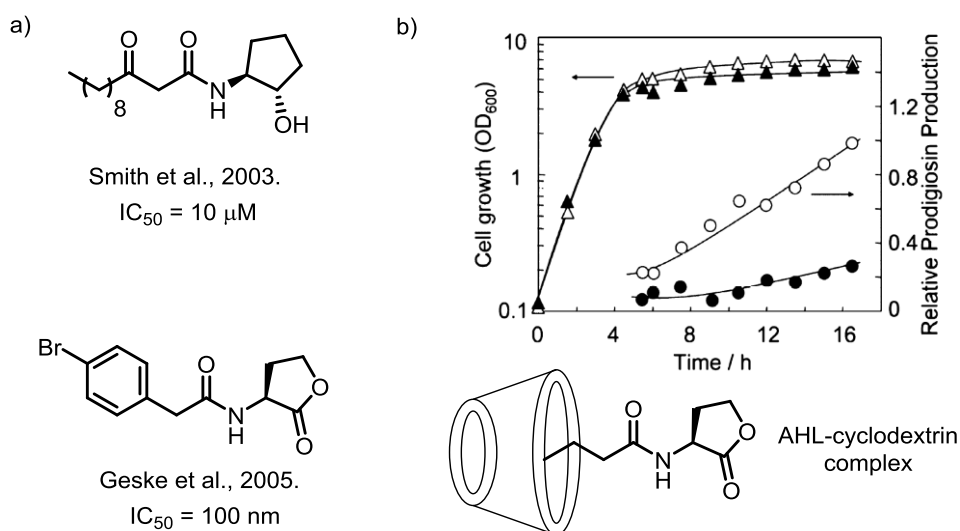
Figure 1.5. Manipulation of the AHL to promote QS Inhibition. a) Select examples of AHL analogs and corresponding IC_{50} values for LasR inhibition in *P.aeurginosa*.[27,7] b) AHL sequestration by cyclodextrins, depicting prodigiosin production (●) and cell growth (○) in the presence compared to the absence of cyclodextrin (▲,△). The reduction in prodigiosin levels indicating a reduction in viable AHLs in solution for QS regulation.[32]

Advances in quorum sensing inhibition have also been afforded in directly impeding the function of the AHL by employing chemical methods to reduce the concentration of the active messenger *in situ*. Janda and coworkers synthesized a small number of AHL-inspired haptens to select for monoclonal antibodies capable of degrading the native ligand. The selected antibody served to catalytically hydrolyze the lactone, presenting the first example

of antibody-mediated quorum sensing inhibition.[33,34]. Taking advantage of the inherent lipophilicity of AHLs, Kato and colleagues found that the addition of immobilized cyclodextrins to cellular assays reduced the in solution concentration of the chemical messengers (Figure 1.5b). The resultant cyclodextrin-AHL complex afforded attenuated production of the secondary metabolite prodigiosin in the human pathogen *S. marcescens* and was hypothesized to gain added stability through ionic interactions between the signal and its acceptor.[32] These approaches capitalize on the intrinsic functionality and reactivity of the autoinducer. Further, the use of cyclodextrins and catalytic antibodies demonstrate the effectiveness of enzyme mimics in quorum quenching, taking advantage of select non-covalent interactions to forward AHL recognition and QS inhibition.

D. Derivatizing AHL Autoinducers for Chemical Biology

The dynamic and complex nature of quorum sensing regulatory pathways has presented difficulties in identifying the biomolecular events that take place from autoinducer binding to gene transcription. Likewise, as more examples of AHL mediated crosstalk between species and eukaryotes surface, great interest lies in developing tools to elucidate environmental factors and the molecular architecture that support these interactions.[5] To generate new chemical biology strategies to study QS, the parent structure of the AHL has again served as a template.[35] Meijler and coworkers completed the synthesis of a 3-oxo-C_{12} AHL analog dually functionalized with a diazirine moiety and terminal alkyne (Figure 1.6a). The unique construct maintained the functional requirements for receptor binding while enabling light-mediated carbene insertion at the diazirine functionality to establish a covalent linkage between the AHL analog and its receptor. Through Huisgen cycloaddition with an azide-functionalized fluorescent tag, the signal-receptor complex was visualized in an *in vitro*

9

P.aeruginosa culture.[36] The Blackwell group, by derivatizing the 3-oxo-C_{12} AHL with a terminal amine, was able to bind and isolate the QscR receptor in *P.aeruginosa* through affinity chromatography. Both methods could serve as valuable tools for elucidating AHL-receptor binding, including identification of receptors in other species that enable the crosstalk though AHL recognition.[37]
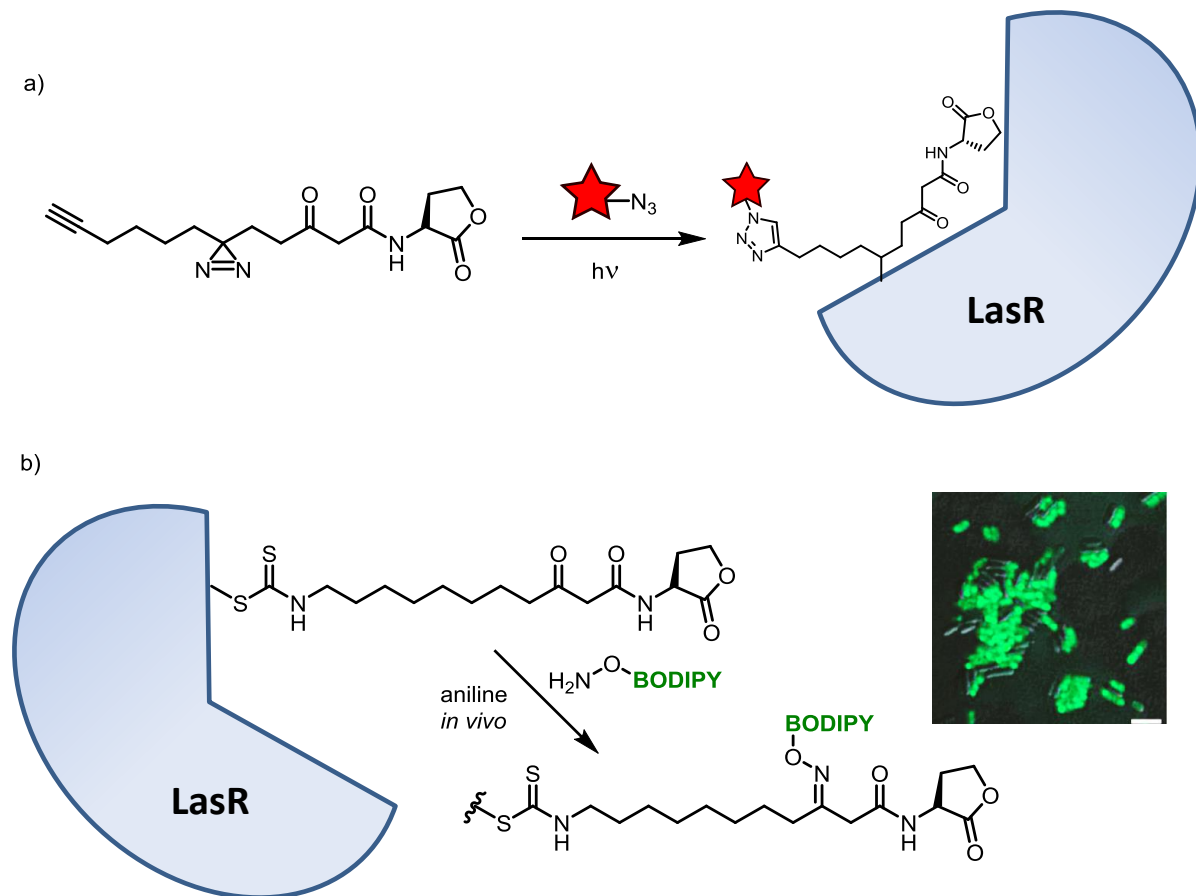
Figure 1.6. Advances in LasR labeling in *P.aeruginosa* by AHL analog synthesis and *in situ* derivatization of the autoinducer. a) upon binding to LasR, a light-mediated carbene insertion covalently links the AHL to the receptor allowing subsequent fluorescent tag attachment via Huisgen cycloaddition to observe the receptor bound signal.[36] b) covalent attachment of an isothiocyanate 3-oxo-C_{12}-AHL analog is exposed to an aminoxy-BODIPY derivative forming the corresponding oxime and allowing *in vivo* visualization of LasR.[38]

Further advances in chemical biology have also been realized through the derivatization of the native AHL *in situ*. Meijler and coworkers covalently attached a 3-oxo-

C_{12}-AHL derivative to its cognate receptor in *P.aeruginosa*, LasR. Taking advantage of the carbonyl reactivity that is uniquely characteristic of the 3-oxo-AHLs, an aminoxy functionalized BODIPY dye was then successfully linked to the bound autoinducer (Figure 1.6b). The resultant oxime enabled live cell labeling of LasR for *in vivo* visualization of the location of the receptor within the bacteria.[38] Such technologies that exploit the unique reactivity of the AHL could be a gateway to tagging and visualizing the autoinducers while active in their role as quorum sensing modulators.

E. Statement of Research

Reflected in this dissertation, research efforts have focused on expanding the suite of chemical based strategies for modifying the *N*-acyl-homoserine lactones. Inspired by the progress made in derivatizing the AHLs *in situ* for QS inhibition and chemical biology, our approach has centered on exploiting the reactivity of the autoinducers to expose covalent and non-covalent interactions that can promote their degradation. As detailed in the following chapters, the use of amine nucleophiles has led to modes of AHL functionalization that focus on both the γ-butyrolactone found in all AHLs and the ketone characteristic of the 3-oxo-AHLs. The supramolecular interactions provided by biomimetic catalysts, both small molecule and peptide-based, were assessed for their ability to activate the AHL for subsequent covalent modification. Ultimately, our approach has enabled AHL derivatization reactions to advance from catalyzing aminolysis reactions of the AHL in organic solvents to the development of a high-throughput reactive tagging assay for identifying peptides capable of rapid derivatization of the 3-oxo-AHL under physiological conditions. The knowledge uncovered regarding intrinsic AHL reactive and the technologies developed in these

investigations contribute to the ongoing effort to understand virulence mechanisms of

quorum sensing while creating new strategies to inhibit them.

REFERENCES

1. Nealson, K H. and Hastings, W. Bacterial Bioluminescence: Its Control and Ecological Significance. *Microbiological Reviews* **43**, 496 - 518 (1979).

2. Waters, C. M. & Bassler, B. L. QUORUM SENSING: Cell-to-Cell Communication in Bacteria. *Annual Review of Cell and Developmental Biology* **21**, 319–346 (2005).

3. Miller, M. B. & Bassler, B. L. Quorum Sensing in Bacteria. *Annual Review of Microbiology* **55**, 165–199 (2001).

4. Geske, G. D., O'Neill, J. C. & Blackwell, H. E. Expanding dialogues: from natural autoinducers to non-natural analogues that modulate quorum sensing in Gram-negative bacteria. *Chemical Society Reviews* **37**, 1432 (2008).

5. Praneenararat, T., Palmer, A. G. & Blackwell, H. E. Chemical methods to interrogate bacterial quorum sensing pathways. *Organic & Biomolecular Chemistry* **10**, 8189 (2012).

6. Li, Y.-H. & Tian, X. Quorum Sensing and Bacterial Social Interactions in Biofilms. *Sensors* **12**, 2519–2538 (2012).

7. Geske, G. D., Wezeman, R. J., Siegel, A. P. & Blackwell, H. E. Small Molecule Inhibitors of Bacterial Quorum Sensing and Biofilm Formation. *Journal of the American Chemical Society* **127**, 12762–12763 (2005).

8. K. Bhardwaj, A., Vinothkumar, K. & Rajpara, N. Bacterial Quorum Sensing Inhibitors: Attractive Alternatives for Control of Infectious Pathogens Showing Multiple Drug Resistance. *Recent Patents on Anti-Infective Drug Discovery* **8**, 68–83 (2013).

9. Cámara, M., Williams, P. & Hardman, A. Controlling infection by tuning in and turning down the volume of bacterial small-talk. *The Lancet Infectious Diseases* **2**, 667–676 (2002).

10. Chhabra, S. *et al.* in *The Chemistry of Pheromones and Other Semiochemicals II* (Schulz, S.) **240**, 279–315 (Springer Berlin Heidelberg, 2005).

11. Tal-Gan, Y., Stacy, D. M., Foegen, M. K., Koenig, D. W. & Blackwell, H. E. Highly Potent Inhibitors of Quorum Sensing in Staphylococcus aureus Revealed Through a Systematic Synthetic Study of the Group-III Autoinducing Peptide. *Journal of the American Chemical Society* **135**, 7869–7882 (2013).

12. Deng, Y., Wu, J., Tao, F. & Zhang, L.-H. Listening to a New Language: DSF-Based Quorum Sensing in Gram-Negative Bacteria. *Chemical Reviews* **111**, 160–173 (2011).

13. Galloway, W. R. J. D., Hodgkinson, J. T., Bowden, S. D., Welch, M. & Spring, D. R. Quorum Sensing in Gram-Negative Bacteria: Small-Molecule Modulation of AHL and AI-2 Quorum Sensing Pathways. *Chemical Reviews* **111**, 28–67 (2011).

14. Nadal Jimenez, P. *et al.* The Multiple Signaling Systems Regulating Virulence in Pseudomonas aeruginosa. *Microbiology and Molecular Biology Reviews* **76**, 46–65 (2012).

15. Dulla, G. F. J. & Lindow, S. E. Acyl-homoserine lactone-mediated cross talk among epiphytic bacteria modulates behavior of Pseudomonas syringae on leaves. *The ISME Journal* **3**, 825–834 (2009).

16. Williams, P. Quorum sensing, communication and cross-kingdom signalling in the bacterial world. *Microbiology* **153**, 3923–3938 (2007).

17. Yates, E. A. *et al.* N-Acylhomoserine Lactones Undergo Lactonolysis in a pH-, Temperature-, and Acyl Chain Length-Dependent Manner during Growth of Yersinia pseudotuberculosis and Pseudomonas aeruginosa. *Infection and Immunity* **70**, 5635–5646 (2002).

18. Kaufmann, G. F. *et al.* Revisiting quorum sensing: Discovery of additional chemical and biological functions for 3-oxo-N-acylhomoserine lactones. *Proceedings of the National Academy of Sciences* **102**, 309–314 (2004).

19. Amara, N., Krom, B. P., Kaufmann, G. F. & Meijler, M. M. Macromolecular Inhibition of Quorum Sensing: Enzymes, Antibodies, and Beyond. *Chemical Reviews* **111**, 195–208 (2011).

20. Dong, Y.-H., Xu, J.-L., Li, X.-Z. & Zhang, L.-H. AiiA, an enzyme that inactivates the acylhomoserine lactone quorum-sensing signal and attenuates the virulence of Erwinia carotovora. *Proceedings of the National Academy of Sciences* **97**, 3526–3531 (2000).

21. Teiber, J. F. *et al.* Dominant Role of Paraoxonases in Inactivation of the Pseudomonas aeruginosa Quorum-Sensing Signal N-(3-Oxododecanoyl)-L-Homoserine Lactone. *Infection and Immunity* **76**, 2512–2519 (2008).

22. Bokhove, M., Jimenez, P. N., Quax, W. J. & Dijkstra, B. W. The quorum-quenching N-acyl homoserine lactone acylase PvdQ is an Ntn-hydrolase with an unusual substrate-binding pocket. *Proceedings of the National Academy of Sciences* **107**, 686–691 (2009).

23. Lin, Y.-H. *et al.* Acyl-homoserine lactone acylase from Ralstonia strain XJ12B represents a novel and potent class of quorum-quenching enzymes: Quorum-quenching AHL-acylase. *Molecular Microbiology* **47**, 849–860 (2003).

24. Yin, J., Deng, Z., Zhao, G. & Huang, X. The N-terminal Nucleophile Serine of Cephalosporin Acylase Executes the Second Autoproteolytic Cleavage and Acylpeptide Hydrolysis. *Journal of Biological Chemistry* **286**, 24476–24486 (2011).

25. Eberhard, A., Widrig, C., McBath, P. & Schineller, J. Analogs of the autoinducer of bioluminescence inVibrio fischer. *Archives of Microbiology* **146**, 35–40 (1986).

26. Chhabra, S. R. *et al.* Autoregulation of carbapenem biosynthesis in Erwinia carotovora by analogues of N-(3-oxohexanoyl)-L-homoserine lactone. *The Journal of Antibiotics* **46**, 441–454 (1993).

27. Smith, K. M., Bu, Y. & Suga, H. Induction and Inhibition of Pseudomonas aeruginosa Quorum Sensing by Synthetic Autoinducer Analogs. *Chemistry & Biology* **10**, 81–89 (2003).

28. Smith, K. M., Bu, Y. & Suga, H. Library Screening for Synthetic Agonists and Antagonists of a Pseudomonas aeruginosa Autoinducer. *Chemistry & Biology* **10**, 563–571 (2003).

29. Ishida, T. *et al.* Inhibition of Quorum Sensing in Pseudomonas aeruginosa by N-Acyl Cyclopentylamides. *Applied and Environmental Microbiology* **73**, 3183–3188 (2007).

30. Reverchon, S., Chantegrel, B., Deshayes, C., Doutheau, A. & Cotte-Pattat, N. New synthetic analogues of N-acyl homoserine lactones as agonists or antagonists of transcriptional regulators involved in bacterial quorum sensing. *Bioorganic & Medicinal Chemistry Letters* **12**, 1153–1157 (2002).

31. Geske, G. D. *et al.* Comparative Analyses ofN-Acylated Homoserine Lactones Reveal Unique Structural Features that Dictate Their Ability to Activate or Inhibit Quorum Sensing. *ChemBioChem* **9**, 389–400 (2008).

32. Kato, N., Morohoshi, T., Nozawa, T., Matsumoto, H. & Ikeda, T. Control of Gram-Negative Bacterial Quorum Sensing with Cyclodextrin Immobilized Cellulose Ether Gel. *Journal of Inclusion Phenomena and Macrocyclic Chemistry* **56**, 55–59 (2006).

33. Kaufmann, G. F. *et al.* Antibody Interference with *N* -Acyl Homoserine Lactone-Mediated Bacterial Quorum Sensing. *Journal of the American Chemical Society* **128**, 2802–2803 (2006).

34. De Lamo Marin, S., Xu, Y., Meijler, M. M. & Janda, K. D. Antibody catalyzed hydrolysis of a quorum sensing signal found in Gram-negative bacteria. *Bioorganic & Medicinal Chemistry Letters* **17**, 1549–1552 (2007).

35. Gomes, J., Huber, N., Grunau, A., Eberl, L. & Gademann, K. Fluorescent Labeling Agents for Quorum-Sensing Receptors (FLAQS) in Live Cells. *Chemistry - A European Journal* **19**, 9766–9770 (2013).

36. Dubinsky, L. *et al.* Species selective diazirine positioning in tag-free photoactive quorum sensing probes. *Chemical Communications* **49**, 5826 - 5828 (2013).

37. Praneenararat, T., Beary, T. M. J., Breitbach, A. S. & Blackwell, H. E. Synthesis and application of an N-acylated l-homoserine lactone derivatized affinity matrix for the isolation of quorum sensing signal receptors. *Bioorganic & Medicinal Chemistry Letters* **21**, 5054–5057 (2011).

38. Rayo, J., Amara, N., Krief, P. & Meijler, M. M. Live Cell Labeling of Native Intracellular Bacterial Receptors Using Aniline-Catalyzed Oxime Ligation. *Journal of the American Chemical Society* **133**, 7469–7475 (2011).

CHAPTER II: THIOUREA AND GUANIDINE CATALYZED AMINOLYSIS OF N-ACYL HOMOSERINE LACTONES

A. Introduction

Chemists have been long inspired by the efficiency and specificity by which nature carries out biochemical processes. Consequently, much time as been devoted to artificially recreating these pathways through synthetic chemistry. The intricate array of hydrogen bonding interactions and proton transfers that in part enable enzyme function has spawned the development of specifically crafted hydrogen bond accepting and donating organocatalysts.[1] Mimicking the supramolecular interactions found in nature, these small molecule catalysts have been developed to improve rates and stereoselectivities of a variety of organic transformations. Two such hydrogen bonding compounds that have garnered wide use are thiourea and guanidine catalysts.

i. Thiourea Catalysis

The thiourea catalyst was first introduced by Jacobsen and coworkers who showcased its ability to accelerate asymmetric Strecker reactions.[2] Further study of the Strecker system revealed that the thiourea operates through a mechanism of dual hydrogen bond donation.[3] (Figure 2.1). The acidity of the thiourea moiety makes it successful in coordinating Lewis basic functionalities such as carbonyls, anions, nitrates, and sulfonic acids.[4] The generality of its method of activation has allowed the thiourea to be employed in Pictet-Spangler reactions[5], Mannich reactions[6,7], Diels-Alder reactions[8], and Michael additions[9–11].
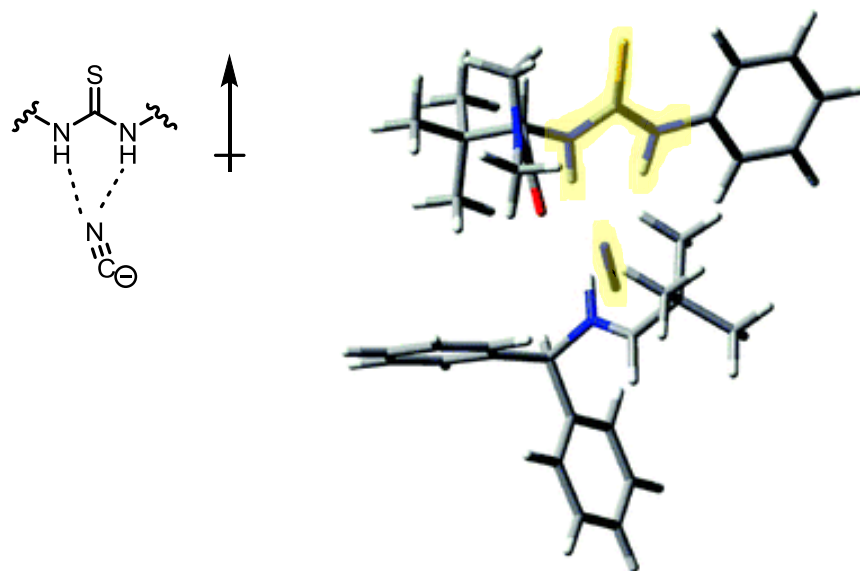
Figure 2.1. Transition state model of Jacobsen's thiourea catalyst for asymmetric Strecker reactions (minor enantiomer). Hydrogen bond donation of the thiourea to the cyanide nucleophile provided a mechanistic rationale for the observed rates and product stereoselectivities. Adapted from Zuend, et al.[12]

Advancements in the field of thiourea catalysis have been forwarded through the use of bifunctional derivatives of the catalyst. These catalysts have been appended to impart an element of catalyst chirality or provide additional sites for non-covalent interactions. Incorporation of a chiral hydrogen bond acceptor in close proximity to the thiourea has been demonstrated to enhance nucleophilic addition reactions in both rate and enantioselectivity (Figure 2.2a). For example, Takemoto and colleagues utilized chiral bifunctional thiourea catalysts in the Michael addition of 1,3 diketones to nitroolefins (Figure 2.2b).[11] The use of the *N,N*-dimethylcyclohexyl functionalized catalyst **3** proved to be the most effective, rapidly affording addition products with up to 99% ee. Through mechanistic studies, the tertiary amine was determined to play a critical role in the activation of the Michael donor serving as a hydrogen bond acceptor to the incoming enol nucleophile.
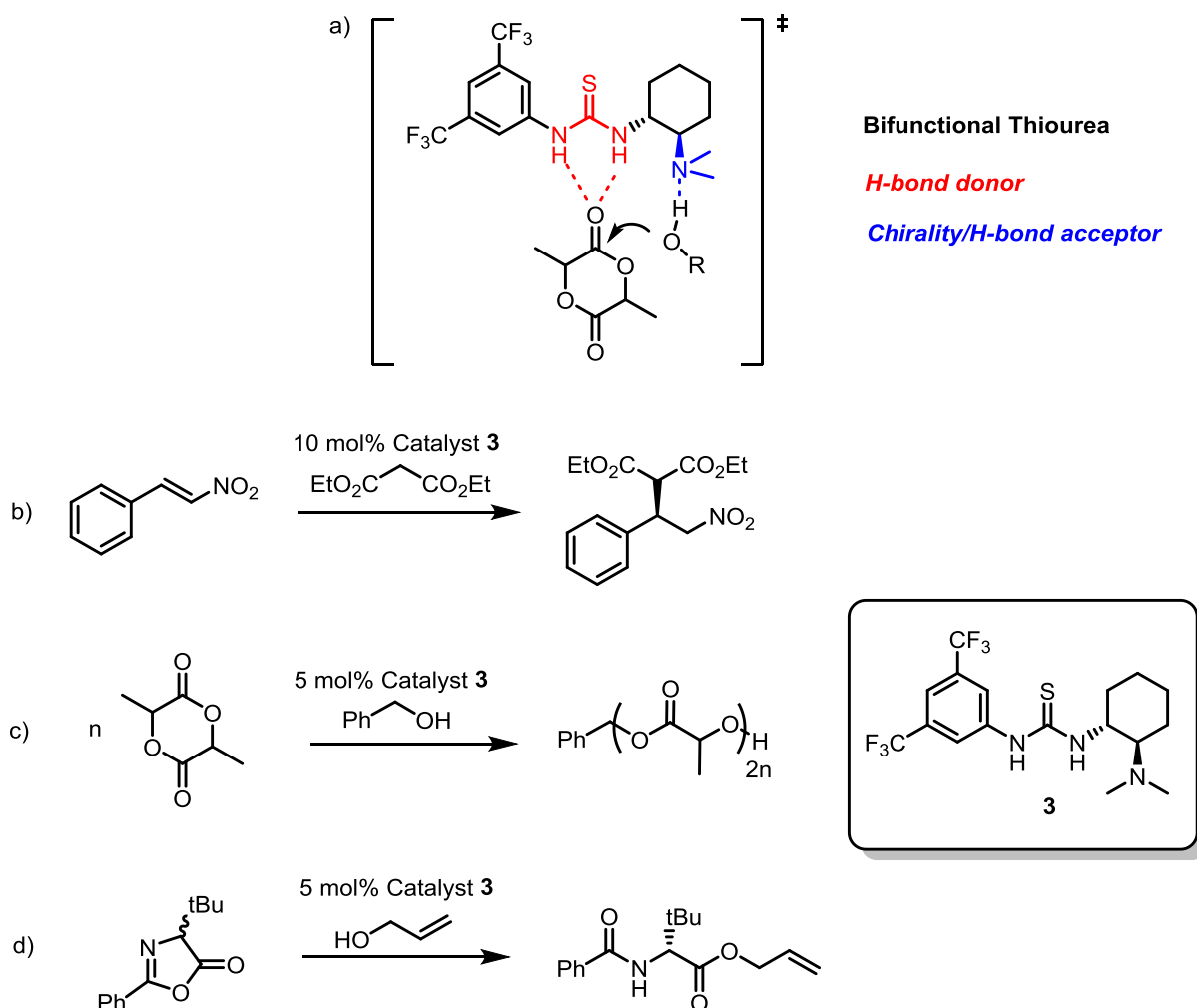
Figure 2.2 – Bifunctional thiourea catalysis with Takemoto's catalyst **3**. a) dual activation by catalyst **3** as described by Hedrick[13] in the transition state of nucleophilic additions to l-lactide. Similar modes of activation have been described in the catalyst's use in b) Michael additions to nitroolefins[11], c) polymerizations of cyclic esters[13], and d) kinetic resolutions of azlactones.[14]

Carbonyl –based substrates, specifically esters and lactones, are also amenable to

activation by thioureas. A racemic version of Takemoto's catalyst was employed by Hedrick

and coworkers in the polymerization of cyclic esters (Figure 2.2c).[13] Through increasing the

electrophilicity of the ester, the bifunctional thiourea effectively advanced rates of

polymerization with only 5 mol % catalyst loading. Comparable rates of polymerization

could not be obtained when the thiourea and dimethylamino moiety were screened

independently, supporting the necessity of the catalyst's bifunctionality for reactivity.

Similar modes of catalyst activation were described by Berkessel and colleagues in their use

of thioureas for the kinetic resolution of azlactones (Figure 2.2d).[14]
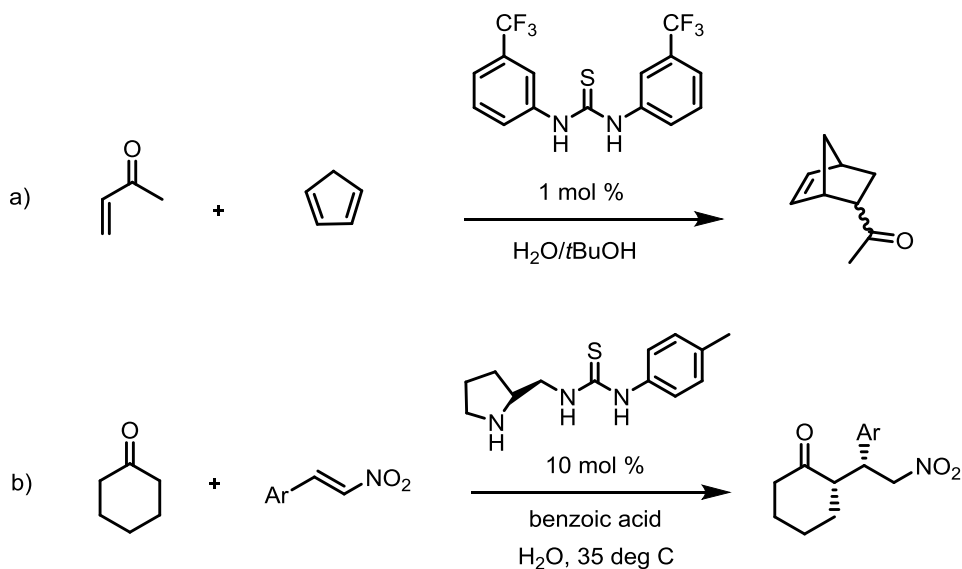
Scheme 2.1. Thiourea catalysis under aqueous conditions. The catalysts have been employed for a) Diels-Alder reactions[15] and b) enantioselective Michael additions to nitroolefins.[10]

Transformations mediated by thiourea catalysis are most readily conducted in

nonpolar, aprotic solvents in order to optimize the hydrogen bonding events necessary for

substrate activation. However, several examples in the literature cite successful thiourea-

catalyzed transformations in water. Schreiner and Wittkopp witnessed moderate rate

accelerations in the Diels-Alder cycloadditions when employing a trifluoromethylated

catalyst in a 9:1 water:*tert*-butanol mixture, observing an 11% increase in yield after 1 h

(Scheme 2.1a). The sustained substrate activation was hypothesized to occur due to the

hydrophobicity of the catalyst and reagents, promoting aggregation of the reaction

components in aqueous media.[8] Xiao and coworkers employed bifunctional proline-thiourea

catalysts for the asymmetric addition of ketones to nitroolefins in water (Scheme 2.1b).

Though catalysis was largely mediated by the addition of 10 mol% benzoic acid, ee's of 79-

99% were obtained across the catalyst and substrate scope, suggesting necessary engagement

of the thiourea during the progression of the reaction.[10] The potential for the thiourea

catalyst to maintain its function of supramolecular activation in water makes it a viable

candidate for screening in biological relevant systems.

ii. Guanidine Catalysis

With arginine as the most prevalent example, guanidines are a motif integral to

natural chemical processes. The functionality has been detected in a variety of natural

products from single-celled prokaryotes to higher order eukaryotes.[16] The uniquely strong

basicity of guanidines renders them protonated across a wide range of pH's, making them

highly capable of anion binding and hydrogen bonding.[17] Enzymes that involve arginine

such as inosine 5'-monophosphate dehydrogenase and fumarate reductase, proceed by

mechanisms that involve the amino acid participating in multiple hydrogen bonding

interactions or serving as general base.[18]
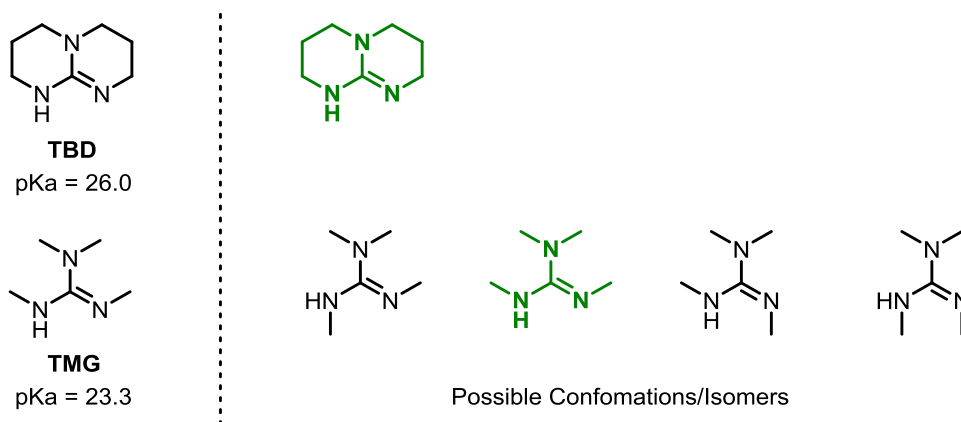
Figure 2.3. Comparison of properties of cyclic guanidine TBD and acyclic TMG.[19] The ring strain in TBD inhibits the delocalization of electrons across the guanidine core, increasing its basicity. The bicycle also restricts C=N isomerization and C-N free rotation to disfavor inactive forms of the catalyst as seen with TMG. The active forms of each catalyst are highlighted in green. TMG = 1,1,3,3-tetramethylguanidine.

The biological relevance of guanidine has inspired its use in organocatalysis. The

functionality has been demonstrated as a suitable catalyst for aldol reactions, carbonylations,

methylations, silylations, and conjugate additions.[20] The most frequently employed

guanidines are bicyclic guanidines, such as 1,5,7-triazabicyclo[4.4.0]dec-5-ene or TBD, due

to the increase in basicity provided by associated ring strain and transition state planarity

relative to their acyclic counterparts. Further, the bicyclic structure preorganizes the catalyst

into the active isomer necessary for optimal substrate interaction with the basic guanidine

core (Figure 2.3).[19] These organocatalysts were originally thought to operate solely through

general base or hydrogen bonding mechanisms, however instances in which the guanidine

serves as nucleophilic catalyst have been well documented.[20,21]
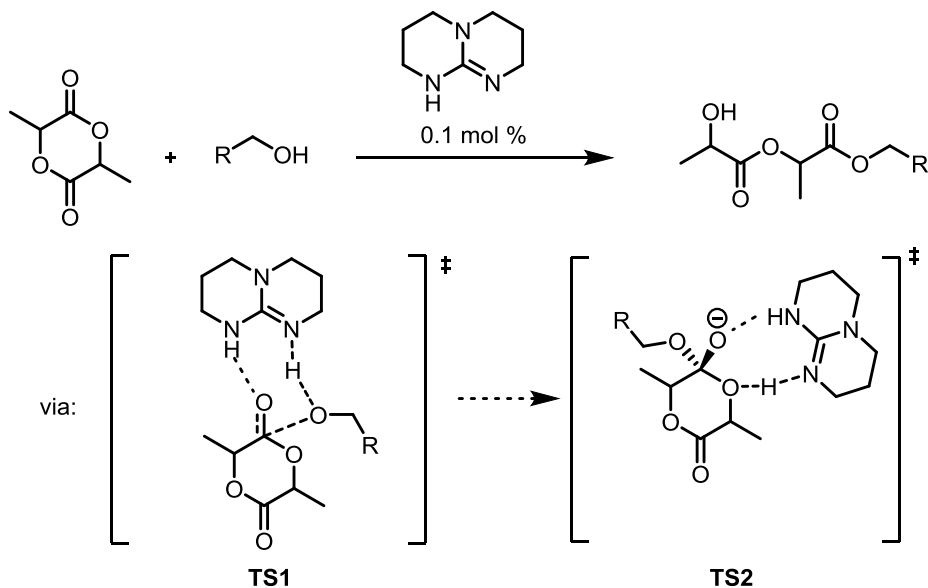
Scheme 2.2. Transition states in the revised mechanism of TBD-catalyzed cyclic ester
polymerizations. TBD operates through a dual hydrogen bonding mechanism,
simultaneously activating both the ester and alcohol (**TS1**). Stabilization of the resultant
oxyanion and hydrogen bonding to oxygen adjacent to the carbonyl (**TS2**) enables rapid
generation of the acyclic product.

Guanidine catalysts have also been demonstrated to be effective in accelerating

transesterifications and acyl transfer reactions by greater than two orders of magnitude over

the uncatalyzed reaction. The mechanism by which these guanidine catalyzed transformations proceed has been debated, being shown to vary depending on the reaction and substrate. Waymouth and colleagues employed TBD as a catalyst for the polymerization of cyclic esters.[22,23] Identification of an *N*-acyl intermediate by ^{1}H NMR led to the conclusion that the increase in polymerization rates was due to TBD serving as a nucleophilic catalyst. DFT calculations by Simon and Goodman on polymerizations of lactones challenged the proposed mechanism, suggesting a lower energy hydrogen bonding pathway. This mechanism depicts the bifunctionality of the catalyst, activating both the incoming nucleophile and substrate, prior to an ultimate proton transfer from the catalyst to the formed tetrahedral intermediate to afford the ring-opening product (Scheme 2.2). Further, β-butyrolactone was not amenable to TBD catalysis but still detectably formed what was deemed a non-productive *N*-acyl intermediate.[24] The hydrogen bonding mechanism was later confirmed by Waymouth in an independent set of computational experiments.[25]
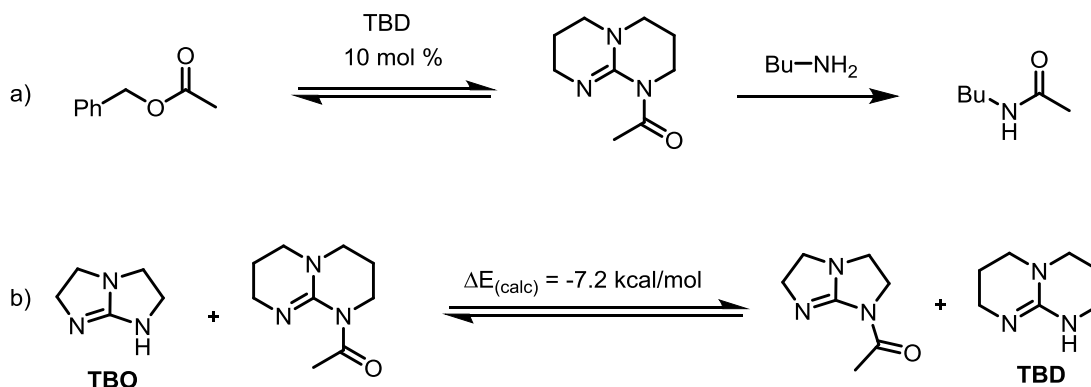
Scheme 2.3. a) TBD-catalyzed amidation of benzyl acetate. Waymouth and colleagues determined catalysis to occur through a nucleophilic mechanism involving first-order formation and decay of an *N*-acylated TBD intermediate. b) *N*-acylated TBD is less energetically stable than the corresponding TBO analog, supporting the increased reactivity of TBD.

In contrast, the ability of TBD to function as a nucleophilic catalyst has been demonstrated in acyl transfer reactions with acyclic esters. Waymouth proved such a

23

mechanism in the amidation of benzyl acetate by observing the reaction to proceed with first order kinetics in both the generation and decay of the corresponding acetylated-TBD intermediate by ^{1}H NMR (Scheme 2.3a). The importance of the structure, namely the N-C=N dihedral angle for reactivity of the formed intermediate, was also highlighted as the rates of reaction decreased on substituting the less spatially constrained 1,4,6-triazabicyclo[3.3.0]oct-4-ene (TBO) for TBD.[26] A twist in the dihedral angle of the acyl-TBD species was determined by DFT calculations, supporting its relatively increased reactivity (Scheme 2.3b). Though variable in its mode of catalysis, TBD is unique in its ability to activate lactone-based substrates for addition reactions by modes inspired by nature.

iii. Rationale for AHL aminolysis

Our investigations into fundamental AHL reactivity and activation began by targeting the lactone of the chemical messenger. Modification of this functionality is a pathway for the deactivation of the signal in nature (see Chapter I) and is a more chemically labile target than the *N*-acyl bond. The γ-butyrolactone is also present across all known *N*-acyl homoserine lactones, holding the potential for our developed methodology to be applicable across multiple gram-negative species.

Initially, we tested the susceptibility of the AHL to modification by transesterification. By employing general base catalysts such as imidazole and N-methylimidazole, the acyclic derivative of the AHL was obtained.[27–29] However, the reaction required solvent quantities of the transesterification agent, in this case methanol. Moreover, in monitoring the reaction by analytical HPLC, it was evident that a solvent dependent equilibrium between the methyl ester and the lactone was established. The resistance of the

24

autoinducers to progress fully to the methanolysis product indicated that the system strongly

favors the reverse reaction and any obtained AHL methyl ester will be readily susceptible to

recyclization (Figure 2.4).
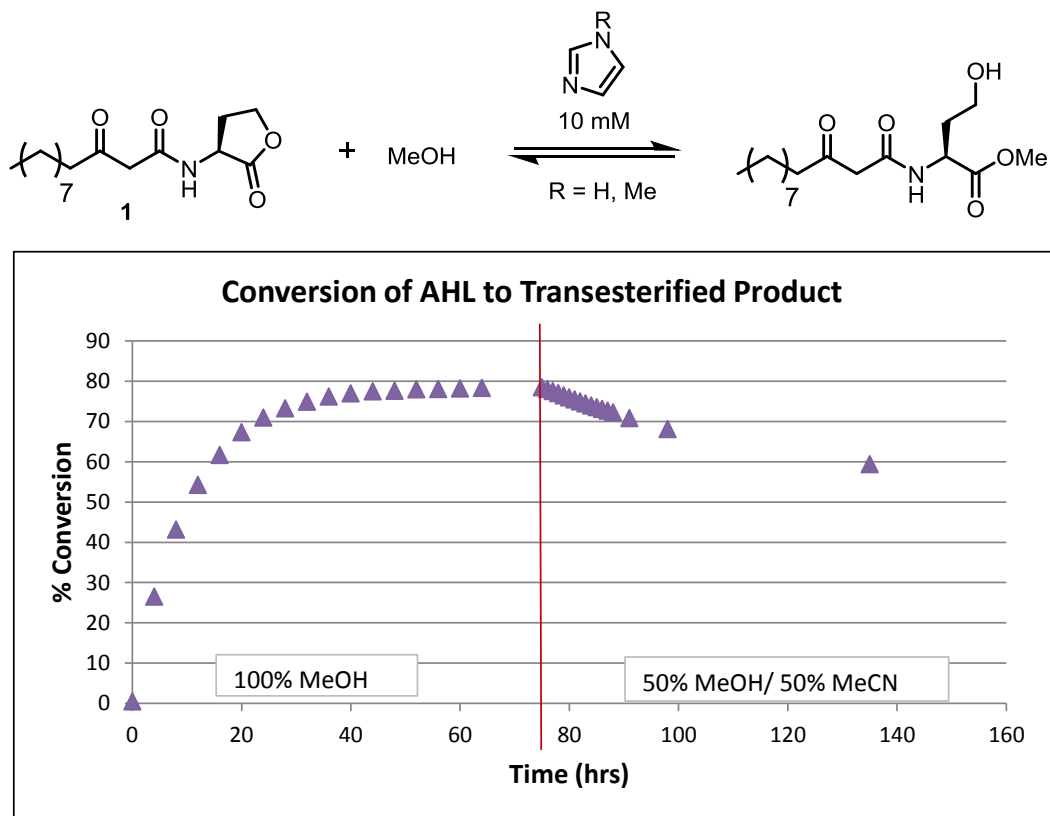
Figure 2.4. Equilibrium established between the 3-oxo-C$_{12}$-AHL (**1**) and its methyl ester. In methanol, 78% of the methyl ester was obtained after 75 hours in the presence of imidazole. Upon introduction of equimolar amounts of acetonitrile (red line), recyclization from the methyl ester to the lactone was observed.

The observed dynamics of AHL transesterification supported the necessity of forming

a more thermodynamically stable acyclic product to irreversibly modify the autoinducer.

Consequently, we investigated amine nucleophiles for AHL lactonolysis, hypothesizing that

the resultant amide from such a transformation would essentially negate the contribution of

the reverse reaction (recyclization). Despite the energy gained in the formation of the amide,

the relatively low ring strain of five membered lactones make them resistant to modification

by a nucleophile.[30] Attempted additions to γ-butyrolactone based substrates have required high temperatures, high amine equivalents, and long reaction times. Hence, Lewis acids, such as AlCl$_3$, and other catalysts have often been employed to increase rates and conversions.[31,32]
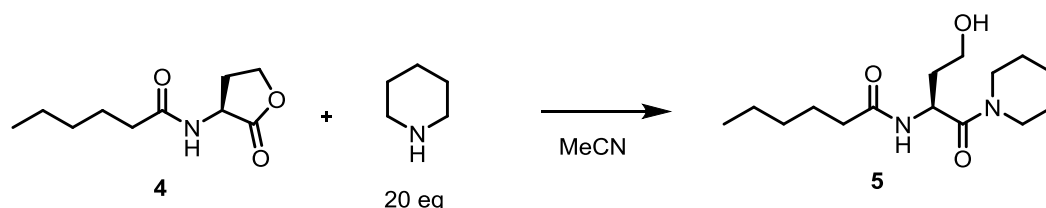
Scheme 2.4. Aminolysis of the C$_6$-AHL with piperidine.

To probe the ability of the AHL to be modified by aminolysis, the C$_6$-AHL (**4**) was combined with 20 eq. of piperidine in MeCN (Scheme 2.4). The reaction reached complete conversion to the corresponding aminolysis product (**5**) after 4 days at RT. Despite the sluggish rates of conversion, the product was isolated with no detected tendency for cycloreversion.
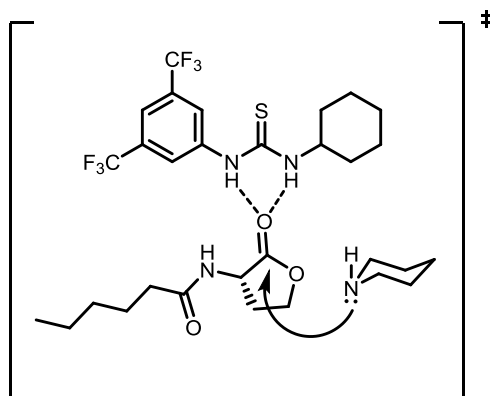
Figure 2.5. Proposed mode of AHL activation by a thiourea catalyst.

As an irreversible modification of the AHL had been achieved, we sought to discover a means of catalyzing this transformation to increase reaction rates and divulge functionality capable of activating the AHL as a substrate. Previous research on thioureas and guanidines

as efficient catalysts for carbonyl additions (see Introduction) made them attractive candidates for screening for AHL aminolysis reactions. We envisioned that both catalysts could serve as hydrogen bond donors to lower the LUMO at the carbonyl and increase the electrophilicity of the lactone, thus activating it for acyl transfer (Figure 2.5). Both catalysts also have the potential to be readily modified to impose elements of bifunctional activation and synthetically tuned to alter properties of acidity and steric constraint for the purpose of optimizing catalytic efficiency.

B. Results and Discussion

i. Thiourea-catalyzed AHL aminolysis[33]

As an initial proof of concept for our proposed mode of activation, thiourea catalyst **7a** was synthesized by addition of cyclohexylamine to the corresponding isothiocyanate and added to the reaction of piperidine and the C_6-AHL. Utilizing 10 mol % of the catalyst, complete conversion was obtained in 19 h, equating to approximately six times the rate of the uncatalyzed reaction in MeCN.

Table 2.1 Thiourea catalyst scope and percent yields.

Catalyst	R	% Yield
7a	(cyclohexyl)	90
7b	(propyl)	84
7c	(ethyl-N-methylamine)	82
7d	(propyl-dimethylamine)	87
7e	(imidazole)	38
3	(cyclohexyl amine)	30
7f	(trimethylammonium)	11
7g	(bis-CF₃ thiourea)	79
7h	(propyl bis-CF₃ thiourea)	83

With the initial success of catalyst **7a**, we synthesized a small library of thioureas to determine if such mild rates of catalysis could be improved. Nine potential organocatalysts were synthesized and can be compared based on their potential for multimodal interactions with the substrate and nucleophile (Table 2.1). Catalysts **7a** and **7b** are monofunctional, relying solely on the thiourea for substrate activation. The remaining catalysts each contain an element of bifunctionality with the potential to further activate the AHL or nucleophile.

28

Catalysts **7c**, **7d**, **7e**, and **3** are all appended with tertiary amines capable of serving as a hydrogen bond acceptors to assist in enhancing the nucleophilicity of piperidine. Tetraalkylammonium **7f** could provide stability to the developing anionic transition-state characteristic of amine additions to carbonyl. Dithiourea catalysts **7g** and **7h** possess two thioureas that may act individually on two AHLs or synergistically on a single molecule of substrate by creating a more extensive surface of available hydrogen bond donors. The 3,5-bis(trifluoromethyl)phenyl group was retained in all catalysts due to its ability to inductively increase the acidity of the thiourea and provide additional stabilization with a uniquely polar ortho-CH bond.[34]
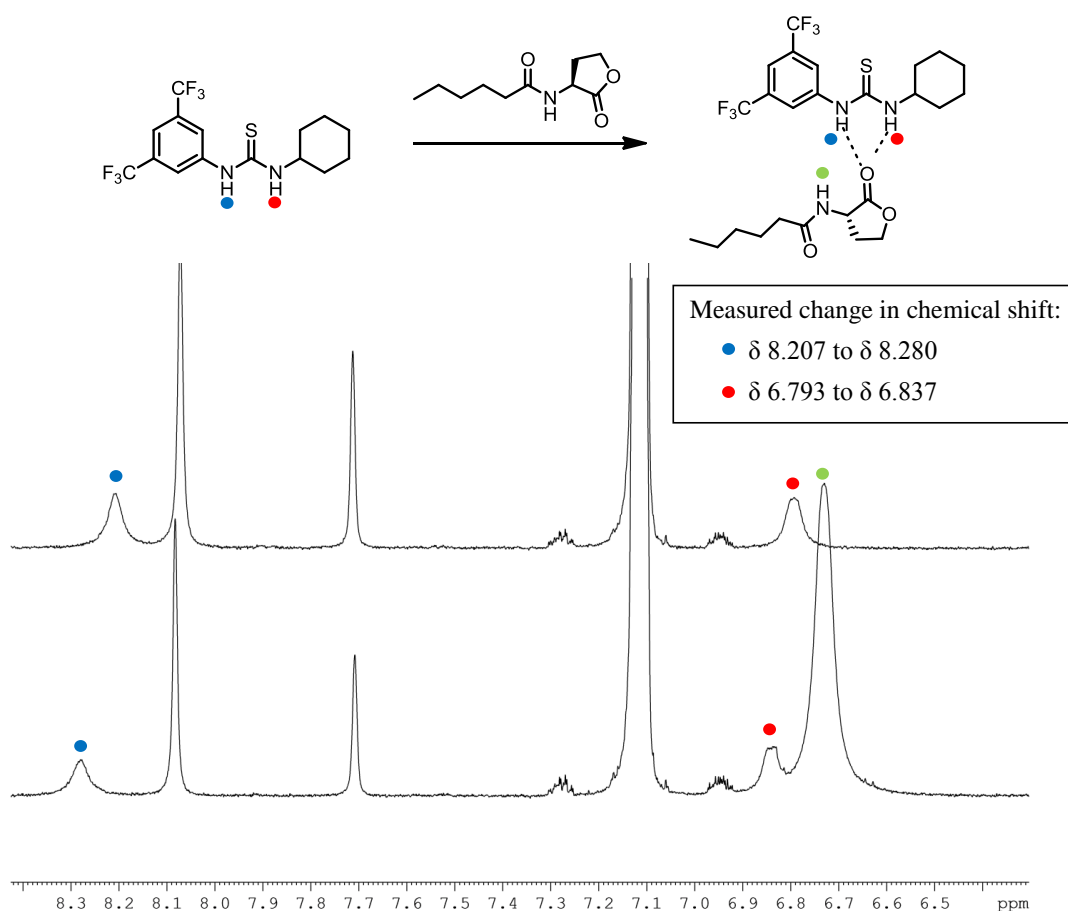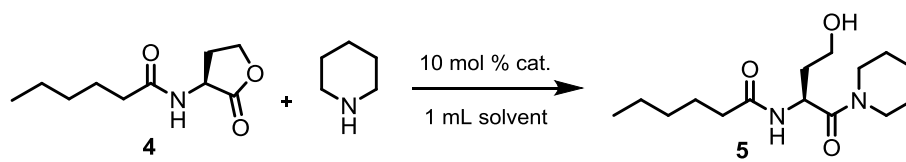
Figure 2.6. Evidence of an AHL-thiourea interaction by ^{1}H NMR. A downfield shift in the N-H resonances of 10 mol % of catalyst **7a** is observed upon addition of the C_6-AHL.

The catalysts were then screened for activity in the same piperidine/C_6-AHL model system as described above by ^{1}H NMR, monitoring the integration of the α-proton resonance over time. Prior to the addition of piperidine, an observable shift was detected in the proton resonances of the thiourea catalyst in the presence of the AHL (Figure 2.6). This confirms the hypothesized interaction between the thiourea and the homoserine lactone.

Table 2.2 Relative rates of thiourea catalyzed aminolysis in CD_3CN and DMF-d_7.
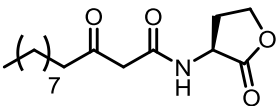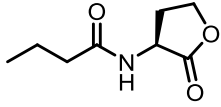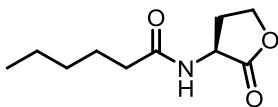
Catalyst	k_{rel} CD_3CN	k_{rel} DMF-d_7
7a	4.5	3.4
7b	5.6	3.6
7c	4.3	3.4
7d	4.4	3.3
7e	5.5	3.2
7f	4.5	-
3	8.2	-
7g	7.9	5.2
7h	10.0	5.3

[a]The reactions were monitored until 50% conversion (t_{50}) was reached

The entire library of catalysts proved active in enhancing rates of AHL aminolysis (Table 2.2). Ring-opening rates up to 8.2 times the uncatalyzed reaction were achieved among the monofunctional and bifunctional catalysts screened with dithiourea catalyst **7h** reaching an increase of an order of magnitude relative to the control. However, in comparing the activity of the monofunctional and bifunctional catalysts, those catalysts which include secondary sites of activation served to provide little to no advantage as the rates obtained were similar. Takemoto's catalyst (**3**) generated the aminolysis product at twice the rate of

any monofunctional thioureas, supporting the involvement of the *N,N,*-dimethylamino group in catalysis. This mild acceleration relative to use of the same catalyst in previously published systems[11,13,14] may be due to the inherent weakness of the interaction of the tertiary amine with the nucleophile, namely the N-H---N hydrogen bond. In the case of catalysts **7c** – **7f**, the lack of conformational constraints to position the bifunctionality at the catalytic active site is one possible explanation for the observed rates.

Table 2.3. Relative rates of aminolysis of different AHLs in CD_3CN^a

AHL	Structure	k_{rel} **7a**	k_{rel} **7h**
1		2.7	4.0
2		4.1	7.3
4		4.5	10

[a]with piperidine as the amine nucleophile in 20-fold excess.

Next, the transferability of the thiourea catalysts across the AHL family was assessed. Inspired by the autoinducers responsible for quorum sensing in *P.aeruginosa*, we screened both catalyst **7a** and **7h** against the 3-oxo-C_{12} (**1**) and C_4-AHL (**2**) (Table 2.3). The C_4-AHL proceeded in a similar fashion to the C_6-AHL. The 3-oxo-C_{12}-AHL showed a marked decrease in its susceptibility to thiourea catalysis achieving rates of only four times the control reaction with catalyst **7h**. The 3-oxo-C_{12}-AHL was also sparingly soluble in CD_3CN and substrate aggregation could negatively impact the interaction of the autoinducer with the catalyst. In addition, the extra carbonyl moiety characteristic of the 3-oxo-AHL could be serving as a site for competitive catalyst binding.

With the ability of AHL aminolysis to be accelerated by H-bonding catalysts established, the impact of solvent background reactivity and catalysis was tested (Table 2.4). First, catalysts **7a** and **7h** were screened in aprotic solvents with a wide range of polarity. Background reaction rates markedly increased as solvent polarity was increased, however catalysis was still observed. Notably, the impact of the thioureas was evident in DMF-d_7, a solvent in which competitive hydrogen bonding was expected to deactivate the catalyst.

Table 2.4. Relative rates of C_6-AHL aminolysis in the presence of catalysts **7a** and **7h** in aprotic solvents and polar protic solvent mixtures

Entry	Solvent (% v/v)	$t_{50}\%^b$ uncat (x 10^3 s)	k_{rel} **7a**	k_{rel} **7h**
1	C_6D_6	5.1	2.0	4.3
2	CD_2Cl_2	3.6	1.0	1.1
3	CD_3CN	35.5	4.5	10
4	DMF-d_7	100.7	3.4	5.3
5	DMSO-d_6	123.2	1.9	2.2
6	10% MeOH-d_4/CD_3CN	14.3	0.9	1.5
7	10% D_2O/ DMSO-d_6	21.0	1.3	1.0
8	10% TFE-d_3/CD_3CN	9.7	1.1	1.0
9	10% D_2O/CD_3CN	4.2	1.0	0.9

[a]with piperidine as the amine nucleophile in 20-fold excess; [b]$t_{50\%}$ represents the reaction time to reach 50% conversion

Next, with the goal of determining if catalysis would be sustained under physiological conditions, the catalysts were screened in a series of protic co-solvents. A significant increase in the uncatalyzed reaction rate was observed with 10% v/v of a protic additive, supporting a component of protic solvent assistance in the aminolysis reaction. Further, the impact of the thiourea catalysts under these conditions was negated. Unlike the previously

discussed examples of thiourea catalysis in water[8,10], the presence of protic additives

inhibited the supramolecular events necessary for catalysis in our system.

ii. Guanidine-catalyzed AHL aminolysis

In an effort to improve upon rates obtained in our thiourea screens, we undertook a

short study of the impact of guanidines on enhancing AHL reactivity. With its success in

catalyzing transesterification and acyl transfer reactions, TBD was selected for an initial

screen in the C_6-AHL/piperidine control reaction described above (Scheme 2.4). Upon

addition of 10 mol % TBD, complete conversion to the aminolysis product was achieved in

1.5 h or 65 times faster than the control reaction. Notably, these rates are 6.5 times faster

than our most successful thiourea catalyst **7h**.

Equilibration Time[a]	$t_{50\%}$(s)
4 days	>86400
5 minutes	3500

[a]refers to time with AHL and TBD in solution prior to piperidine addition
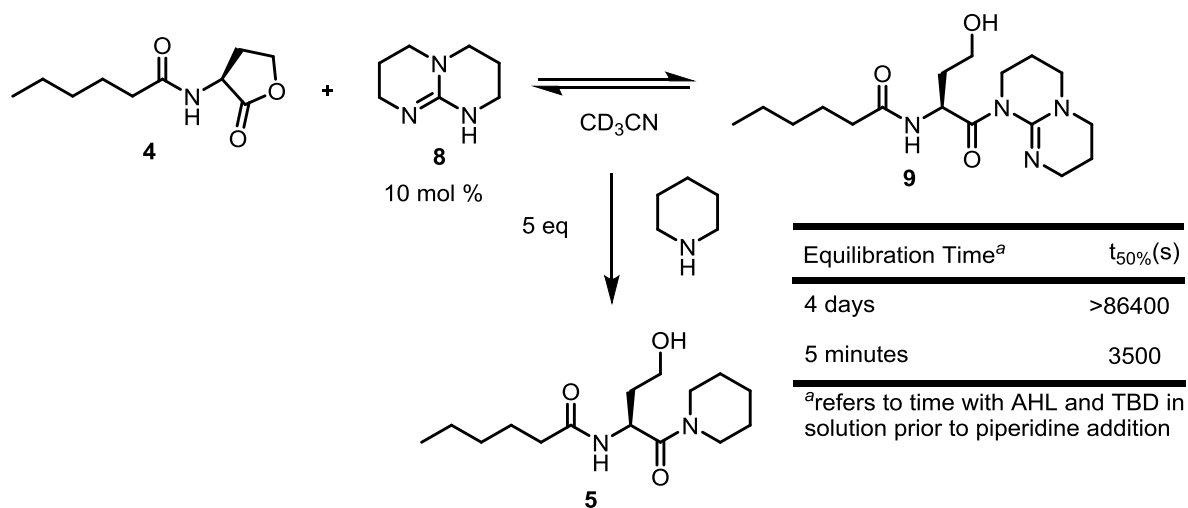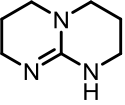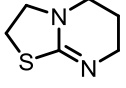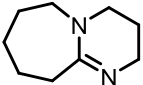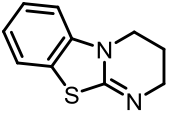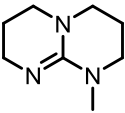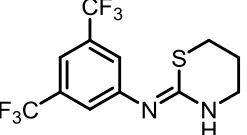
Scheme 2.5. Generation of *N*-acylated TBD intermediate (**9**) at variable equilibration times. Preforming the *N*-acyl intermediate inhibits formation of AHL aminolysis product. Relative $t_{50\%}$ values were determined by ^{1}H NMR.

The significant rate enhancement compared to the previously screened thiourea

catalysts made further study of the TBD system critical for understanding the mode of AHL

activation. As noted in beginning of Chapter 2, TBD has been proposed to serve as both a

nucleophilic catalyst and hydrogen bond donor depending on the reaction and substrate. To

assess the possibility of catalysis by a nucleophilic pathway, the C_6-AHL (**5**) was combined

with a stoichiometric amount of TBD in the absence of piperidine to test for the formation of

an *N*-acyl intermediate (**9**) by ^{1}H NMR. Observable shifts in the catalyst and substrate proton

resonances were detected and the corresponding intermediate was confirmed by 2D NMR

spectroscopy. However, upon addition of piperidine to a solution containing the preformed

intermediate, the rates of conversion to aminolysis product **6** dramatically decreased (Scheme

2.5), suggesting that formation of the *N*-acyl intermediate was catalytically unproductive. If

the acylation of TBD was a key step in the catalytic cycle, the intermediate would have

readily dissipated in the presence of a nucleophile. Hence, similar to Goodman's

observations in the transesterification of β-butyrolactone, the aminolysis of the AHL was

likely not proceeding through a nucleophilic pathway and more reasonably by acting through

a hydrogen bond mediated mechanism.[24]

      To demonstrate the importance of hydrogen bond donation in the TBD-catalyzed

aminolysis of the autoinducer, a series of amidine and isothiourea catalysts (Table 2.5) were

synthesized and screened. Both amidines and isothioureas have been employed in acyl

transfer catalysis but are incapable of serving as hydrogen bond donors.[35–39] When combined

with the C_6-AHL in the presence of piperidine, no increase in reaction rate was afforded

relative to the control. The same decrease in activity was observed in screening MTBD

(**10b**), in which methylation of the guanidine expunges the potential of the catalyst to

participate hydrogen bond donation to the substrate. Both examples corroborate the function

of TBD as a hydrogen bond donor and not a nucleophilic catalyst in our system.

Table 2.5. Relative rates of amidine and isothiourea-mediated C_6-AHL aminolysis with piperidine in CD_3CN.

Catalyst		k_{rel}	Catalyst		k_{rel}
8		64.8	**10c**		1.1
10a		2.0	**10d**		1.1
10b		1.5	**10e**		1.1

Establishing the importance of TBD as a hydrogen bond donor, we sought to assess the interplay of the basicity of the guanidine in the increasing aminolysis rates in addition to its potential for bifunctional activation.[26] An equimolar amount of trifluoroacetic acid was titrated into a reaction mixture containing the catalyst and substrate to fully protonate the guanidine and eliminate secondary modes of activation beyond hydrogen bond donation (Scheme 2.6). Upon the addition of piperidine, the resulting guanidinium (**11**) was inactive as rates obtained were similar to the uncatalyzed reaction. The inactivity of the protonated guanidine demonstrates that TBD is not acting solely through a mechanism of hydrogen bond donation and does employ a secondary mode of activation in the derivatization of the QS autoinducer.
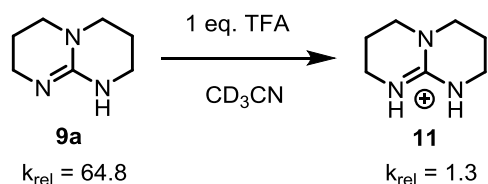
Scheme 2.6. Relative rates of aminolysis upon TBD protonation. An equivalent of trifluoroacetic acid (TFA) was added to form the corresponding guanidinium ion (**11**). The loss of catalytic activity indicates that TBD does not exclusively serve as an H-bond donor.
Table 2.6. Relative rates of C_6-AHL aminolysis with decreasing catalyst basicity in CD_3CN.

Catalyst	Structure	pKa[a]	k_{rel}
8		26.0	64.8
12a		(12.5)	2.0
12b		(5.3)	1.5

[a]pKa in CD_3CN; parenthesis indicate pKa in MeOH-d_4/D_2O

To further explore the importance of basicity to catalyst function, catalysts **12a** and

12b were obtained and tested due to their reduced pKa values relative to TBD. When each

was added in 10 mol % quantities to the control reaction of C_6-AHL with piperidine,

attenuation of catalytic rates was observed (Table 2.6). The decrease in relative rates of

catalysis directly correlates to the decrease of the pKa of the catalyst compared to TBD.

Thus, the basicity of TBD is critical in achieving accelerated rates of AHL aminolysis.
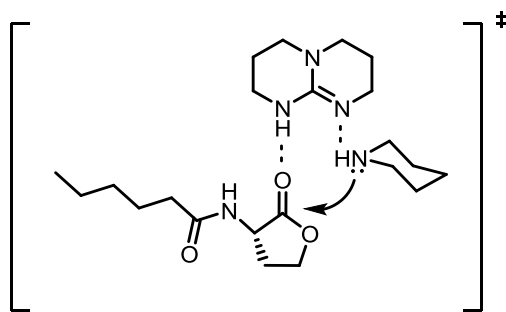
Figure 2.7. Bifunctional activation of the AHL and amine nucleophile by TBD.

The collection of results from this short study led us to hypothesize that the TBD is

acting through a bifunctional model of activation, similar to that described by Waymouth and

colleagues.[26] As the contribution of hydrogen bond donation to the catalytic efficiency of

TBD has been proven, the neighboring basic site could reasonably be serving as a hydrogen

bond acceptor to activate piperidine during nucleophilic attack (Figure 2.7). This dual mode

of activation is likely supported by the uniquely small dihedral angle of TBD that permits both donor and acceptor functions of the catalyst to work in tandem. Further mechanistic investigation and catalyst development is necessary to confirm these mechanistic details, but the decision was made to not to complete these studies in lieu of as to pursuing novel modes of activating and modifying the AHLs under aqueous conditions (Chapter 3 & 4).

C. Conclusions

By probing the reactivity of the characteristic γ-butyrolactone of the AHL family of quorum sensing autoinducers, their susceptibility to ring-opening by amine nucleophiles was demonstrated. In contrast to attempts at transesterification of the lactone, complete conversion was obtained through the formation of a more thermodynamically stable, amidated product. The introduction of thiourea catalysts demonstrated that the incorporation of hydrogen bond donors can increase the electrophilicity of the autoinducer for subsequent addition. Employing a guanidine catalyst, TBD, in a similar fashion reinforced substrate activation by hydrogen bond donation while achieving greater conversion rates. From our experimental evidence, it is reasonable to attribute this increase in rate to the elevated basicity of TBD and complimentary structure of the guanidine core that supports an effective bifunctional catalytic pathway for lactone aminolysis.

This is the first time small molecule organocatalysts have been employed to activate the QS autoinducers and have provided valuable information into the non-covalent interactions that advance their derivatization. Though the catalytic activity of both the thiourea and guanidine catalysts was not sustained in protic environments, these interactions relate to those observed in enzymatic catalytic sites that have evolved for degradation of the signaling molecule. Moving away from small molecule catalysts towards peptide-based

enzyme mimics may provide the opportunity to exploit our findings about AHL reactivity in an aqueous milieu.

D. Experimental

i. General Reagents and Catalyst Synthesis

Commercial reagents and catalysts, including TBD (**8**), MTBD (**10b**), DBU (**10a**), and THQPO (**12b**) were obtained from Sigma-Aldrich and Fisher Scientific. Column chromatography of all compounds, except catalyst **7f**, was completed using Fisher 230-400 Mesh Grade 60 silica gel. Catalyst **7f** was purified using a Waters semi-prep HPLC/UV-Vis with an XBridge 5μM C_{18} column as detailed in the procedure below. NMR solvents were purchased from Cambridge Isotopes Laboratories. Product characterization and kinetic experiments were completed on either a 600 MHz or 500 MHz Bruker NMR spectrometer. All related coupling constants are reported in Hertz and shifts in ppm. Elemental analyses (C, H and N) were completed by Robertson Microlit Laboratories, Inc. High resolution mass spectrometry (HRMS) was completed by the Mass Spectrometry Laboratory at the School of Chemical Sciences, University of Illinois using ESI on a Waters Q-ToF Ultima mass spectrometer.

General Procedure for Thiourea Catalyst Synthesis Preparation

To a 25-mL Schlenk flask flushed with N_2, 3,5-bis(trifluoromethyl)phenyl isothiocyanate **6** (0.336 mL, 1.84 mmol) was added and then solvated in benzene (1 mL). The corresponding amine (1.84 mmol) was added slowly to the flask. The walls of flask were washed with benzene (1 mL) and the reaction was allowed to stir at room temperature for 3 h. The reaction progress was monitored by TLC. The reaction mixture was concentrated under

vacuum and redissolved in DCM. The product was purified by column chromatography on silica gel with a gradient mobile phase [DCM to MeOH/DCM (1:9)].[7,11]

1-(3,5-bis(trifluoromethyl)phenyl)-3-cyclohexylthiourea (7a)
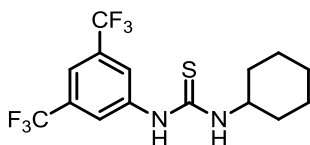
δ_H (DMSO-d_6, 500 MHz) 9.88 (1H, s), 8.24 (2H, s), 8.18 (1H, s), 7.72 (1H, s), 4.12 (1H, br s), 1.92 (2H, m), 1.71 (2H, m), 1.58 (1H, m), 1.35 – 1.29 (5H, m); δ_C (DMSO-d_6, 125 MHz) 179.1, 141.9, 130.0 (q, J_{CF} = 33.9 Hz), 123.2 (q, J_{CF} = 272.7 Hz), 121.6, 115.7, 52.2, 31.5, 25.0, 24.3; HRMS (ESI) calcd for $C_{15}H_{17}N_2F_6S$: 371.1017, found: 371.1014 (M + H).

1-(3,5-bis(trifluoromethyl)phenyl)-3-propylthiourea (7b)
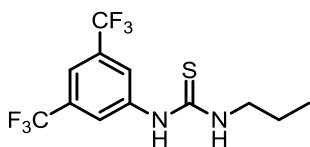
δ_H (DMSO-d_6, 500 MHz) 10.00 (1H, s), 8.23 (3H, br s), 7.69 (1H, s), 7.72 (1H, s), 3.40 (2H, m), 1.56 (2H, dt, J = 7.5 Hz), 0.89 (3H, t, J = 7.5 Hz); δ_C (DMSO-d_6, 125 MHz) 180.2, 141.7, 129.8 (q, J_{CF} = 32.7 Hz), 122.9 (q, J_{CF} = 272.9 Hz), 121.4, 115.5, 45.3, 21.4, 11.0; HRMS (ESI) calcd for $C_{12}H_{13}N_2F_6S$: 331.0712, found: 331.0704 (M + H); Anal. Calc. for $C_{12}H_{13}N_2F_6S$: C, 43.64; H, 3.66; N, 8.48; found: C, 43.56, H, 3.66, N, 8.35.

1-(3,5-bis(trifluoromethyl)phenyl)-3-(2-(dimethylamino)ethyl)thiourea (7c)
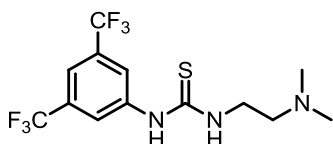
δ_H (DMSO-d_6, 500 MHz) 10.27 (1H, s), 8.26 (2H, s), 8.10 (1H, s), 7.72 (1H, s), 3.56 (2H, br q), 2.44 (br t, 2H), 2.19 (6H, s); δ_C (DMSO-d_6, 150 MHz) 180.0, 141.9, 130.2 (q, $J = 33.2$ Hz), 123.2 (q, $J = 273.1$ Hz), 121.3, 115.8, 56.8, 44.9, 41.7; HRMS (ESI) calcd for $C_{13}H_{16}N_3F_6S$: 360.0696, found: 360.0692 (M + H).

1-(3,5-bis(trifluoromethyl)phenyl)-3-(3-(dimethylamino)propyl)thiourea (7d)
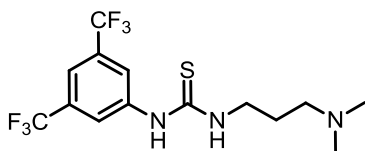
δ_H (DMSO-d_6, 600 MHz) δ10.09 (1H, s), 8.33 (1H, s), 8.23 (2H, s), 7.70 (1H, s), 3.51 (2H, br s), 2.27 (2H, t, $J = 6.60$ Hz), 2.12 (6H, s), 1.69 (2H, p, $J = 6.60$ Hz); δ_C (DMSO-d_6, 150 MHz) δ180.3, 141.9, 130.2 (q, $J_{CF} = 33.2$ Hz), 123.2 (q, $J_{CF} = 273.1$ Hz), 121.8, 115.9, 56.8, 45.0, 42.6, 25.9; HRMS (ESI) calcd for $C_{14}H_{18}N_3F_6S$: 374.1126, found: 374.1126 (M + H).

1-(2-(1H-imidazol-4-yl)ethyl)-3-(3,5-bis(trifluoromethyl)phenyl)thiourea (7e)
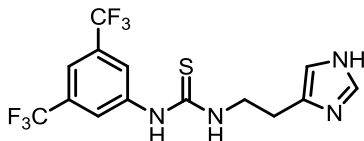
δ_H (DMSO-d_6, 500 MHz) 11.90 (1H, br s), 10.21 (1H, s), 8.27 (3H, br s), 7.72 (1H, s), 7.57 (1H, s), 6.88 (1H, s), 3.76 (2H, br q), 2.81 (2H, t, J = 7.5 Hz); δ_C (DMSO-d_6, 125 MHz) 180.2, 141.8, 134.4, 130.0 (q, $J_{CF} = 32.7$ Hz), 128.2, 123.1 (q, $J_{CF} = 272.9$ Hz), 121.6, 115.8,

43.8, 26.0; HRMS (ESI) calcd for $C_{14}H_{13}N_4F_6S$: 383.0765, found: 383.0772 (M + H); Anal. Calc. for $C_{14}H_{13}N_4F_6S$: C, 43.98, H, 3.16, N, 14.65; found: C, 44.01, H, 3.20, N, 14.61.

1-(3,5-bis(trifluoromethyl)phenyl)-3-((1R,2R)-2-(dimethylamino)cyclohexyl)thiourea (3)
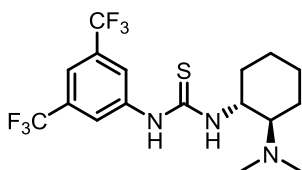
δ_H (DMSO-d_6, 600 MHz) 10.02 (1H, s), 8.23 (1H, s), 8.17 (2H, s), 7.69 (1H, s), 4.10 (1H, br s), 2.54 (1H, s), 2.22 (7H, s), 1.85 (1H, br s), 1.76 (1H, br s), 1.64 (1H, d, J = 10.2 Hz), 1.32 − 1.09 (4H, m); δ_C (DMSO-d_6, 125 MHz) 179.0, 142.4, 130.8 (q, J_{CF} = 27.5), 123.7 (q, J_{CF} = 226 Hz), 121.4, 115.9, 65.5, 55.7, 32.1, 25.1, 25.0, 21.5; MS (ESI) calcd for $C_{17}H_{21}N_3F_6S$: 414.13; found: 414.17 (M+H)

Synthesis of Catalyst **7f**

Catalyst **7f** was synthesized through a modified version of the general procedure above. In a 2-mL eppendorf tube, (2-aminoethyl)trimethylammonium chloride hydrochloride (50 mg, 0.286 mmol) was combined with N,N-diisopropylethylamine (0.050 mL, 0.286 mmol). Then, **6** (0.052 mL, 0.286 mmol) was then added to the tube. The reaction mixture was vortexed for 10 min in the eppendorf tube. The reaction mixture was quenched by adding 2 mL of MeOH to the tube.   The reaction mixture was concentrated and redissolved in distilled water. The resultant aqueous solution was filtered and diluted to prepare for purification. The product was purified by semi-prep HPLC with a gradient mobile phase [MeCN/H$_2$O (1:4) to MeCN/H$_2$O (1:1)]. Notably, a small percentage of trifluoroacetic acid was retained by the catalyst after purification and is present in the ^{13}C NMR. Given the large

excess of piperidine present in the catalyst screening, this trace acid did not significantly

affect the rate of AHL aminolysis.

2-(3-(3,5-bis(trifluoromethyl)phenyl)thioureido)-N,N,N-trimethylethanaminium (7f)
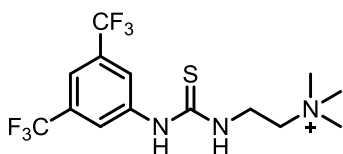
δ_H (DMSO-d$_6$, 500 MHz) 10.78 (1H, br s), 8.80 (1H, s), 8.26 (2H, s), 7.80 (1H, s), 3.99 (2H,

m), 3.54 (1H, t, J = 6.50), 3.14 (9H, s); δ_C (CD$_3$CN-d$_3$, 125 MHz) 182.9, 160.8 (q, J = 35.2),

142.4, 131.5 (q, J_{CF} = 32.7 Hz), 124.1 (q, J_{CF} = 271.6 Hz), 123.5, 64.8, 54.1, 38.7; HRMS

(ESI) calcd for C$_{14}$H$_{18}$N$_3$F$_6$S: 374.1126, found: 374.1120 (M + H).

Synthesis of Catalysts **7g** *and* **7h**

Catalysts **7g** and **7h** were synthesized following the general procedure but reacting 2 eq (3.68

mmol) of **6** with 1 eq (1.84 mmol) of a diamine. Ethylenediamine was the diamine chosen to

construct **7g** and 1,3 diaminopropane to make **7h**.

1,1'-(ethane-1,2-diyl)bis(3-(3,5-bis(trifluoromethyl)phenyl)thiourea) (7g)
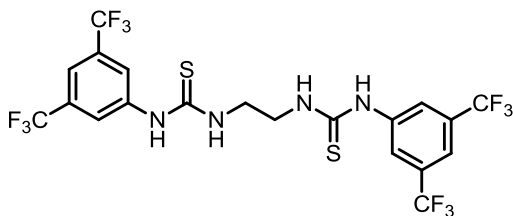
δ_H (DMSO-d$_6$, 500 MHz) 10.14 (2H, s), 8.34 (2H, s), 8.22 (4H, s), 7.72 (2H, s), 3.77 (4H, br

s); δ_C (DMSO-d$_6$, 125 MHz) 180.7, 141.4, 129.9 (q, J_{CF} = 32.7 Hz), 122.9 (q, J_{CF} = 272.9

Hz), 122.0, 116.0, 42.5; HRMS (ESI) calcd for $C_{20}H_{15}N_4F_{12}S_2$: 603.0547, found: 603.0546

(M + H); Anal. Calc. for $C_{20}H_{15}N_4F_{12}S_2$: C, 39.87; H, 2.34; N, 9.30; found: C, 40.15; H, 2.47;

N, 9.06.

1,1'-(propane-1,3-diyl)bis(3-(3,5-bis(trifluoromethyl)phenyl)thiourea) (7h)
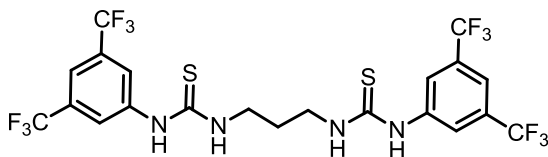
δ_H (DMSO-d_6, 600 MHz) 10.09 (2H, s), 8.26 (2H, s), 8.22 (4H, s), 7.70 (2H, s), 3.57 (4H, s),

1.89 (2H, p, J = 6.6 Hz); δ_C (DMF-d_7, 125 MHz) 181.6, 142.7, 131.1 (q, J_{CF} = 32.7 Hz),

123.8 (q, J_{CF} = 271.5 Hz), 122.6, 116.5, 42.1, 28.3; HRMS (ESI) calcd for $C_{21}H_{17}N_4F_{12}S_2$

617.0703, found 617.0699 (M + H); Anal. Calc. for $C_{21}H_{17}N_4F_{12}S_2$: C, 40.91; H, 2.62; N,

9.09, found: C, 40.64; H, 2.58; N, 8.86.

Synthesis of Catalyst **10e**

To a N_2 flushed flask, **6** (1.00 mL, 8.4 mmol) was dissolved in 20 mL of THF followed by

the addition of 3-aminopropan-1-ol (0.61 mL, 8.0 mmol). The reaction mixture was allowed

to stir at RT for 5 hours and then concentrated under vacuum. The reaction mixture was

redissolved in concentrated HCl and stirred at 80°C for 4h. After cooling the reaction to

room temperature, 15 mL of 2.5 M NaOH was added and allowed to stir for ten minutes.

The resultant reaction mixture was vacuum filtered to afford the desired product.

(Z)-N-(3,5-bis(trifluoromethyl)phenyl)-1,3-thiazinan-2-imine (10e)
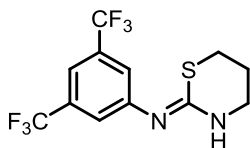
51% yield. δ_H (CD$_3$CN, 600 MHz) 7.67 (2H, s), 7.57 (1H, s), 3.48 (2H, t), 3.09 (2H, t), 2.02 (2H, m); δ_C (CD$_3$CN, 125 MHz) 152.7, 148.1, 131.4 (q, J_{CF} = 27.5 Hz), 123.6 (q, J_{CF} = 225.0 Hz), 121.85, 115.0, 42.6, 26.9, 21.9; HRMS (ESI) calcd for C$_{12}$H$_{10}$F$_6$N$_2$S 329.0542, found 329.0549 (M + H);

Synthesis of Catalysts **10c** *and* **10d**

Catalysts **10c** and **10d** are known compounds and were synthesized according to known procedures.[38] Spectral data below is included for completeness.

2,3,6,7-tetrahydro-5H-thiazolo[3,2-a]pyrimidine (10c)
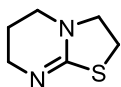
δ_H (CD$_3$CN, 600 MHz) 3.48 (2H, J = 7.2 Hz, t), 3.28 (1H, J = 5.4 Hz, t), 3.22 (2H, J = 6.0 Hz, t), 3.10 (2H, J = 6.6 Hz, t), 1.80 (2H, m); δ_C (CD$_3$CN, 125 MHz) 160.0, 54.3, 45.5, 45.1, 26.4, 21.2.

3,4-dihydro-2H-benzo[4,5]thiazolo[3,2-a]pyrimidine (10d)
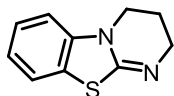
δ_H (CD$_3$CN, 600 MHz) 7.34 (1H, d), 7.23 (1H, td, J = 9.6, 0.6 Hz, 1H), 6.99 (1H, td, J = 9.0,

0.6 Hz, 1H), 6.84 (1H, J = 9.6 Hz), 3.78 (2H, t), 3.46 (2H, t), 1.97 (2H, m); δ_C (CD$_3$CN, 125

MHz) 157.3, 141.4, 126.1, 122.5, 121.9, 121.7, 107.5, 45.7, 42.3, 20.0.

Synthesis of Catalyst **12a**

LiAlH$_4$ (106 mg, 2.80 mmol) was added to an oven-dried round bottom flask and suspended

in dry Et$_2$O. Catalyst **12b** (225 mg, 1.12 mmol) was added to the slurry and the reaction

mixture was refluxed for 20 h under N$_2$. The reaction mixture was then cooled and placed on

ice. With stirring, 0.11 mL of H$_2$O was added slowly to the mixture followed by 0.22 mL of

10% NaOH and then 0.33 mL of H$_2$O to quench excess reducing agent. The mixture was

allowed to stir for ten minutes and then vacuum filtered. The filter cake was added to 25 mL

of stirring chloroform and heated to 40°C. The reaction mixture was allowed to stir for 10

minutes to dissolve the desired product. Following a second vacuum filtration, the filtrate

was collected and concentrated to yield the desired product.

1,3,4,6-tetrahydro-2H-pyrimido[2,1-b]quinazoline (12a)
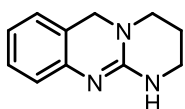
Yield 70%. δ_H (CD$_3$CN, 400 MHz) 6.97 (1H, J = 7.2 Hz, t), 6.83 (1H, J = 7.2 Hz, d), 6.67

(1H, J = 7.2 Hz, t), 6.57 (2H, J = 7.6 Hz, d), 4.24 (2H, s), 3.21 (1H, J = 5.6, t), 3.11 (1H, J =

6.0, t), 1.97 (2H, m); HRMS (ESI) calcd for C$_{11}$H$_{12}$N$_3$O 202.0976, found 202.0975 (M + H);

General Procedure for N-Acyl Homoserine Lactone (AHL) Synthesis

The C_4, C_6, and 3-oxo-C_{12} AHLs are known compounds and were synthesized following previously published procedures.[40–42]

_N_-Hexanolyl-L-homoserine Lactone (4)
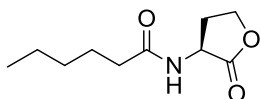
63.8% Yield; δ_H (DMSO-d$_6$, 500 MHz) 8.30 (1H, s), 4.49 (1H, m), 4.31 (1H, td, J_1 = 9.0 Hz, J_2 =1.5 Hz), 4.17 (1H, m), 2.35 (1H, m), 2.13-2.06 (3H, m), 1.47 (2H, m, J = 7.5 Hz), 1.26-1.21 (4H, m), 0.84 (3H, t, J = 7.0 Hz); δ_C (DMSO-d$_6$, 125 MHz) 175.9, 172.7, 65.7, 48.3, 35.5, 31.2, 28.7, 25.2, 22.3, 14.3; MS (ESI) calcd for $C_{10}H_{17}NO_3$: 200.13, found: 200.12 (M + H).

_N_-Butyryl-L-homoserine Lactone (2)
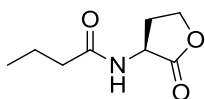
56.1% Yield; δ_H (DMSO-d$_6$, 500 MHz) 8.30 (1H, s), 4.51 (1H, m), 4.32 (1H, td, J_1 = 8.5 Hz, J_2 = 2.0 Hz), 4.18 (1H, m), 2.36 (1H, m), 2.14-2.05 (3H, m), 1.59 (2H, m, J = 7.5 Hz), 0.84 (3H, t, J = 7.5 Hz); δ_C (DMSO-d$_6$, 150 MHz) 175.3, 172.0, 65.1, 47.7, 36.9, 28.2, 18.5, 13.4; MS (ESI) calcd for $C_8H_{13}NO_3$: 172.10, found: 172.06 (M + H).

_N_-(3-Oxododecanolyl)-L-homoserine Lactone (1)
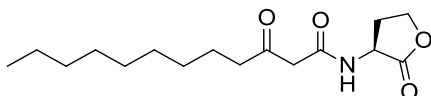
45.2% Yield; δ_H (CDCl$_3$, 600 MHz) 7.75 (1H, d, J = 6.6 Hz), 4.62 (1H, m), 4.48 (1H, td, J_1 = 9.0 Hz, J_2 = 1.2Hz), 4.29 (1H, m), 3.48 (2H, s), 2.73 (1H, m), 2.54 (2H, t, J = 7.2 Hz), 2.27 (1H, m), 1.58 (2H, p, J = 7.2 Hz), 1.31-1.26 (12H, m), 0.88 (3H, t, J = 6.6 Hz); δ_C (CDCl$_3$, 150 MHz) 206.5, 175.0, 166.6, 65.9, 49.0, 48.3, 43.8, 31.8, 29.6, 29.4, 29.3, 29.2, 29.0, 23.4, 22.7, 14.1; MS (ESI) calcd for C$_{16}$H$_{27}$NO$_4$: 298.20, found: 298.18 (M + H).

ii. Catalyst Screening by ^{1}H NMR

General Procedure for Catalytic Experiments by ^{1}H NMR

In a 4-mL scintillation vial, **4** (10.0 mg, 0.0502 mmol) and the thiourea/guanidinium catalyst being screened (0.00502 mmol) were combined. The catalyst and substrate were then dissolved in 1 mL of the deuterated solvent of choice. As an internal standard, 1,4-difluorobenzene (5.16 μL, 0.00502 mmol) was added to the reaction mixture. Piperidine (99.0 μL, 0.1004 mmol) was transferred into the vial and the reaction mixture was vortexed and quickly transferred to an NMR tube for analysis. ^{1}H NMR experiments were acquired in a sequence with a spectra being acquired between every 376 – 669 s depending on the experiment. The integration of the α-proton resonance of the lactone was monitored over time to track the conversion of starting material to product.

(S)-N-(4-hydroxy-1-oxo-1-(piperidin-1-yl)butan-2-yl)hexanamide (5)
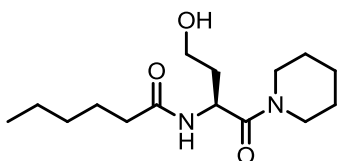
δ_H (CD$_3$CN-d$_3$, 500 MHz) 6.86 (1H, s), 4.92 (1H, m), 3.58 (1H, dd, J_1 = 2.5 Hz, J_2 = 5.0 Hz), 3.53-3.41 (6H, m), 2.21-2.17 (3H, m), 1.81 (1H, m), 1.62 (2H, m), 1.56 (4H, m), 1.50-1.45

(3H, m), 1.32-1.26 (4H, m), 0.88 (3H, t, J = 7.0 Hz); δ_C (CD$_3$CN-d$_3$, 125 MHz) 173.8, 170.0, 57.8, 46.4, 46,2, 43.0, 36.2, 36.0, 31.5, 26.4, 25.7, 25.6, 24.5, 22.5, 13.6; MS (ESI) calcd for C$_{15}$H$_{28}$N$_2$O$_3$: 285.22, found: 285.20 (M + H); Anal. Calc. for C$_{15}$H$_{28}$N$_2$O$_3$: C, 63.35; H, 9.92; N, 9.85; found: C, 63.34; H, 9.76; N, 9.80.

REFERENCES

1. Taylor, M. S. & Jacobsen, E. N. Asymmetric Catalysis by Chiral Hydrogen-Bond Donors. *Angewandte Chemie International Edition* **45**, 1520–1543 (2006).

2. Sigman, M. S. & Jacobsen, E. N. Schiff Base Catalysts for the Asymmetric Strecker Reaction Identified and Optimized from Parallel Synthetic Libraries. *Journal of the American Chemical Society* **120**, 4901–4902 (1998).

3. Vachal, P. & Jacobsen, E. N. Structure-Based Analysis and Optimization of a Highly Enantioselective Catalyst for the Strecker Reaction. *Journal of the American Chemical Society* **124**, 10012–10014 (2002).

4. Kelly, T. R. & Kim, M. H. Relative Binding Affinity of Carboxylate and Its Isosteres: Nitro, Phosphate, Phosphonate, Sulfonate, and .delta.-Lactone. *Journal of the American Chemical Society* **116**, 7072–7080 (1994).

5. Taylor, M. S. & Jacobsen, E. N. Highly Enantioselective Catalytic Acyl-Pictet−Spengler Reactions. *Journal of the American Chemical Society* **126**, 10558–10559 (2004).

6. Yoon, T. P. & Jacobsen, E. N. Highly Enantioselective Thiourea-Catalyzed Nitro-Mannich Reactions. *Angewandte Chemie International Edition* **44**, 466–468 (2005).

7. Han, B. *et al.* Discovery of Bifunctional Thiourea/Secondary-Amine Organocatalysts for the Highly Stereoselective Nitro-Mannich Reaction of α-Substituted Nitroacetates. *Chemistry - A European Journal* **14**, 8094–8097 (2008).

8. Wittkopp, A. & Schreiner, P. R. Metal-Free, Noncovalent Catalysis of Diels−Alder Reactions by Neutral Hydrogen Bond Donors in Organic Solvents and in Water. *Chemistry - A European Journal* **9**, 407–414 (2003).

9. Cao, C.-L., Ye, M.-C., Sun, X.-L. & Tang, Y. Pyrrolidine−Thiourea as a Bifunctional Organocatalyst: Highly Enantioselective Michael Addition of Cyclohexanone to Nitroolefins. *Organic Letters* **8**, 2901–2904 (2006).

10. Cao, Y.-J., Lai, Y.-Y., Wang, X., Li, Y.-J. & Xiao, W.-J. Michael Additions in Water of Ketones to Nitroolefins Catalyzed by Readily Tunable and Bifunctional Pyrrolidine—Thiourea Organocatalysts. *Tetrahedron Letters*, **48**, 21-24 (2007).

11. Okino, T., Hoashi, Y., Furukawa, T., Xu, X. & Takemoto, Y. Enantio- and Diastereoselective Michael Reaction of 1,3-Dicarbonyl Compounds to Nitroolefins Catalyzed by a Bifunctional Thiourea. *Journal of the American Chemical Society* **127**, 119–125 (2005).

12. Zuend, S. J. & Jacobsen, E. N. Mechanism of Amido-Thiourea Catalyzed Enantioselective Imine Hydrocyanation: Transition State Stabilization via Multiple Non-

Covalent Interactions. *Journal of the American Chemical Society* **131**, 15358–15374 (2009).

13. Dove, A. P., Pratt, R. C., Lohmeijer, B. G. G., Waymouth, R. M. & Hedrick, J. L. Thiourea-Based Bifunctional Organocatalysis: Supramolecular Recognition for Living Polymerization. *Journal of the American Chemical Society* **127**, 13798–13799 (2005).

14. Berkessel, A. *et al.* Structural optimization of thiourea-based bifunctional organocatalysts for the highly enantioselective dynamic kinetic resolution of azlactones. *Organic & Biomolecular Chemistry* **4**, 4319 (2006).

15. Berlinck, R. G. S., Trindade-Silva, A. E. & Santos, M. F. C. The chemistry and biology of organic guanidine derivatives. *Natural Product Reports* **29**, 1382 (2012).

16. Best, M. D., Tobey, S. L. & Anslyn, E. V. Abiotic guanidinium containing receptors for anionic species. *Coordination Chemistry Reviews* **240**, 3–15 (2003).

17. Guillén Schlippe, Y. V. & Hedstrom, L. A twisted base? The role of arginine in enzyme-catalyzed proton abstractions. *Archives of Biochemistry and Biophysics* **433**, 266–278 (2005).

18. Ghobril, C. *et al.* Structure-Reactivity Relationship Studies for Guanidine-Organocatalyzed Direct Intramolecular Aldolization of Ketoaldehydes. *ChemCatChem* **2**, 1573–1581 (2010).

19. Taylor, J. E., Bull, S. D. & Williams, J. M. J. Amidines, isothioureas, and guanidines as nucleophilic catalysts. *Chemical Society Reviews* **41**, 2109 (2012).

20. Fu, X. & Tan, C.-H. Mechanistic considerations of guanidine-catalyzed reactions. *Chemical Communications* **47**, 8210 (2011).

21. Pratt, R. C., Lohmeijer, B. G. G., Long, D. A., Waymouth, R. M. & Hedrick, J. L. Triazabicyclodecene: A Simple Bifunctional Organocatalyst for Acyl Transfer and Ring-Opening Polymerization of Cyclic Esters. *Journal of the American Chemical Society* **128**, 4556–4557 (2006).

22. Lohmeijer, B. G. G. *et al.* Guanidine and Amidine Organocatalysts for Ring-Opening Polymerization of Cyclic Esters. *Macromolecules* **39**, 8574–8583 (2006).

23. Simón, L. & Goodman, J. M. The Mechanism of TBD-Catalyzed Ring-Opening Polymerization of Cyclic Esters. *The Journal of Organic Chemistry* **72**, 9656–9662 (2007).

24. Chuma, A. *et al.* The Reaction Mechanism for the Organocatalytic Ring-Opening Polymerization of l-Lactide Using a Guanidine-Based Catalyst: Hydrogen-Bonded or Covalently Bound? *Journal of the American Chemical Society* **130**, 6749–6754 (2008).

25. Kiesewetter, M. K. *et al.* Cyclic Guanidine Organic Catalysts: What Is Magic About Triazabicyclodecene? *The Journal of Organic Chemistry* **74**, 9490–9496 (2009).

26. Kirsch, J. F. & Jencks, W. P. Base Catalysis of Imidazole Catalysis of Ester Hydrolysis. *Journal of the American Chemical Society* **86**, 833–837 (1964).

27. Jencks, W. P. & Carriuolo, J. Imidazole Catalysis: II. Acyl Transfer and the Reactions of Acetyl Imidazole with Water and Oxygen Anions. *Journal of Biological Chemistry* **234**, 1272–1279 (1959).

28. Gagliano, R. A., Knowlton, R. C. & Byers, L. D. Methylimidazole-catalyzed ester hydrolysis: nonlinear kinetics. *The Journal of Organic Chemistry* **54**, 5247–5250 (1989).

29. Brown, J. M., Conn, A. D., Pilcher, G., Leitão, M. L. P. & Meng-Yan, Y. On the strain energy of 5-ring and 6-ring lactones. *Journal of the Chemical Society, Chemical Communications* 1817 (1989).

30. Blay, G., Cardona, L., García, B., García, C. L. & Pedro, J. R. A non-catalyzed ring-opening aminolysis reaction of sesquiterpene lactones. *Tetrahedron Letters* **35**, 931–934 (1994).

31. Liu, W., Xu, D. D., Repič, O. & Blacklock, T. J. A mild method for ring-opening aminolysis of lactones. *Tetrahedron Letters* **42**, 2439–2441 (2001).

32. Bertucci, M. A., Lee, S. J. & Gagné, M. R. Thiourea-catalyzed aminolysis of N-acyl homoserine lactones. *Chemical Communications* **49**, 2055 (2013).

33. Lippert, K. M. *et al.* Hydrogen-Bonding Thiourea Organocatalysts: The Privileged 3,5-Bis(trifluoromethyl)phenyl Group. *European Journal of Organic Chemistry*, **30**, 5919-5927 (2012).

34. Zhang, W. & Shi, M. DBU catalyzed cyanoacylation of ketones with acyl cyanides. *Organic & Biomolecular Chemistry* **4**, 1671 (2006).

35. Price, K. E. *et al.* Mild and Efficient DBU-Catalyzed Amidation of Cyanoacetates. *Organic Letters* **11**, 2003–2006 (2009).

36. Kobayashi, M. & Okamoto, S. Unexpected reactivity of annulated 3H-benzothiazol-2-ylideneamines as an acyl transfer catalyst. *Tetrahedron Letters* **47**, 4347–4350 (2006).

37. Birman, V. B., Li, X. & Han, Z. Nonaromatic Amidine Derivatives as Acylation Catalysts. *Organic Letters* **9**, 37–40 (2007).

38. Joannesse, C. *et al.* Isothiourea-Mediated Asymmetric O- to C-Carboxyl Transfer of Oxazolyl Carbonates: Structure-Selectivity Profiles and Mechanistic Studies. *Chemistry - A European Journal* **18**, 2398–2408 (2012).

39. Pomini, A. M. & Marsaioli, A. J. Absolute Configuration and Antimicrobial Activity of Acylhomoserine Lactones. *Journal of Natural Products* **71**, 1032–1036 (2008).

40. Chhabra, S. *et al.*in *The Chemistry of Pheromones and Other Semiochemicals II* (Schulz, S.) **240**, 279–315 (Springer Berlin Heidelberg, 2005).

41. Chhabra, S. R. *et al.* Synthetic Analogues of the Bacterial Signal (Quorum Sensing) Molecule *N* -(3-Oxododecanoyl)- L -homoserine Lactone as Immune Modulators. *Journal of Medicinal Chemistry* **46**, 97–104 (2003).

CHAPTER III: HYDRAZINE MEDIATED TRANSAMIDATION OF 3-OXO-*N*-ACYL HOMOSERINE LACTONES

A. Introduction

i. Amines as Nucleophiles in Water

Reactions that employ amines as nucleophiles in water are central to all life processes. Enzyme-mediated amine additions, namely through acyl transfer reactions, are pervasive in cellular and molecular biology. Amide bond formation, the key linkage in protein biosynthesis, is achieved by the addition of the *N*-terminus of a tRNA-tethered amino acid via acyl transfer to a growing polypeptide chain.[1] Posttranslational modifications to histone lysine residues are mediated by a series of transferases that catalyze acyl transfer reactions of the amine side chain with their respective coenzymes. These modifications, such as lysine methylation, acetylation, and ubiquitination, have been shown to be critical for DNA processing and gene regulation while also being linked to a variety of human diseases.[2,3]
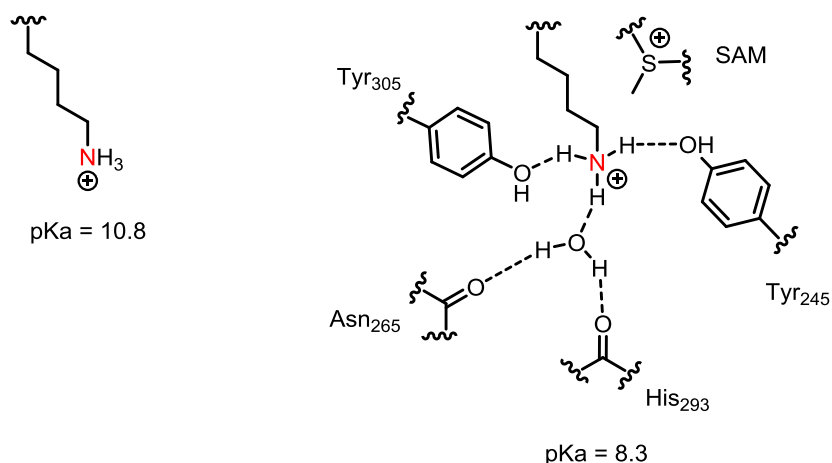
Figure 3.1. Comparison of lysine pKa values in solution and in the active site of histone lysine monomethyltransferase SET7/9. The presence of the sulfonium ion has been computationally demonstrated to effectively reduce lysine's pKa from 10.8 to 8.3. Participation of local amino acids in hydrogen bonding lysine resultantly increases its nucleophilicity and enables transfer of the methyl group to lysine from S-adenosylmethionine (SAM).[3,4]

Harnessing the nucleophilicity of amines for acyl transfer under physiological conditions in a non-enzymatic environment is not trivial. Part of the difficulty associated with achieving these transformations synthetically lies in the interdependence of nucleophilicity and basicity. In general, amines with higher pKa values are more nucleophilic. However, the basicity of the amines renders them almost fully protonated when well-solvated at physiological pH. The effective concentration of the neutral amine in solution resultantly decreases, attenuating its capacity to serve as a nucleophile.[5,6] In an enzyme, nucleophilicity is modulated by both the hydrophobicity of the catalytic site and the presence of ordered hydrogen bond networks, often forwarded by suppression in amine pKa.[7] (Figure 3.1). Thus, amine nucleophilicity in water is highly dependent on the amine selected and local environment in which the reaction proceeds.
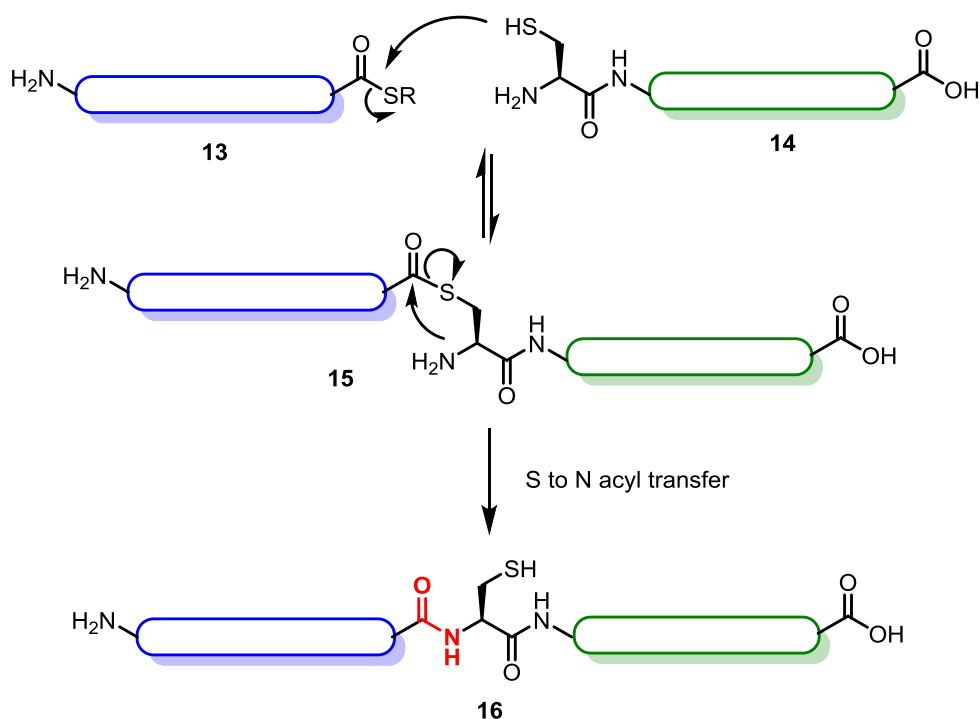
Figure 3.2. Amide bond formation by native chemical ligation.[8]

Despite this setback, synthetic chemists have developed methodologies to elicit amine

nucleophilicity for organic transformations in water. Intramolecular additions have proven to

be an effective strategy for promoting the reaction of amine nucleophiles despite the extant

equilibrium favoring the corresponding ammonium species. Installing such an element of

preorganization increases the effective concentration of the neutral amine at the electrophilic

site, thus decreasing entropic barriers to reaction. Such principles have been implemented to

advance synthesis of peptide sequences beyond fifty residues through the process of native

chemical ligation (NCL) (Figure 3.2).[8] Two peptide fragments, one containing a C-terminal

thioester fragment (**13**) and the other containing an N-terminal cysteine (**14**), react to form

the corresponding thioester (**15**). The formation of the thioester is rapid and reversible at

neutral pH. However, the pendant α-amino group of the cysteine is positioned to undergo an

intramolecular S$\rightarrow$N acyl transfer through a favorable five membered transition state. The

result is the ligation product (**16**) of the two shorter peptide fragments through the irreversible formation of a native peptide bond. NCL has been effectively employed to perform ligations on the time scale of hours at micromolar concentrations, with the amine of the N-terminal cysteine greater than 90% protonated at physiological pH.[9] Similar modes of exploiting amine nucleophilicity in water are present in the mechanisms of both expressed protein ligation and intein chemistry.[10,11]

The nucleophilicity of an amine in water is also altered by its neighboring atom. Influence of the α-effect, or the presence of an adjacent heteroatom containing at least one pair of non-bonded electrons to the nucleophilic site, enhances nucleophilicity without a significantly modifying basicity.[12,13] The adjacent lone pair of electrons destabilizes the ground state of the amine through electron repulsion, increasing its general reactivity.[14] The presence of the electron withdrawing heteroatom leads to greater desolvation of the unbonded electrons on nitrogen, enhancing its propensity for addition to an electrophile. Even when partially protonated at physiological pH, these amines still retain a high nucleophilicity parameter. Hydroxylamine and hydrazine are two such examples of amines influenced by the α-effect.[6]

ii. Applications of Hydrazine as a Nucleophile in Medicinal Chemistry and Chemical Biology

The enhanced nucleophilicity of hydrazine and hydroxylamine has become a valuable tool for both medicinal chemistry and chemical biology. Both amines react with aldehydes and ketones to form the corresponding hydrazone and oxime in water (Scheme 3.1). As aldehydes and ketones are absent from cell surfaces, hydrazone and oxime formation is an example of a bioorthogonal reaction or an organic transformation that proceeds without

interfering with biological processeses. Consequently, the chemoselective condensation can be employed *in vitro* and *in vivo* to selectively conjugate biomolecules, label cellular targets, and engineer immunotherapies.[15–18]
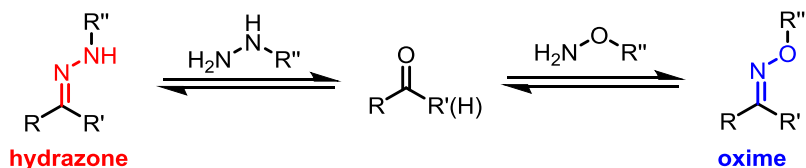
Scheme 3.1. Oxime and hydrazone formation in the presence of an aldehyde or ketone.

In a seminal work incorporating hydrazone formation into a biological setting for imaging, Heitzmann & Richards employed hydrazine functionalized biotin molecules as conjugates to membrane-bound glycoproteins for visualization of the cell membranes by electron microscopy.[19] More recently, hydrazinonicotinic acid has been employed for labeling cancer cells. Two notable examples include use of the hydrazine to conjugate RGD peptide derivatives, known for selectively binding α,β-integrins on cancerous cells, to ^{18}F radiolabels and ^{99m}Tc to VEGF, an overexpressed growth factor in tumors (Figure 3.3a).[20,21] Hydrazone formation for the incorporation of fluorescent tags has been similarly employed for visualizing biochemical pathways and binding events in both prokaryotic and eukaryotic cellular environments.[16,22–24]
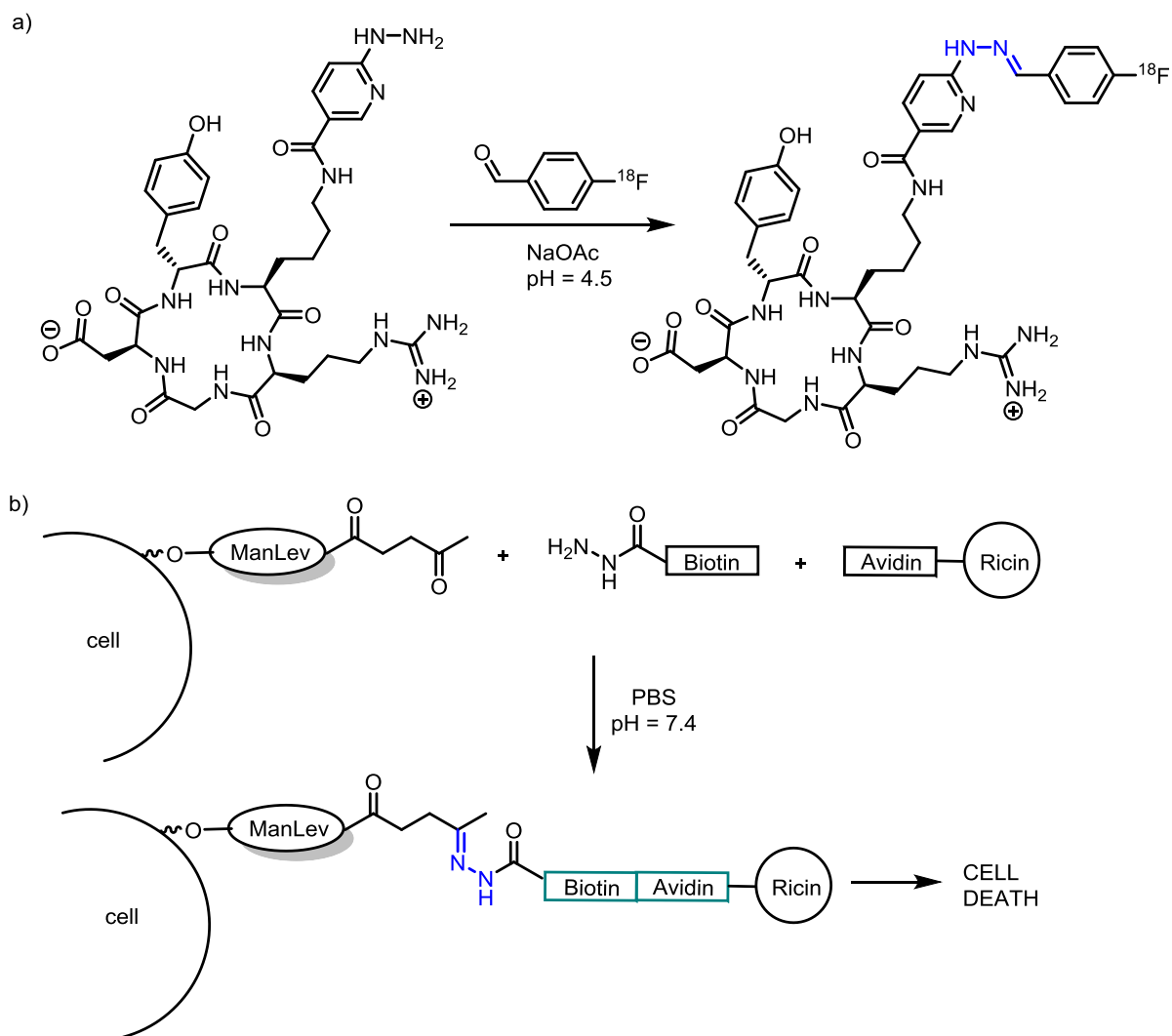
Figure 3.3. Select applications of hydrazone formation in medicinal chemistry and chemical biology. a) A radiolabeled RGDyK peptide conjugate is prepared by hydrazone formation (blue) between hydrazinonicotinic acid and an ^{18}F-functionalized benzaldehyde for *in vivo* tumor imaging.[20] b) Ricin toxin A is selectively conjugated to Jurkat cells presenting a ketone-functionalized ManLev derivative through hydrazone formation (blue), resulting in cell death.[25]

The chemoselectivity of the hydrazone ligation for biomolecular conjugation also allows for the engineered modification of cellular function (Figure 3.3b). This was demonstrated by Bertozzi and colleagues through use of a biotinylated hydrazide for recognition of manufactured ketone-containing *N*-Levulinoylmannosamine (ManLev) derivatives on T-lymphocytes. An avidin-ricin toxin conjugate was then introduced to bind

58

biotin for direct delivery of the toxin to the cell surface, leading to cell death in the sugar

presenting lymphocytes. These results demonstrated that use of hydrazine derived

conjugates can enable new strategies in drug delivery and stimulating immunological

recognition and response.[25]
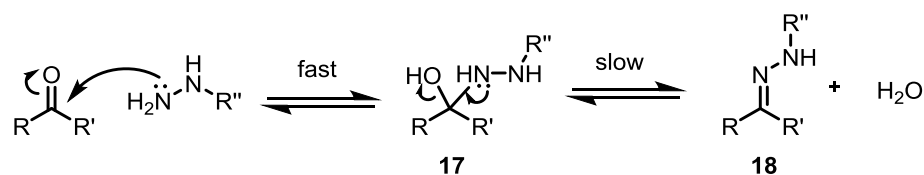
Scheme 3.2. Concerted mechanism of hydrazone formation. Protonation of the tetrahedral intermediate (**17**) under acidic conditions enhances leaving group ability (⁻OH vs. H_2O) and thus the rate of hydrazone formation (**18**).

While the application of the reactions is broad, oxime and hydrazone formation have

their innate limitations. Considering the mechanism of the reaction in conditions where

nucleophilic attack at the carbonyl carbon is fast, the rate-determining step is protonation of

the tetrahedral intermediate **17** to eliminate water and form the corresponding C=N

condensation product **18** (Scheme 3.2). Thus, both oxime and hydrazone formation are

accelerated under acidic conditions. This impedes the rates of the condensations at

physiological pH, requiring hours or even days to reach maximum conversion. As a result, a

large excess of either the amine or carbonyl are generally required at millimolar

concentrations for achieving practical rates of bioconjugation.[26] A study conducted by

Dirksen and Dawson compared the rates of both ligation reactions. Hydrazone formation

was shown to proceed at rates 20-fold faster than oxime formation, supporting the use of

hydrazines to reduce reaction times.[27] Further, phenylhydrazines were demonstrated to

undergo hydrazone formation more rapidly than aliphatic hydrazine derivatives.[28,29]

The poor kinetics of hydrazone and oxime formation were greatly improved when the

amenability of both reactions to nucleophilic catalysis by aniline was introduced by Dirksen

and Dawson in 2006. Peptide ligation rates were shown to improve more than 400 times that of the uncatalyzed reaction at physiological pH.[26,30] Since then, successive generations of aniline-based catalysts, including anthranilic acids, phosphonates, and phenylenediamines have been introduced to improve reaction rates, catalyst loadings, and catalyst solubility.[31–33] In most cases, superstoichimetric quantities of the catalyst are still necessary to afford significant increases in ligation rates. Crisalli and Kool offered an exception by optimizing the nucleophilic and electrophilic partners for hydrazone formation to eliminate the need of a nucleophilic catalyst. Through the use 2-carboxylphenylhydrazine (**19**) and quinoline-8-carboxaldehyde (**20**), greater than 90% hydrazone formation was achieved in under 2h at pH 7.4 (Scheme 3.3). These increased rates are attributed to both optimized electronics, specifically an electron poor aldehyde, and the presence of acidic and basic functionality to catalyze the breakdown of the formed tetrahedral intermediate.[28] While these rates are highly compatible for applications in chemical biology, the substrate specificities currently limit broad employment of the reactivity.
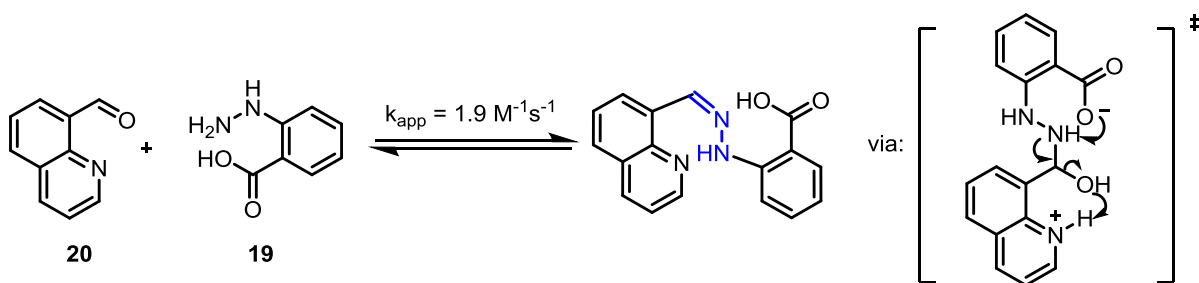
Scheme 3.3. Rapid hydrazone formation in the absence of aniline derivatives. The use of pyridyl and carboxyl groups intramolecularly catalyzes conversion from the tetrahedral intermediate to the hydrazone at rates greater than other common bioorthogonal reactions, such as strain-promoted azide-alkyne cycloadditions.[28]

Though great progress has been made in achieving rate enhancement, one underlying drawback of hydrazone and oxime formation is the reversibility of the ligation. Both

hydrazones and oximes have been experimentally proven to be more stable than simple imines, but are still prone to hydrolysis. The resultant ligation products have half-lives that vary from days to hours, making the chemistry less desirable when irreversible conjugations are required.[34] In the following chapter, a hydrazine-mediate method for the selective degradation of 3-oxo-AHLs is described. The irreversibility of the transformation and its ability to proceed in both acidic and neutral media has the potential to circumvent current drawbacks of hydrazone ligation while derivatizing a critical quorum sensing target.

B. Results and Discussion

i. Aminolysis of the AHL under Aqueous Conditions

In Chapter I, the ability to amidate the γ-butyrolactone of the AHL was demonstrated in organic solvents. To progress toward derivatization of the AHL in conditions more relevant to the natural environment of the autoinuducer, we sought to conduct the ring opening reaction under aqueous conditions. However, the nucleophile employed during our catalytic experiments, piperidine, has a pKa of 11.2. This renders the nucleophile inactive at physiological pH as it lies almost exclusively in its protonated form. As a result, the control reaction of piperidine and the C_6-AHL presented in Chapter I failed to proceed with identical amine and substrate concentrations in pH 7 buffer.

To identify amines capable of rapid aminolysis under aqueous conditions, a competitive screen of potential nucleophiles against the AHL was prepared. Further, the screen would enable the aminolysis rates to be compared to the background rate of lactone hydrolysis.[35] The selection of amines for the screen was focused to those with a pKa at or below that of piperidine (Table 3.1). Understanding the varied nucleophilicity of each of the amines, we hypothesized that the content of neutral amine present in solution would largely

dictate reactivity with the AHL.[36,37] A cocktail of amines was prepared by combining six amines in an equimolar ratio in PBS buffer. The pH of the solution was adjusted with HCl, and then combined with the autoinducer. The reaction progress was monitored by LC-MS, allowing for separation, identification, and relative quantification of the formed aminolysis products.

Table 3.1. Product masses in C_6-AHL aminolysis competitive screen.

Amine	Observed [M+H][a]	pKa[b]	Amine	Observed [M+H][a]	pKa[b]
H_3N^+–NH_2 (hydrazine)	232.1	8.1	NH_3^+ (propylamine)	-	10.7
HO–NH_2 (hydroxylamine)	233.1	6.0	NH_2 (aniline)	-	4.6
morpholine (NH_2^+)	-	8.4	imidazole–NH_2 (histamine)	-	5.0, 9.7
piperidine (NH_2^+)	-	11.2	H_2N–NH_3^+ (ethylenediamine)	260.1	6.9, 10.0
pyrrolidine (NH_2^+)	-	11.2	aziridine	-	7.9
azetidine (NH_2^+)	-	11.2	H_3N^+ ... O^-, HS (cysteine)	-	10.8
AHL hydrolysis (**21**)	218.2	-			

[a]reference to C_6-AHL (**5**) observed mass of 200.1 m/z [M+H]; [b]pKa's obtained from reported values

A series of aminolysis products were detected by mass spectrometry, proving our desired reactivity. Upon consumption of the AHL, products corresponding to the addition of hydrazine, hydroxylamine, and ethylenediamine to the AHL were observed, with the product corresponding to the addition of hydrazine having the greatest LC yield. Each of these amines has a pKa of 8.12 or lower, displaying the impact of protonation state on the amine's participation in the acyl transfer reaction. The effectiveness of hydrazine and hydroxylamine

can be attributed to enhanced nucleophilicity by the α-effect (see Introduction). At 20 eq. of

hydrazine, formation of the aminolysis product outcompeted background hydrolysis of the

AHL (**21**). This provides promise for using hydrazine to achieve more rapid degradation of

the autoinducer than the naturally imposed hydrolysis of the signaling molecule during its

extracellular transport.

Hydrazine, hydroxylamine, and ethylenediamine were all screened independently to

validate relative rates of conversion in the absence of the other amines contained in the initial

cocktail. Each proceeded with similar relative rates of conversion as observed in the

competitive screen, disproving any contribution by synergistic effects. As the competitive

screen was designed simply to identify the most effective amines for AHL aminolysis,

assessment of nucleophilicity beyond the three most readily detected was not pursued.

ii. Hydrazine-mediated Transamidation of 3-oxo-AHLs

As hydrazine proved to be the standout nucleophile from our aqueous competitive

screen, we sought to test it with the 3-oxo variant of the AHL. As displayed in the

competitive screens with the C_6-AHL, both aminolysis and hydrolysis of the lactone of the

autoinducer were expected to occur. However, the additional carbonyl functionality in this

AHL subfamily serves as a secondary site for nucleophilic attack to form the corresponding

hydrazone by condensation. Hydrazone formation would also uniquely position the α-amine

proximal to the N-acyl moiety of the AHL and we hypothesized that an additional lytic

pathway could be achieved in cleaving the amide bond (Scheme 3.4).
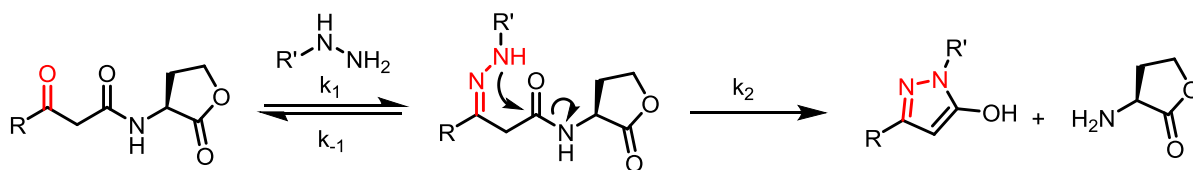
Scheme 3.4. Proposed route to 3-oxo-AHL amide cleavage through hydrazone formation and subsequent transamidation.

With multiple pathways of degradation identified, the 3-oxo-C$_8$-AHL (**22**) was synthesized as model substrate for screening due to its miscibility in water. The autoinducer was combined with 10 eq. of hydrazine buffered at pH 7 to determine the distribution of products by LC-MS. Upon consumption of the AHL, the major product generated had a mass of 155.1 m/z [M+H], indicating cleavage of the parent AHL structure (242.1 m/z [M+H]). The truncated mass was identified to be hydroxypyrazole **23**. The total mass chromatogram contained only trace amounts of both the aminolysis and hydrolysis product relative to the cleavage product, divulging that the observed transformation is both a novel and dominant pathway to reduce the active form of the autoinducer *in situ*.

Further modification of reaction conditions by decreasing the amine equivalents demonstrated that the hydroxypyrazole can be generated as the major product with only stoichiometric quantities of hydrazine. This is in contrast to the 20 eq. of hydrazine required for lactone aminolysis to out compete rates of background hydrolysis. Decreasing the pH of the reaction media to 4.5 to mitigate hydrolysis of the lactone allowed for exclusive formation of the hydroxypyrazole product (Figure 3.4). The reaction was replicated on a larger scale to allow for isolation and characterization of the hydroxypyrazole by ^{1}H and ^{13}C NMR.
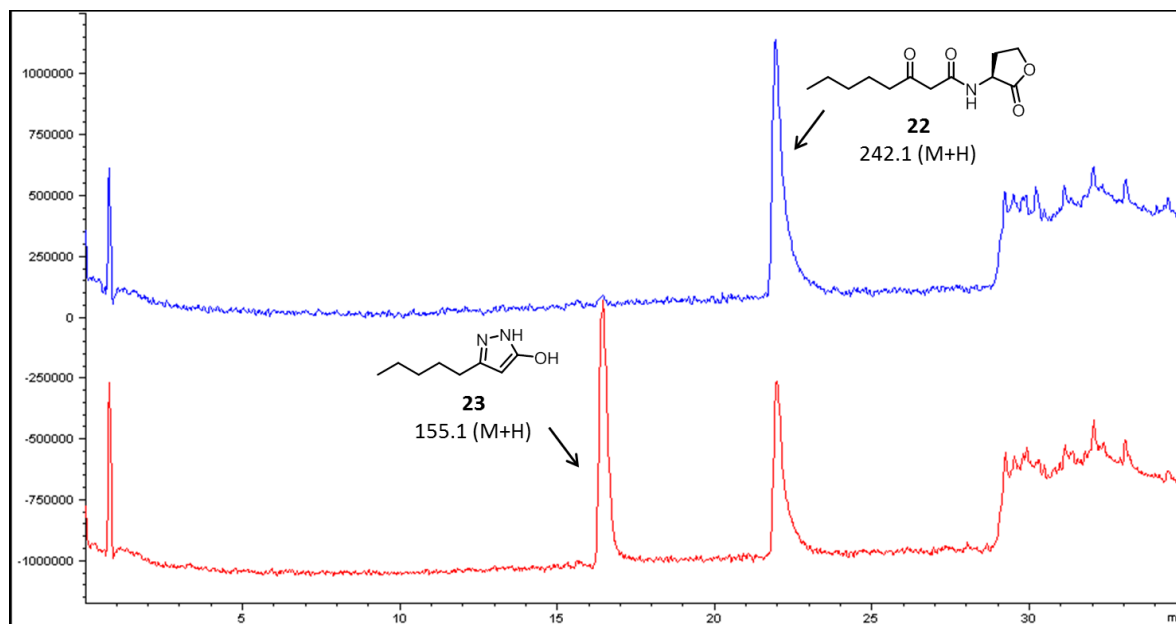
Figure 3.4. Total ion chromatogram of hydrazine-mediated AHL transamidation. The trace displays clean conversion of the 3-oxo-C_8 AHL (**22**) (1.0 mM) to the corresponding hydroxypyrazole (**23**) product at pH 4.5 in NaOAc buffer.

Recalling our initial hypothesis, condensation of hydrazine onto the 3-oxo-position of the AHL followed by transamidation through intramolecular cyclization presents a viable pathway for the generation of the 5-hydroxypyrazole product (Scheme 3.4). The predicted 5-membered cyclic transition state for nucleophilic attack is reminiscent of native chemical ligation, an already well-established method for amide bond formation under aqueous conditions. The aromaticity of the resultant pyrazole product likely provides an additional thermodynamic driving force to enable the observed AHL cleavage. The hydrazone (256.2 m/z [M+H]), which is the putative intermediate in the transformation, was only observed in trace amounts by LC-MS during the course of the reaction. The hydrazone was found to build up more significantly when substituted hydrazines (Section iv) and hydrazine-containing peptides were employed (Chapter IV).

iii. Reaction Selectivity and pH Dependence

As described in Chapter 1, the communication networks in gram-negative bacteria that are regulated by quorum sensing often employ identical *N*-acyl homoserine lactones across different species. In addition, multiple AHLs are often responsible for the regulation of gene expression in an individual species (Figure 1.3). A reaction that selectively modifies a single class of AHLs could give insight into the importance of a singular autoinducer in influencing a colony phenotype or permit selective inhibition of quorum-based communication in a multi-species environment. To determine the ability of hydrazine to selectively react with 3-oxo-AHLs in the presence of other AHLs, a competition experiment containing a representative member of each AHL structural subfamily was conducted. The C_6, 3-OH-C_8, and 3-oxo-C_8-AHLs were combined and subjected to a single equivalent of hydrazine at pH 4.5 (Figure 3.5). The reaction was monitored by HPLC and unambiguously demonstrated that the 3-oxo-C_8-AHL was the only species consumed amongst the other autoinducers. Accordingly, the resultant 5-hydroxypyrazole transamidation product was the only species to be amplified in the trace over time. This selective depletion of the 3-oxo-AHL supports the importance of hydrazone formation in the transamidation mechanism as the non-keto functionalized AHLs proved unreactive. The exclusive generation of the hydroxypyrazole also reinforces the kinetic dominance of the condensation-cyclization pathway compared to AHL modification by lactone aminolysis.
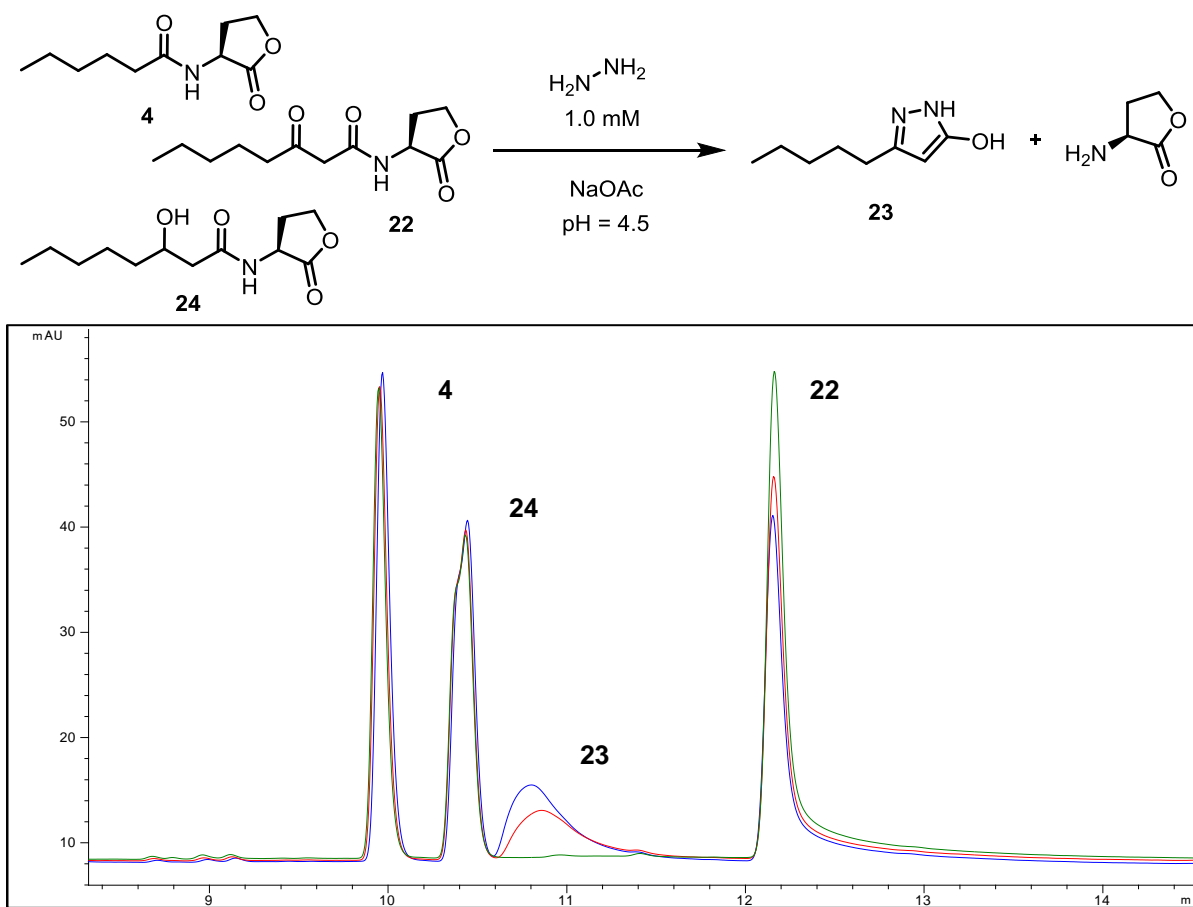
Figure 3.5. AHL selectivity in hydrazine-mediated transamidation. The 3-oxo-C$_8$-AHL (**22**) is cleaved in the presence of the 3-OH-C$_8$-AHL (**24**) and the C$_6$-AHL (**4**) to form hydroxypyrazole (**23**). The overlaid green, red, and blue lines on the HPLC trace represent injections made at 0 h, 14 h, and 44 h, respectively.

To investigate the impact of pH on the rate of transamidation, the 3-oxo-C$_8$ AHL was screened in a series of NaOAc and PBS buffers of variable pH. Four reactions were conducted from pH 4.5 to 7.4 with 5 eq. of hydrazine and monitored by HPLC. The autoinducer was converted to hydroxpyrazole most efficiently at pH 7.4, with a relative rate of AHL consumption that was almost five times the rate at pH 4.5 (Figure 3.6). Importantly, the background rates of AHL hydrolysis also increase with increased pH and significant hydrolysis product was observed at pH 7.4. Hence, we determined pH 6.5 to be an optimal pH for further reaction development.
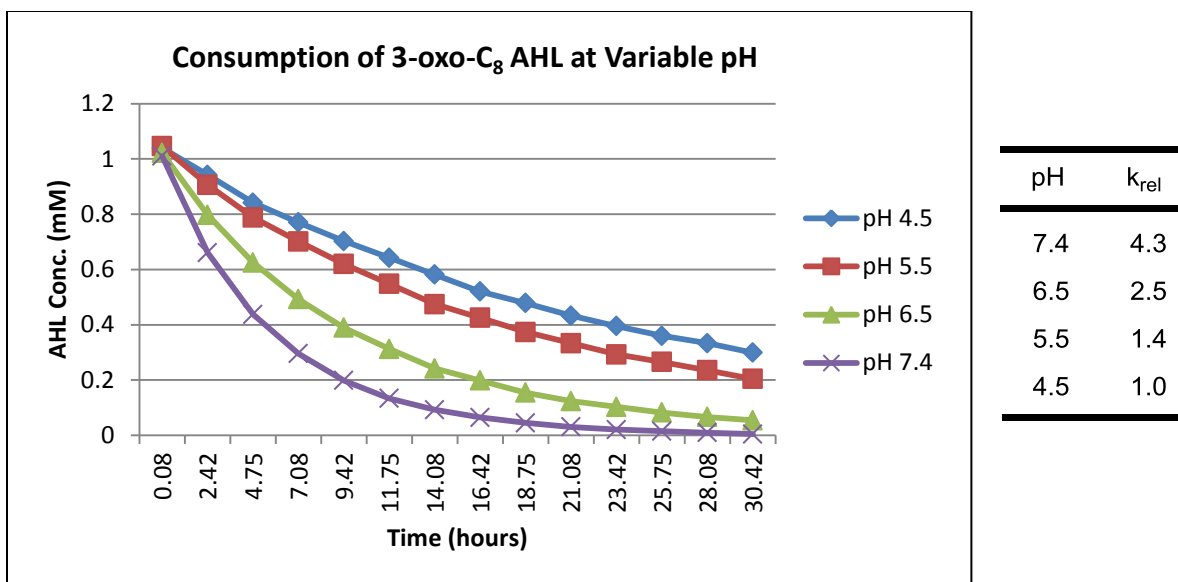
Figure 3.6. pH dependence on 3-oxo-C_8 AHL rates of consumption with hydrazine. Reaction progress was monitored by analytical HPLC at 210 nm with a 5:1 ratio of hydrazine to AHL.

By the known mechanism of hydrazone formation, the rate-determining step of the reaction is protonation of the tetrahedral intermediate. Consequently, hydrazone formation is known to be acid catalyzed (Figure 3.6). The reversal of the anticipated pH dependence on reaction rate distinguishes the contribution of both the condensation and cyclization to the kinetics of the reaction. Hydrazone formation slows as the solution becomes more basic, decreasing k_1 (Scheme 3.4). However, the effective concentration of the neutral α-amine of the hydrazone is greater at increased pH, enhancing its nucleophilicity. This increases the contribution of k_2 to the overall reaction, reflected in the increased rate of pyrazole formation at higher pH. Thus, it is reasonable that intramolecular attack of the amino imine onto the amide to yield the hydroxypyrazole is rate-determining in AHL transamidation.

iv. Reaction Scope

After characterizing the selectivity and pH dependence of the hydrazine-mediated 3-oxo-AHL transamidation reaction, a series of commercially available hydrazines were

screened to probe substituent effects on rate and reactivity. The selected hydrazines (Table

3.2) were tested individually in 5-fold excess in the presence of the 3-oxo-C_8 AHL at pH 6.5.

Table 3.2. Transamidation of the 3-oxo-C_8 AHL in the presence of hydrazine derivatives.

Entry	R	% Conversion at 30 h[a]	Entry	R	% Conversion at 30 h[a]
1	AHL hydrolysis	28.7	5	H₃C	60.2
2		36.9	6	HO	86.7
3		40.5	7	H	96.7
4		43.0	8		100

[a]Percent conversion determined by monitoring the integration of **22** over time on an analytical HPLC at 210nm
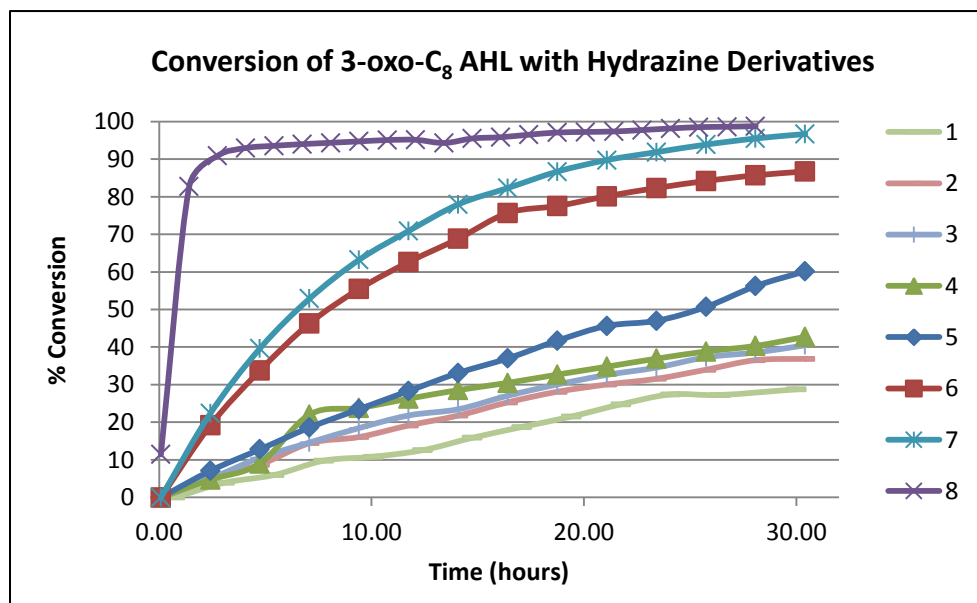
Figure 3.7. Percent conversion of the 3-oxo-C_8 AHL (**22**) in the presence of hydrazine derivatives. The numbers displayed in the legend correspond to the entries listed in Table 3.2.

The nature of the hydrazine employed had a significant impact on rate and the relative content of hydrazone and hydroxypyrazole product. Alkylated derivatives of hydrazine (Table 3.2, Entries 4-6) were noticeably less reactive with the AHL, but still possess the capability to cleave at the *N*-acyl moiety as the corresponding pyrazole fragment masses were detected by LC-MS. Rates also decreased with increased substituent size and pKa, factors that would expectedly attenuate amine nucleophilcity under aqueous conditions. Hydrazides (Table 3.2 , Entries 2-3), which are common functionalities chosen for hydrazone formation in bioorthogonal chemistry,[17,38] proved essentially unreactive with the autoinducers, yielding only trace amounts of the corresponding hydrazone. Failure of the hydrazides to cyclize can be attributed to the decreased nucleophilicity of the α-amine when in direct resonance with a carbonyl. Delocalization of the non-bonded α-amine electrons in stabilized amide resonance forms decreases the propensity for addition to the AHL.

By comparison, phenylhydrazine (Table 3.2, Entry 8) proved to be the most efficient hydrazine in derivatizing the AHL, reaching 82% conversion after 2.5 h. The rapid depletion of the AHL was driven by formation of the corresponding hydrazone, the dominant product detected by LC-MS. From 2.5 to 30 h, the concentration of the AHL steadily declined as the hydrazone proceeded to cyclize to the *N*-phenylhydroxypyrazole. Complete conversion of the AHL was obtained, proving that phenylhydrazone is a competent nucleophile for transamidation. Thus, the known increased ligation rates provided by phenylhydrazine translated to 3-oxo-AHL derivatization, while obviating the susceptibility of resultant hydrazone to hydrolysis by coupling its formation with an irreversible amide cleavage.[34]

C. Conclusions

To uncover new chemical strategies for *N*-acyl homoserine lactone functionalization under physiological conditions, the susceptibility of AHLs towards amine additions was probed in aqueous solutions. Aminolysis of the γ-butyrolactone was achieved by the employment of α-effect nucleophiles, such as hydroxylamine or hydrazine. With the proper excess of amine, the amidated product proved to be more kinetically favorable than AHL hydrolysis.

By strategically exploiting their unique β-ketoamide moiety, the first example of a non-enzymatic amide cleavage of 3-oxo-AHLs in aqueous media using hydrazine and hydrazine derivatives was reported. Through detection of transient hydrazone masses by LC-MS, we hypothesize that reversible association of the hydrazine to the AHL enables irreversible, intramolecular acyl transfer to form the observed hydroxylpyrazole product. The low activation energy of the 5-membered transition state for hydrazone cyclization coupled with the thermodynamic driving force provided by the aromaticity of the pyrazole product are each important in overcoming the high barrier for amide cleavage in water.

Hydrazine-mediated transamidation presents a new platform for the study and manipulation of quorum sensing pathways that contain 3-oxo-AHLs, such as in *P.aeruginosa*. The irreversible transformation proceeds most readily at physiological pH. Moreover, the selectivity of hydrazine for the 3-oxo-AHL was demonstrated in the presence of other known AHL substructures. This provides precedence for the use of hydrazine derivatives for the functionalization of the autoinducer in a multispecies environment and in quorum sensing circuits that employ multiple AHLs. As rates of transamidation are improved, the methodology could be an alternative route to quorum quenching by reducing

the extracellular concentration of the signaling molecule *in situ*. Our strategy to optimize the 3-oxo-AHL transamidation reaction through the generation of hydrazine-containing peptide libraries is discussed in Chapter IV.

D. Experimental

i. General Reagents and Synthesis

Commercial reagents and solvents, including hydrazine derivatives, were purchased from Sigma-Aldrich and Fisher Scientific. Hydrazine competition experiments were monitored on an Agilent 1200 Series LC-MS using a 2.7μM HALO C_{18} column. Reaction kinetics were monitored on an HP 1100 Series analytical HPLC/UV-Vis using a 2.7μM HALO C_{18} column at 210 nm. Hydroxypyrazole **23** was purified using a Waters semi-prep HPLC/UV-Vis with a Waters 4.2μM C_{18} column. Product characterization (^{1}H and ^{13}C) was completed on a 500 or 600 MHz Bruker NMR spectrometer. All related coupling constants are reported in Hertz and shifts in ppm. NMR solvents were purchased from Cambridge Isotopes Laboratories. High resolution mass spectra were obtained on an Agilent Accurate LC-TOF Mass Spectrometer (Agilent Series 6220) operating in positive ion mode with an electrospray ionization source (fragmentor = 175 V). The data was analyzed using an Agilent MassHunter Workstation Software, Qualitative Analysis (V. B.02.00).

General Procedure for the Characterization of Hydroxypyrazole Products

To a 20-mL scintillation vial, **22** (12.1 mg, 0.0501 mmol) was added to 10.0 mL of 200 mM PBS buffer at pH 7.4 and vortexed. The hydrazine derivative (0.250 mmol) was then added to the reaction mixture. The reaction was allowed to stir at RT and reaction progress was monitored by LC-MS. Upon complete conversion to the hydroxypyrazole product, the

reaction mixture was directly purified by semi-prep HPLC under neutral conditions. Separations were performed in a mobile phase of 20 to 50% B over 20 minutes where A = 100% water, 0.1% methanol and B = 100% acetonitrile. Products were then confirmed by HRMS and ^{1}H, ^{13}C NMR where possible. Several of the hydrazines screened did not progress to the corresponding hydroxypyrazole products by LC-MS (Table 3.2, Entries 2-4) and therefore could not be isolated for mass analysis.

3-pentyl-1H-pyrazol-5-ol
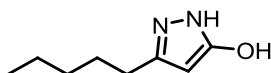
δ_H (DMSO-d$_6$, 600 MHz) 11.2 (1H, s), 9.26 (1H, s), 5.21 (1H, s), 2.41 (2H, t, J = 6.6 Hz), 1.52 (2H, p, J = 7.8 Hz), 1.29 (4H, m), 0.86 (3H, t J = 6.6 Hz); δ_C (DMSO-d$_6$, 150 MHz) 161.4, 144.7, 88.3, 31.3, 28.8, 26.1, 22.3, 14.4; HRMS (ESI) calcd for C$_8$H$_{14}$N$_2$O: 155.1179, found: 155.1181 (M + H).

1-methyl-3-pentyl-1H-pyrazol-5-ol
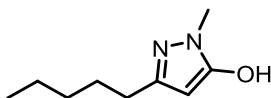
δ_H (DMSO-d$_6$, 600 MHz) 5.36 (1H, s), 3.48 (3H, s), 2.42 (2H, t, J = 6.0 Hz), 1.54 (2H, p, J = 7.2 Hz) 1.27 (4H, m), 0.86 (3H, t J = 7.2 Hz); δ_C (DMSO-d$_6$, 150 MHz) 150.5, 87.3, 32.6, 31.3, 28.5, 27.6, 22.3, 14.3; HRMS (ESI) calcd for C$_9$H$_{16}$N$_2$O: 169.1335, found: 169.1336 (M + H).

1-(2-hydroxyethyl)-3-pentyl-1H-pyrazol-5-ol
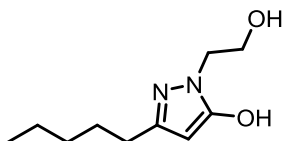
δ_H (DMSO-d_6, 600 MHz) 5.37 (1H, s), 3.88 (2H, t, $J = 6.0$ Hz), 3.63 (2H, t, $J = 6.0$ Hz), 2.43 (2H, t, $J = 7.8$ Hz), 1.54 (2H, p, $J = 7.2$ Hz) 1.30 (4H, m), 0.87 (3H, t, $J = 6.6$ Hz); δ_C (DMSO-d_6, 150 MHz) 150.5, 87.2, 59.5, 48.2, 31.3, 28.5, 27.6, 22.3, 14.3; HRMS (ESI) calcd for $C_{10}H_{18}N_2O_2$: 199.1441, found: 199.1446 (M + H).

3-pentyl-1-phenyl-1H-pyrazol-5-ol*
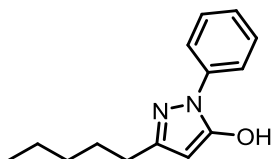
δ_H (DMSO-d_6, 600 MHz) 11.43 (1H, s), 7.71 (2H, d, $J = 7.8$ Hz), 7.42 (2H, t, $J = 7.8$ Hz), 7.21 (1H, t, $J = 7.2$ Hz), 5.38 (1H, s), 2.44 (2H, t, $J = 7.8$ Hz), 1.58 (2H, m), 1.32 (4H, m), 0.88 (3H, t); δ_C (DMSO-d_6, 150 MHz) 162.2, 153.4, 139.5, 129.2, 125.4, 121.0, 87.0, 31.5, 28.8, 25.8, 22.4, 14.4; HRMS (ESI) calcd for $C_{14}H_{18}N_2O$: 231.1492, found: 231.1495 (M + H). *the keto tautomer (minor) was also observed by NMR but only the resonances for the enol are reported.

General Procedure for N-Acyl Homoserine Lactone (AHL) Synthesis

The 3-OH-C_8 AHL and 3-oxo-C_8 AHL are known compounds and were synthesized following previously published procedures.[39,40]

N-(3-hydroxyoctanoyl)-L-homoserine Lactone (24)
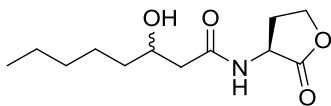
51.3% Yield (racemate); δ_H (CDCl$_3$, 600 MHz) 6.85-6.80 (1H, br d), 4.56 (1H, m), 4.47 (1H, m), 4.28 (1H, m), 4.00 (1H, br s), 3.38-3.31 (1H, br d), 2.76 (1H, m), 2.44 (1H, m), 2.33 (1H, m), 2.22 (1H, m), 1.43 (1H, m), 1.32 (2H, m), 1.29 (5H, m), 0.88 (3H, t); δ_C (CDCl$_3$, 150 MHz) 175.7, 173.0, 68.6, 66.2, 49.1, 42.6, 36.9, 31.9, 30.0, 25.1, 22.6, 14.0; MS (ESI) calcd for C$_{12}$H$_{21}$NO$_4$: 244.2, found: 244.2 (M + H).

N-(3-Oxooctanoyl)-L-homoserine Lactone (22)
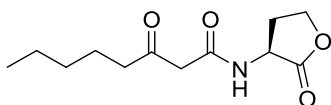
53.1% Yield; δ_H (CD$_3$CN, 500 MHz) 7.21 (1H, s), 4.48 (1H, m), 4.35 (1H, td, J_1 = 7.5 Hz, J_2 = 1.5 Hz), 4.20 (1H, m), 3.34 (2H, s), 2.50-2.46 (3H, m), 2.22 (1H, m), 1.52 (2H, p, J = 7.0 Hz), 1.31-1.20 (4H, m), 0.87 (3H, t, J = 7.0 Hz); δ_C (DMSO-d$_6$, 150 MHz) 210.0, 175.5, 166.7, 65.8, 50.7, 48.6, 42.3, 31.1, 28.7, 23.0, 22.4, 14.3; MS (ESI) calcd for C$_{12}$H$_{19}$NO$_4$: 242.1, found: 242.1 (M + H).

ii. Competition and Kinetics Experiments

Procedure for Amine Competition Experiment

In a 20-mL scintillation vial, hydrazine (3.16 μL, 100 μmol), hydroxylamine (6.13 μL, 50% v/v in water, 100 μmol), morpholine (3.16 μL, 100 μmol), piperidine (3.16 μL, 100 μmol), pyrrolidine (3.16 μL, 100 μmol), and azetidine (3.16 μL, 100 μmol) were combined and dissolved in 10.0 mL of PBS. While stirring, the pH of the amine cocktail was adjusted to 7.04 by titration with concentrated HCl. The C$_6$-AHL (**4**) (1.00 mg, 5.02 μmol) was then

added to the reaction mixture. The reaction was monitored by LC-MS with automated

injection every hour. Separations were performed in a mobile phase of 15% B over 12

minutes where A = 95:5 H_2O:acetonitrile, 0.1% formic acid and B = 0:100 water:acetonitrile,

0.1% formic acid. The presence and relative distribution of aminolysis products was

determined by comparing the integration of the total ion chromatogram (TIC) peaks

generated for each product. The same procedure was repeated for the other six amines

displayed in Table 3.1.

Procedure for AHL Competition Experiment

In a 20-mL scintillation vial, **4** (1.99 mg, 10.0 µmol), **24** (2.43 mg, 10.0 µmol), and **22** (2.41

mg, 10.0 µmol) were all combined and dissolved in 10.0 mL of NaOAc buffer at pH 4.5.

Hydrazine (0.32 µL, 10. µmol) was then added to the reaction mixture. The reaction progress

was monitored by analytical HPLC with automated injection every 40 minutes. Separations

were performed in a mobile phase of 25 to 45% B over 25 minutes where A = 95:5

water:acetonitrile and B = 0:100 water:acetonitrile. After 44 h, the products were analyzed

by LC-MS.

General Procedure for Comparative Kinetics (pH Dependence & Hydrazine Derivatives)

Stock solutions of both the 3-oxo-C_8 AHL (**22**) (2.0 mM) and the corresponding hydrazine

(100 mM) were prepared in distilled water and 400 mM PBS or NaOAc buffer, respectively.

The hydrazine was then diluted 10x in buffer to a final concentration of 10 mM. In a 2.0-mL

vial, 500 µL of both the AHL and hydrazine stock solutions were combined. The reaction

progress was monitored by analytical HPLC with automated injection every 160 minutes.

Separations were performed in a mobile phase of 30 to 50% B for phenylhydrazine and the hydrazide derivatives (Table 3.2, Entries 2, 3, and 8) and a mobile phase of 5 to 40% B over 22 minutes for the remaining hydrazines. Percent conversions were obtained by integration of the peak corresponding to the AHL after each injection with concentrations determined by a prepared standard curve. Products were analyzed by LC-MS.

REFERENCES

1. Pattabiraman, V. R. & Bode, J. W. Rethinking amide bond synthesis. *Nature* **480**, 471–479 (2011).

2. Fierz, B. & Muir, T. W. Chromatin as an expansive canvas for chemical biology. *Nature Chemical Biology* **8**, 417–427 (2012).

3. Smith, B. C. & Denu, J. M. Chemical mechanisms of histone lysine and arginine modifications. *Biochimica et Biophysica Acta (BBA) - Gene Regulatory Mechanisms* **1789**, 45–57 (2009).

4. Zhang, X. & Bruice, T. C. Enzymatic mechanism and product specificity of SET-domain protein lysine methyltransferases. *Proceedings of the National Academy of Sciences* **105**, 5728–5732 (2008).

5. Jencks, W. P., Haber, M. T., Herschlag, D. & Nazaretian, K. L. Decreasing reactivity with increasing nucleophile basicity. The effect of solvation on β_{nuc} for phosphoryl transfer to amines. *Journal of the American Chemical Society* **108**, 479–483 (1986).

6. Anslyn, E. V. *Modern physical organic chemistry*. (University Science, 2006).

7. Harris, T. K. & Turner, G. J. Structural Basis of Perturbed pKa Values of Catalytic Groups in Enzyme Active Sites. *IUBMB Life (International Union of Biochemistry and Molecular Biology: Life)* **53**, 85–98 (2002).

8. Hackenberger, C. P. R. & Schwarzer, D. Chemoselective Ligation and Modification Strategies for Peptides and Proteins. *Angewandte Chemie International Edition* **47**, 10030–10074 (2008).

9. Dawson, P. E. & Kent, S. B. H. Synthesis of Native Proteins by Chemical Ligation. *Annual Review of Biochemistry* **69**, 923–960 (2000).

10. Muir, T. W., Sondhi, D. & Cole, P. A. Expressed protein ligation: A general method for protein engineering. *Proceedings of the National Academy of Sciences* **95**, 6705–6710 (1998).

11. Shah, N. H. & Muir, T. W. Inteins: nature's gift to protein chemists. *Chemical Science* **5**, 446 (2014).

12. Jencks, W. P. & Carriuolo, J. General Base Catalysis of the Aminolysis of Phenyl Acetate. *Journal of the American Chemical Society* **82**, 675–681 (1960).

13. Edwards, J. O. & Pearson, R. G. The Factors Determining Nucleophilic Reactivities. *Journal of the American Chemical Society* **84**, 16–24 (1962).

14. Um, I.-H., Lee, E.-J., Seok, J.-A. & Kim, K.-H. The α-Effect in Reactions of sp-Hybridized Carbon Atom: Michael-Type Reactions of 1-Aryl-2-propyn-1-ones with Primary Amines. *The Journal of Organic Chemistry* **70**, 7530–7536 (2005).

15. Kalia, J. & Raines, R. Advances in Bioconjugation. *Current Organic Chemistry* **14**, 138–147 (2010).

16. Prescher, J. A. & Bertozzi, C. R. Chemistry in living systems. *Nature Chemical Biology* **1**, 13–21 (2005).

17. Sletten, E. M. & Bertozzi, C. R. Bioorthogonal Chemistry: Fishing for Selectivity in a Sea of Functionality. *Angewandte Chemie International Edition* **48**, 6974–6998 (2009).

18. Ulrich, S., Boturyn, D., Marra, A., Renaudet, O. & Dumy, P. Oxime Ligation: A Chemoselective Click-Type Reaction for Accessing Multifunctional Biomolecular Constructs. *Chemistry - A European Journal* **20**, 34-41 (2013).

19. Heitzmann, H. & Richards, F. M. Use of the Avidin-Biotin Complex for Specific Staining of Biological Membranes in Electron Microscopy. *Proceedings of the National Academy of Sciences* **71**, 3537–3541 (1974).

20. Lee, Y.-S. *et al.* An improved method of 18F peptide labeling: hydrazone formation with HYNIC-conjugated c(RGDyK). *Nuclear Medicine and Biology* **33**, 677–683 (2006).

21. Surfraz, M. B.-U., King, R., Mather, S. J., Biagini, S. C. G. & Blower, P. J. Trifluoroacetyl-HYNIC Peptides: Synthesis and ^{99m}Tc Radiolabeling. *Journal of Medicinal Chemistry* **50**, 1418–1422 (2007).

22. Chen, I., Howarth, M., Lin, W. & Ting, A. Y. Site-specific labeling of cell surface proteins with biophysical probes using biotin ligase. *Nature Methods* **2**, 99–104 (2005).

23. Iyer, G. *et al.* Aromatic Aldehyde and Hydrazine Activated Peptide Coated Quantum Dots for Easy Bioconjugation and Live Cell Imaging. *Bioconjugate Chemistry* **22**, 1006–1011 (2011).

24. Rayo, J., Amara, N., Krief, P. & Meijler, M. M. Live Cell Labeling of Native Intracellular Bacterial Receptors Using Aniline-Catalyzed Oxime Ligation. *Journal of the American Chemical Society* **133**, 7469–7475 (2011).

25. Mahal, L. K., *et al.* Engineering Chemical Reactivity on Cell Surfaces Through Oligosaccharide Biosynthesis. *Science* **276**, 1125–1128 (1997).

26. Dirksen, A., Hackeng, T. M. & Dawson, P. E. Nucleophilic Catalysis of Oxime Ligation. *Angewandte Chemie International Edition* **45**, 7581–7584 (2006).

27. Dirksen, A. & Dawson, P. E. Rapid Oxime and Hydrazone Ligations with Aromatic Aldehydes for Biomolecular Labeling. *Bioconjugate Chemistry* **19**, 2543–2548 (2008).

28. Kool, E. T., Park, D.-H. & Crisalli, P. Fast Hydrazone Reactants: Electronic and Acid/Base Effects Strongly Influence Rate at Biological pH. *Journal of the American Chemical Society* **135**, 17663-17666, (2013).

29. Dirksen, A., Yegneswaran, S. & Dawson, P. E. Bisaryl Hydrazones as Exchangeable Biocompatible Linkers. *Angewandte Chemie International Edition* **49**, 2023–2027 (2010).

30. Dirksen, A., Dirksen, S., Hackeng, T. M. & Dawson, P. E. Nucleophilic Catalysis of Hydrazone Formation and Transimination: Implications for Dynamic Covalent Chemistry. *Journal of the American Chemical Society* **128**, 15602–15603 (2006).

31. Crisalli, P. & Kool, E. T. Water-Soluble Organocatalysts for Hydrazone and Oxime Formation. *The Journal of Organic Chemistry* **78**, 1184–1189 (2013).

32. Rashidian, M. *et al.* A Highly Efficient Catalyst for Oxime Ligation and Hydrazone–Oxime Exchange Suitable for Bioconjugation. *Bioconjugate Chemistry* **24**, 333–342 (2013).

33. Wendeler, M., Grinberg, L., Wang, X., Dawson, P. E. & Baca, M. Enhanced Catalysis of Oxime-Based Bioconjugations by Substituted Anilines. *Bioconjugate Chemistry* 25, 93-101, (2013).

34. Kalia, J. & Raines, R. T. Hydrolytic Stability of Hydrazones and Oximes. *Angewandte Chemie International Edition* **47**, 7523–7526 (2008).

35. Yates, E. A. *et al.* N-Acylhomoserine Lactones Undergo Lactonolysis in a pH-, Temperature-, and Acyl Chain Length-Dependent Manner during Growth of Yersinia pseudotuberculosis and Pseudomonas aeruginosa. *Infection and Immunity* **70**, 5635–5646 (2002).

36. Mayr, H. & Ofial, A. R. Do general nucleophilicity scales exist? *Journal of Physical Organic Chemistry* **21**, 584–595 (2008).

37. Brotzel, F., Chu, Y. C. & Mayr, H. Nucleophilicities of Primary and Secondary Amines in Water. *The Journal of Organic Chemistry* **72**, 3679–3688 (2007).

38. Eldridge, G. M. & Weiss, G. A. Hydrazide Reactive Peptide Tags for Site-Specific Protein Labeling. *Bioconjugate Chemistry* **22**, 2143–2153 (2011).

39. Chhabra, S. R. *et al.* Synthetic Analogues of the Bacterial Signal (Quorum Sensing) Molecule *N* -(3-Oxododecanoyl)- L -homoserine Lactone as Immune Modulators. *Journal of Medicinal Chemistry* **46**, 97–104 (2003).

40. Chhabra, S. R. *et al.* Autoregulation of carbapenem biosynthesis in Erwinia carotovora by analogues of N-(3-oxohexanoyl)-L-homoserine lactone. *The Journal of Antibiotics* **46**, 441–454 (1993).

CHAPTER IV: DEVELOPMENT OF HYDRAZINE-CONTAINING PEPTIDES FOR 3-OXO-AHL DERIVATIZATION THROUGH COMBINATORIAL METHODS

A. Introduction

i. Synthetic Peptides as Enzyme Mimics

Enzymes are the envy of the synthetic chemist. Their exquisite selectivity and efficiency in carrying out chemical transformations is of the highest standard, with single molecule affinities and rates reaching greater than 10^9 that of the uncatalyzed reaction.[1] Thus, efforts to recreate enzymatic activity via synthetic mimics have been undertaken to better understand the chemical basis of enzyme function and to harness their reactivity to advance organic transformations and intervene in biological processes.[2] The diversity of functional enzyme mimics includes small molecule catalysts (Chapter II), macromolecular assemblies,[3] and catalytic antibodies.[4]

At the core of enzyme catalysis is the sequence of amino acids that promotes the observed enzyme function. The connectivity and spatial arrangement of the amino acids advantageously presents the corresponding functional groups to mediate substrate binding and modification. The resultant enzyme active site is a coordinated array of covalent and non-covalent interactions, such as hydrogen bonding, ion pairing, acylation, and proton transfer.[5] Despite the size and complexity of enzymes, only a few of the amino acid residues are active participants in catalysis, inspiring chemists to consider minimalist structures to afford comparable reactivity. Synthesizing peptides, or short sequences of amino acids

ranging from 2 – 50 residues in length, has become a strategy for reconstituting these interactions.[6]
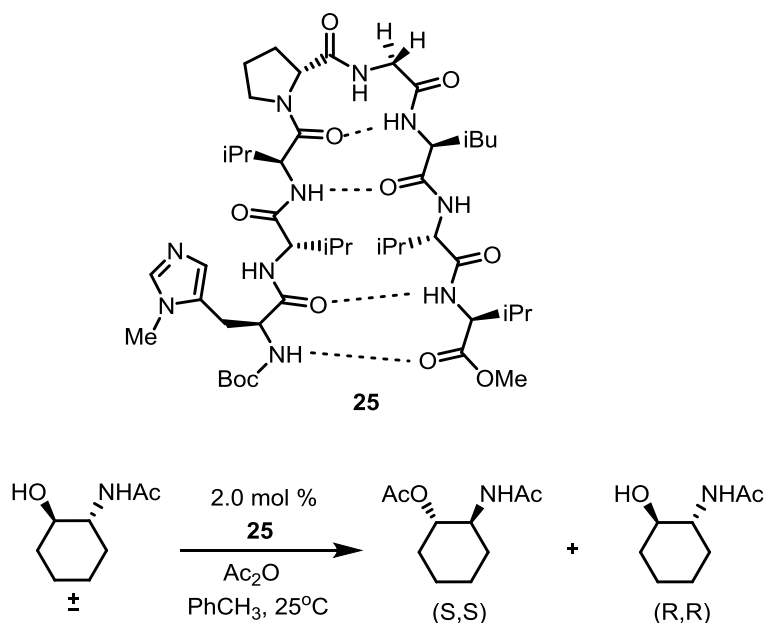
Scheme 4.1. Kinetic resolution of secondary alcohols by Miller's octapeptide **25**. The rigidity of the β-hairpin of the peptide's secondary structure along with the diversity of its primary sequence has been demonstrated to lead to the increase acylation rates of the (S,S) enantiomer.

In organic solvents, peptides have been employed as asymmetric catalysts to enhance rates and selectivity of several well-known organic transformations, such as Aldol reactions, Michael additions, and oxidations.[6,7] The use of *N*-methylhistidine-containing β-hairpin mimics for acyl transfer catalysis was realized by Miller and colleagues, in the kinetic resolution of secondary alcohols (Scheme 4.1). Through the comparison of both tetra- and octapeptide derivatives, increased sequence length improved the rigidity of the catalyst, realized in a 50-fold enhancement in selectivity. This selectivity was attenuated in Pro-AIB and stapled β-hairpin analogs, displaying the importance of the peptide secondary structure and cross-strand hydrogen bonding for the preferential acylation of the (S,S) enantiomer.[8,9]

Derivatives of the *N*-methylhistidine catalysts provided similar enzyme-like substrate-peptide interactions for site-specific acylation reactions and alcohol desymmetrizations.[10–12]

Peptide: YKLLKELLAKLKWLLEKLLGPTCL-NH$_2$
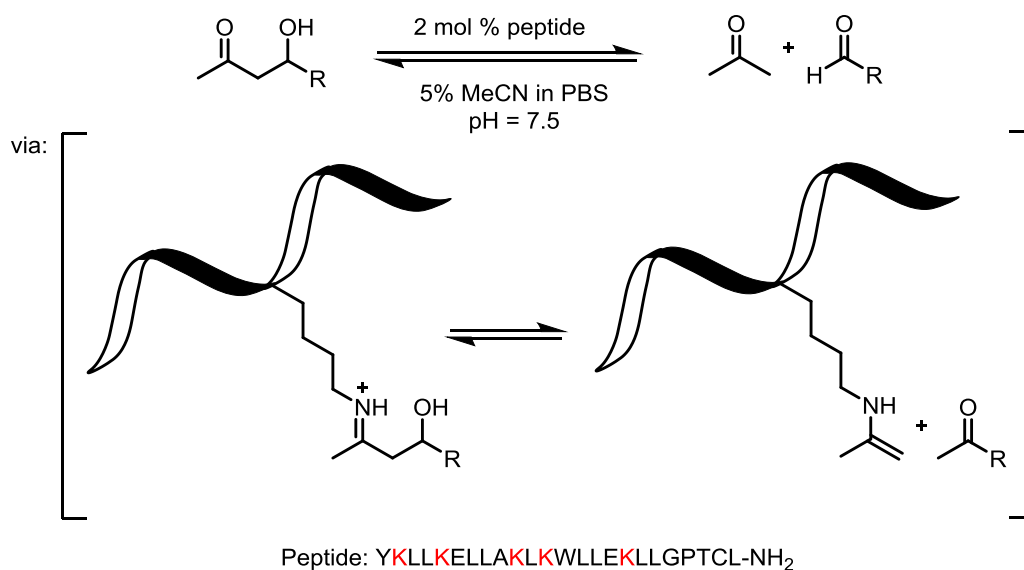
Scheme 4.2. Peptide enzyme mimics for retro-aldol additions by lysine-mediated imine formation. In a study conducted by Tanaka *et al.*, the displayed poly-lysine sequence provided the greatest aldolase activity.[13]

The non-covalent interactions critical to peptide folding are amplified when in organic solvents, providing an advantage in decreasing peptide length while still observing appreciable rate accelerations and product selectivity. Employing synthetic peptides in aqueous media often requires larger or uniquely well-folded peptide assemblies due to the presence of competitive solvent interactions.[14] However, several efficient constructs have still proven quite successful in replicating nucleophilic enzyme-like pathways. Baltzer and coworkers designed a helix-loop-helix dimer capable of accelerated p-nitrophenyl ester hydrolysis up to three orders of magnitude greater than the non-peptide acyl transfer catalyst *N*-methylimidazole. The reactivity of the dimer was attributed to a cooperative general acid and nucleophilic catalysis by two neighboring histidine residues.[15] A second generation of

the peptide improved hydrolysis rates by the incorporation of arginine residues to promote stabilization of the developing negative charge of the *N*-acyl histidine species.[16]

Barbas and coworkers employed a 24-residue poly-lysine peptide sequence to mimic aldolase activity through imine formation.[13] Peptides that contained greater helical content achieved rates up to 1900 times greater than the uncatalyzed reaction, rationalized by formation of an amphipathic surface leading to an increase in lysine nucleophilicity (Scheme 4.2). Using the known structures of the miniature proteins, Allemann and colleagues have rationally engineered catalysts that elicit esterase and decarboxylase-like activity.[17,18] In the esterase study, site-specific incorporation of two histidine residues on the α-helical portion of bovine pancreatic polypeptide create a catalytic HisH$^+$-His motif for p-nitrophenyl fumarate cleavage (Scheme 4.3). The assembled "active site" was proven to be further supported by ionic interactions of neighboring aspartic acid and arginine residues, displaying enzyme-like behavior even on a solvent-exposed surface.
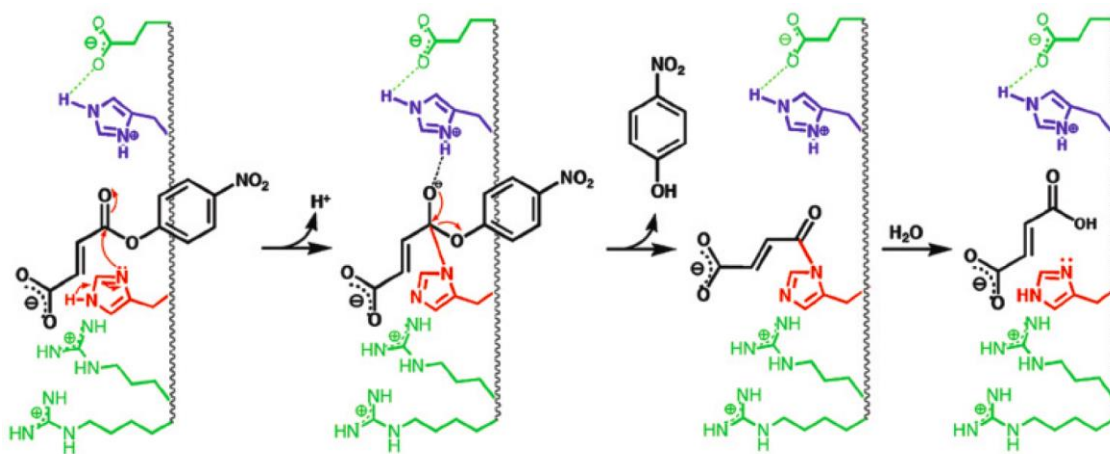
Scheme 4.3. Miniature proteins for ester hydrolysis. Hypothesized mechanism of esterase activity of a dihistidine modified bovine pancreatic peptide displaying the functional coordination of ionic and hydrogen boding interactions in hydrolysis of nitrophenyl esters. Adapted from Nicoll and Allemann.[18]

Our approach is to channel the enzyme-like characteristics of peptides to develop a hydrazine-containing peptide for rapid 3-oxo-AHL transamidation (Chapter III). The peptide would serve as a biologically relevant scaffold to reduce the concentration of the active autoinducer, inhibiting the bacterial quorum sensing mechanism. By establishing a productive network of non-covalent interactions, we hypothesize that the peptide could increase rates of transamidation though such mechanisms as enhancing the nucleophilicity of the hydrazine moiety or promoting localization of the AHL to the reactive surface (Figure 4.1). As the required sequence and structure for attaining the envisioned active site is difficult to rationally predict, we chose to employ combinatorial chemistry to design and identify our target peptides.
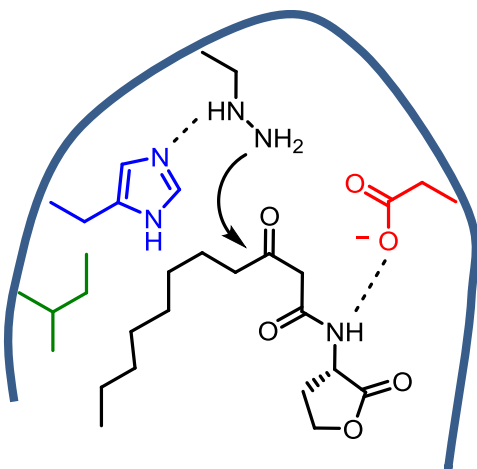
Figure 4.1. Peptide enzyme mimics for AHL transamidation. The hypothetical active site displays how non-covalent interactions could advance the 3-oxo-AHL transamidation. The presence of lipophilic (green), anion (red), and basic (blue), and other residues along the peptide scaffold could aid in AHL localization and enhancing the reactivity of the hydrazine or ketone.

ii. Methods of Combinatorial Synthesis and Screening of Peptide Libraries

Beyond their structural parallels, peptides are attractive candidates for the development of enzyme mimics due their facile and robust synthesis. In addition, they offer an immense diversity of sequence space that can be probed using both natural and unnatural

amino acids. To take advantage of these two characteristics, such peptides are often

synthesized in library format using combinatorial methods and then screened in a high-

throughput fashion to probe the reactivity of the peptide with the target substrate.
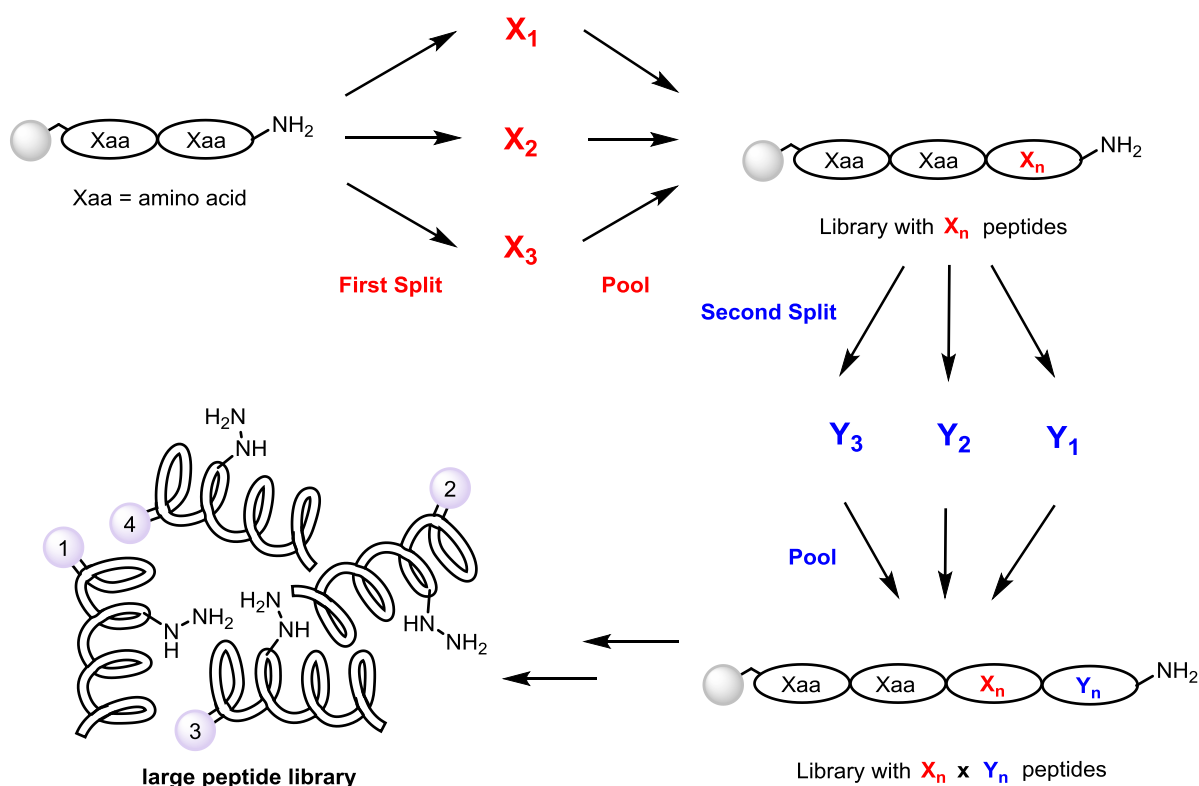
Figure 4.2. Split and pool synthesis of peptide libraries. Variable residues (X and Y) can be natural or unnatural amino acids introduced to increase library diversity.

Split and pool synthesis is one widely used strategy for the rapid construction large

peptide libraries (Figure 4.2).[19,20] The technique is derived from the universally employed

Merrifield method for solid-phase peptide synthesis (SPPS) that allows for the stepwise

construction of amino acid sequences on a polymeric resin or bead.[21,22] With the peptides

bound to the solid support, the resin can be apportioned at any point during the synthesis into

separate reaction vessels, allowing for the introduction of variable amino acids into the

sequence. After coupling, the beads are pooled into a single reaction vessel, generating a

library with a size equal to the number of variable residues incorporated. Subsequent

splitting, coupling, and pooling of the beads allows for a multiplicative increase in the size of the peptide library with minimal synthetic effort. Despite repeated separation and recombination of the resin, each bead retains up to 10^{13} copies of a single peptide sequence, also known as the one-bead-one-compound (OBOC) concept. Consequently, an entire library of peptides can then be screened while assessing the reactivity of just a single library member.[23]
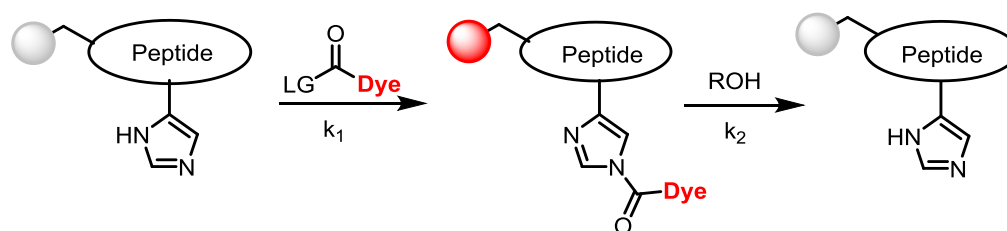
Scheme 4.4. Reactive tagging strategy for colorimetric identification of peptides for acyl transfer catalysis. Covalent attachment and removal of the dye from the peptide through the formed N-acyl intermediate colorizes (k_1) and decolorizes (k_2) the resin. The beads that most rapidly change color were resynthesized for solution phase screening for acyl transfer catalysts. Assay developed by Bezer *et al.*[24]

High-throughput screening strategies are utilized in conjunction with split and pool synthesis for efficient identification of the most reactive sequences or "hits" in a given OBOC peptide library. Colorimetric reactive tagging assays have become a valuable tool for the completion of such screens as the selected sequences can be identified by a color change in the resin. Covalent capture of a dye-tagged substrate has been employed in identifying peptides for small molecule catalysis in acyl transfer reactions,[25–27] aldol additions,[28] and oxime-based protein bioconjugations[29]. The Gagné and Waters groups have recently employed the strategy for the identification of histidine-containing peptides for acyl transfer catalysis.[24] Disperse red functionalized activated esters were synthesized and reacted with solid phase helical peptide libraries to monitor rates of acylation and deacylation at the histidine residue. The peptides capable of rapid acylation (k_1) colorized most readily while

88

those susceptible to deacylation (k_2) quickly decolored in the presence of a weak nucleophile (ROH) (Scheme 4.4). Through optimization of a hit obtained in the k_1 screen, the assay proved fruitful in identifying a catalyst displaying a rate of acyl transfer 2800 times the background reaction in solution.
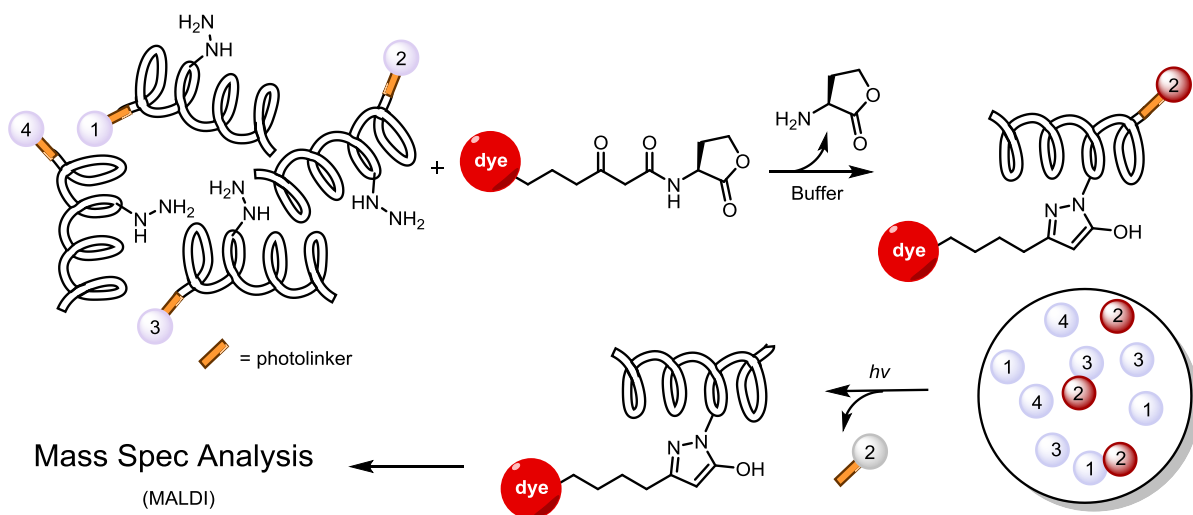
Figure 4.3. Reactive tagging scheme for identifying hydrazine-containing peptides for AHL transamidation.

We envision that a similar method can be employed for the high-throughput screening of hydrazine-containing peptides for AHL derivatization (Figure 4.3). The peptide libraries will be constructed using split and pool synthesis, with the inclusion of a photolabile linker between the resin and the peptide sequence to allow for light-mediated cleavage of the peptide from the solid support. By development of a dye-tagged AHL, the substrate can then be screened with the peptide library, leading to a color change upon the reaction of the peptide and the autoinducer. The darkest colored beads will then be manually selected and cleaved from the resin under UV light. The liberated peptide "hits" can then be identified by MALDI-MS. The designed library screening protocol allows for visual identification of the most reactive peptides for AHL transamidation. Upon determining peptides capable of the

89

transformation, their structure and sequence can then be analyzed to deduce important amino acids and through-space interactions that afford the observed reactivity.

B. Results and Discussion

i. Preparation of Hydrazine-Containing Peptides

To successfully generate peptide libraries for screening in our proposed reactive tagging assay, a method for facile incorporation of hydrazine into a peptide sequence needed to be developed. Inspired by the widespread use of thiol additions to maleimides in bioconjugation chemistry[30–32], we sought to determine if conjugate addition to an unnatural maleimide residue would be viable for rapid installation of hydrazine. A series of test peptides (**26a, 26b, 26c**) were synthesized with 3-maleimidopropionic acid included at the N-terminal residue of each sequence (Figure 4.4a). While on solid support, the peptides were then shaken in a 2% v/v solution of hydrazine in DMF. Upon cleaving the peptides from resin, a mass corresponding to the desired succinimoyl-hydrazine (**27**) was detected by MALDI-MS. However, two other masses corresponding to a second addition of hydrazine to the maleimide (**28**) and complete cleavage of the maleimide residue from the sequence (**29**) were also observed (Figure 4.4b). Stepwise optimization of the conjugate addition, including decreasing hydrazine equivalence, decreasing reaction times, and altering the solvent, were made in order to disfavor the propensity of the nucleophile for overaddition. The presence of both side products was greatly reduced through use of 1% v/v solution of hydrazine in ethanol.
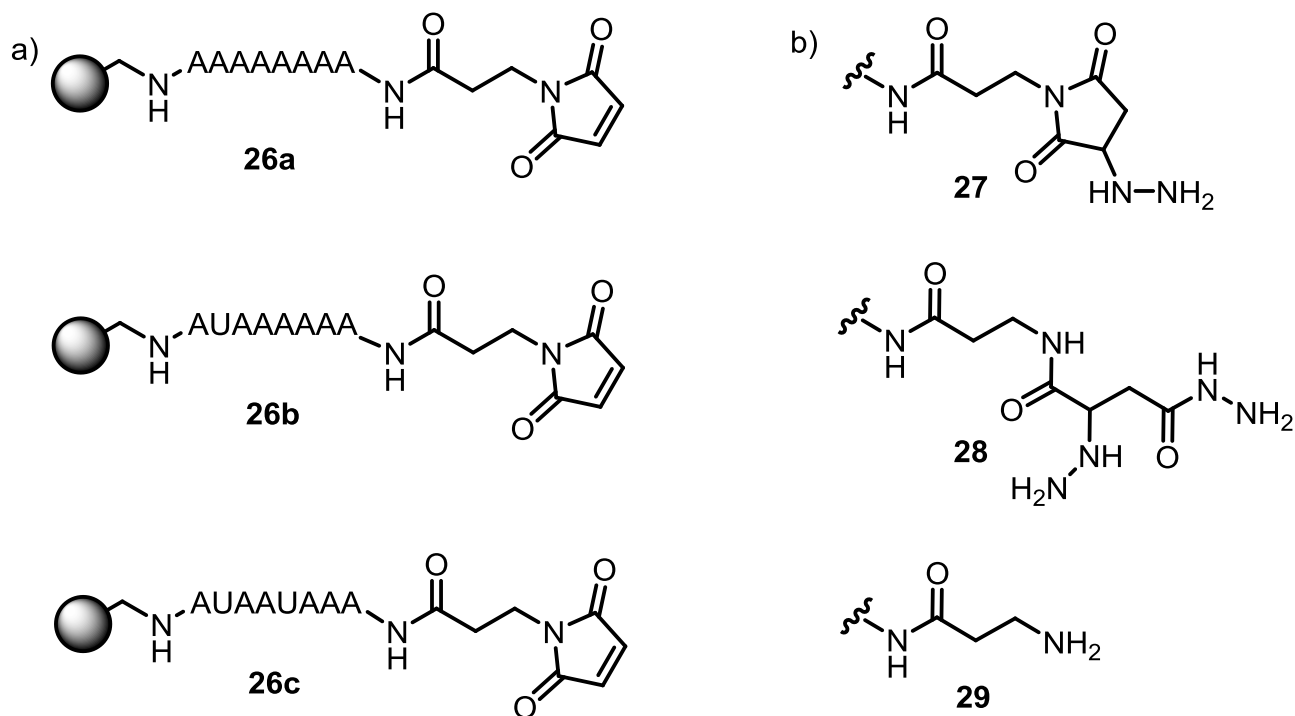
Figure 4.4. Conjugate addition of hydrazine to maleimide-functionalized peptides and corresponding side products. a) test peptides synthesized for optimizing hydrazine addition conditions, where A=alanine and U=α-aminoisobutyric acid b) products observed, as determined by MALDI-MS, upon the reaction of hydrazine with the test peptides.

As an initial proof of concept for the peptide's ability to undergo transamidation with the quorum sensing autoinducers, the succinimoyl-hydrazine derivative of peptide **26a** was combined with 3-oxo-C$_8$-AHL (**22**), in 50 mM NaOAc buffer. After 1h, the corresponding hydroxypyrazole product was observed by MALDI-MS. Detection of the peptide-pyrazole adduct validated the basic reactivity necessary for pursing our combinatorial approach. However, the presence of overaddition and cleavage products persisted in subsequent screens of the control peptides. Also, the degree to which the side products formed was observed to vary based on peptide sequence. This differential reactivity could inadvertently bias the eventual peptide library screening.

As a result, we turned to synthesizing a series of Boc-protected hydrazines that could be installed on the peptide via standard Fmoc-SPPS conditions. This would ensure the uniform distribution of the nucleophilic residue amongst the library members while allowing for liberation of the hydrazine-functionality during global acid deprotection of the remaining amino acid side chains. As hydrazine proved to be too reactive to yield a single Michael adduct, *tert*-butyl carbazate was employed to simultaneously decrease the nucleophilicity of the Michael donor while installing the desired Boc-protecting group for SPPS. The Boc-protected succinimoyl-hydrazine (**30**) was isolated as a single product in 90% yield (Figure 4.5a). To enhance the diversity of the hydrazines to include in the library screens, Boc-protected phenylhydrazine (**31**) and hydrazinoacetic acid (**32**) were also prepared. Phenylhydrazine proved to be the most reactive hydrazine in the small molecule screens with the 3-oxo-C_8-AHL (Chapter III) and hydrazinoacetic acid, though electronically similar to the succinimoyl-hydrazine, provides a much shorter linker length between the peptide and the hydrazine residue. This could prove important for optimizing the non-covalent interactions provided by the peptide to achieve the desired transamidation rate enhancement.
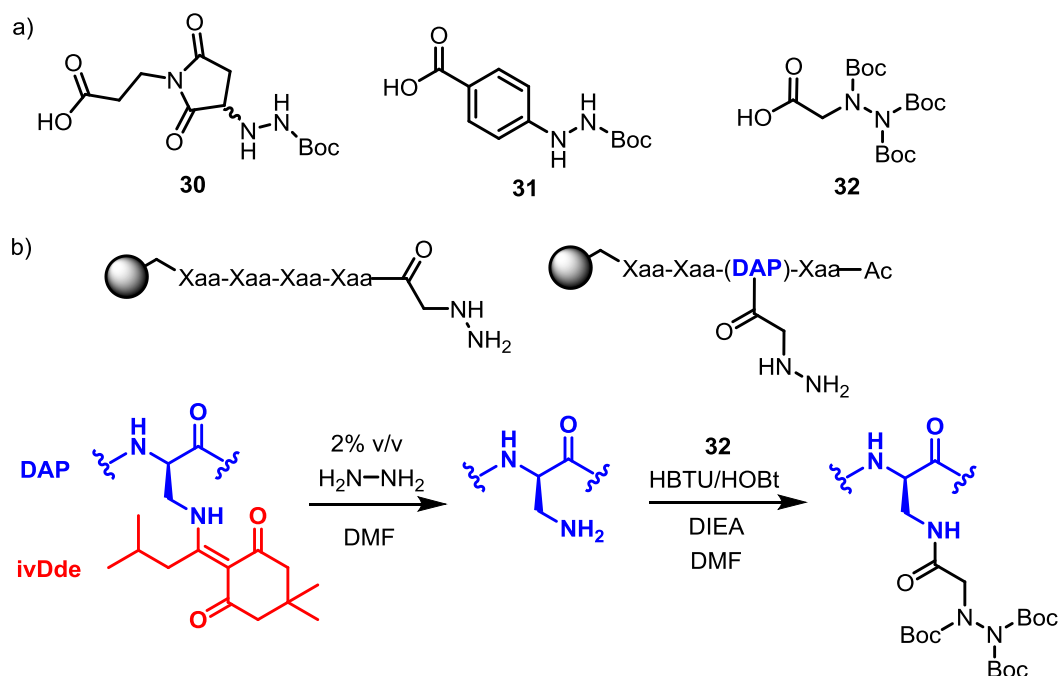
Figure 4.5. Synthesis of peptide libraries using Boc-protected hydrazines. a) Boc-protected hydrazine derivatives synthesized for use in AHL transamidation library design b) Strategy for site-selective hydrazine incorporation at the N-terminus of a peptide library or through an orthogonally DAP(ivDde) residue, where Xaa represents any amino acid.

As in our initial test peptide screens, the carboxylic acid moiety of each Boc-protected hydrazine allows it to be easily coupled to the N-terminus of a peptide during library synthesis. However, accessing a wider variety of library members would require a method for incorporating the hydrazine residue at any location along the peptide sequence. To address this issue, Fmoc-2,3-diaminopropionic acid (DAP) with an orthogonal ivDde side chain protecting group was employed (Figure 4.5b). The unnatural amino-serine analog is introduced as any other amino acid during SPPS. At the completion of the synthesis, the ivDde group is selectively removed and a Boc-protected hydrazine is coupled to the resultant free amine. Site-specifically introduction of hydrazine at the DAP residue lengthens the distance of the hydrazine from the core of the peptide, but increases the primary and secondary structures that can be evaluated by our high-throughput screen.

ii. First Generation Library Synthesis

Our strategy for the development of peptide libraries for selective and rapid derivatization of the 3-oxo AHLs involves the use of minimalist peptide sequences that could present a surface of functionality to both attract the substrate and enhance the reactivity of the hydrazine. Thus, in designing our first generation of libraries, short sequences that have been previously determined to display secondary structure in water were employed. Short poly-Ala-AIB peptides (Table 4.1, **L1**) have demonstrated helical propensity, generally existing as a mixture of $\alpha/3_{10}$-helix based on the present ratio of AIB:Ala residues.[24,33] In addition to its lipophilicity serving as a potential advantage in recruiting the AHL to the peptide surface, the library was constructed to modify a single amino acid adjacent to the hydrazine to determine any steric or electronic implications the substitution may have on reactivity. A β-hairpin inspired library, including a dPro-Gly turn motif, was also constructed to include variable residues cross-strand to the hydrazine to observe their impact on foldedness and AHL reactivity (Table 4.1, **L2**).[33,34] Finally, another poly-Ala-AIB sequence was appended with a type II' dPro-Pro turn followed by three variable residues in hopes of directing the variable residues back towards the hydrazine while presenting a novel surface for peptide-substrate interaction (Table 4.1, **L3**).

Table 4.1. First generation of peptide libraries for AHL transamidation.
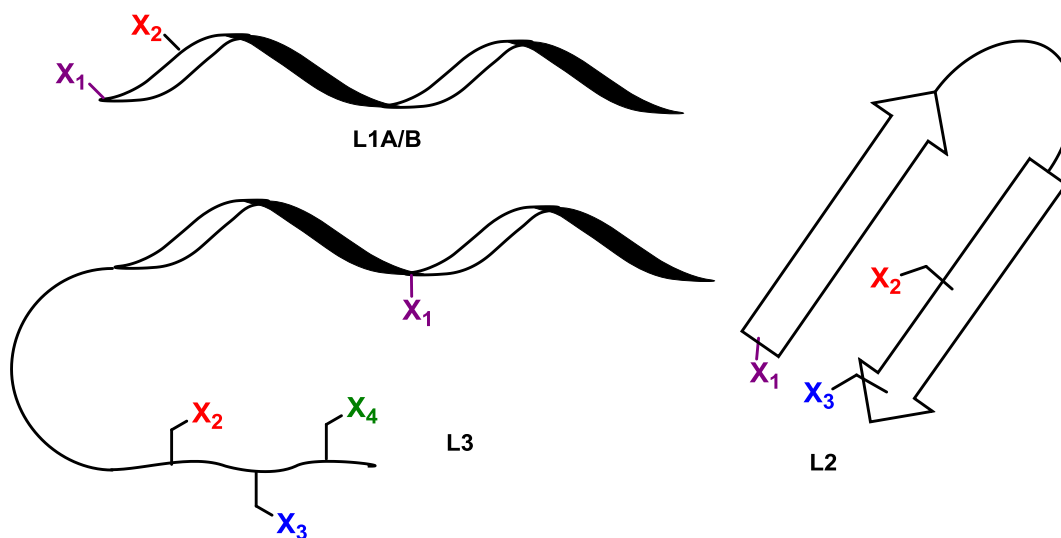
Library	Library Sequence[a]	Variable Residue[a]
1	X_1X_2AAUAAUA-NH$_2$	X_1: **30** (L1A), **31** (L1B) X_2: AIB, Ser, Ala, DAB, Phg, Gly, 3-NO$_2$Phe
2	X_1VWVdPGOX_2VX_3-NH$_2$	X_1: **30** X_2: Lys, His, Phe, Trp, Leu, Ser, Arg X_3: Tyr, 2-Nal, Val, His, Orn, Glu, Cit
3	Ac-$X_4X_3X_2$PdPUAAX_1AAUA-NH$_2$	X_1: **30** X_2: Phe, Lys, Phg, Tyr X_3: Phe, Orn, Cha, 3,5-diFPhe X_4: Phe, His, Trp, Ile

[a]See Abbreviations section above for interpretation of amino acids by single and triple letter codes

A variety of natural and unnatural amino acids were incorporated in the libraries to provide a diversity of non-covalent interactions. Anionic, cationic, aromatic, lipophilic, hydrogen bonding, and conformation inducing residues were inserted non-selectively at the variable sites chosen in each library design.

iii. Development of a Colorimetric Screening Method

With synthesis of our first generation libraries completed, development of a colorimetric tag was necessary to visualize the most reactive library members. As proposed in Figure 4.3, the employment of a dye-functionalized AHL analog as the substrate for the

screen would lead to a color change in the peptides that most rapidly converted the AHL to the corresponding hydroxypyrazole products. In an effort to prepare an AHL-dye conjugate capable of screening under aqueous conditions, 5(6)-carboxyfluorescein was coupled to an amine-functionalized AHL derivative. The resultant fluorescein-AHL (**33**) was obtained in milligram quantities after purification by semi-prep HPLC. However, preliminary control screens of our first generation libraries with the fluorescein-AHL led to a series of false positive "hits", promoting resin coloration in the presence of protected peptide libraries and the resin alone. Screening of alternative non-AHL functionalized water-soluble dyes, including Orange G and Aniline Blue, also led to resin coloration. Non-specific interactions between peptide library members and colorimetric indicators in water, especially due to hydrophobic effects, are not uncommon in solid-phase combinatorial screens.[35,36] We hypothesized that the fluorescein-AHL was not sufficiently miscible at the low millimolar concentrations being utilized for library screening, leading to its affinity for both the protected peptides and the resin.
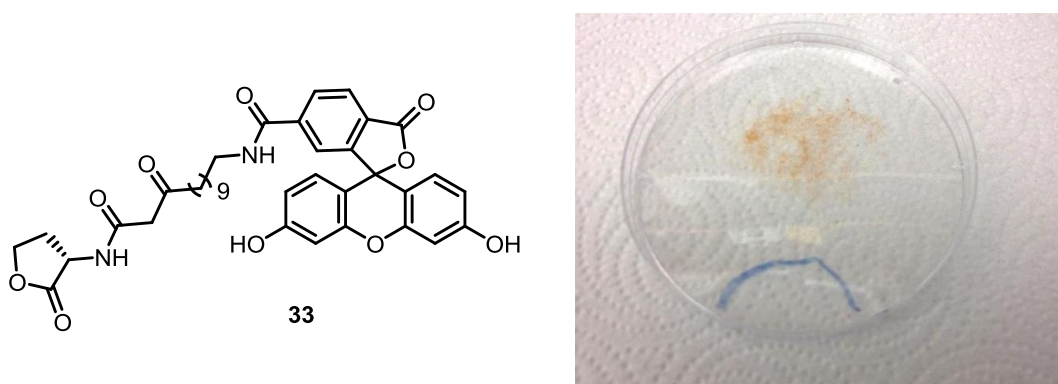
Figure 4.6. Non-specific interactions of the fluorescein-AHL. Without the presence of a hydrazine-containing peptide, coloration was observed upon agitating acylated Tentagel resin in a buffered solution of **33**.
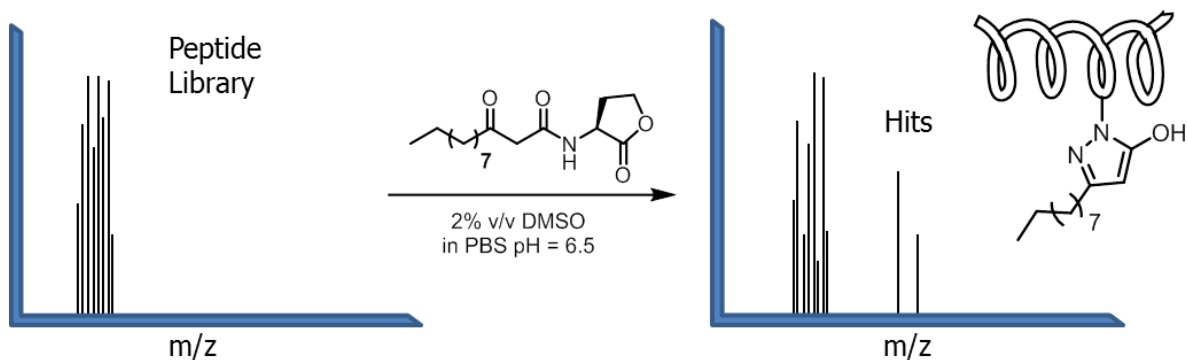
Figure 4.7. AHL transamidation hit identification without a colorimetric tag. Library hits were identified by detection of shift in mass corresponding to the hydroxypyrazole adduct of the 3-oxo-C$_{12}$-AHL and the peptide.

As an alternative strategy, screening of **L1, L2**, and **L3** was completed without the fluorescein-functionalized AHL. The resin-bound libraries were shaken with a buffered solution in the presence of the parent 3-oxo-C$_{12}$-AHL containing 2% DMSO for enhanced AHL solubility. The screen was terminated by cleaving the entire library from resin to observe a shift in mass (+178.1 m/z) by MALDI-MS corresponding to the formation of the peptide-AHL conjugates (Figure 4.7). We hypothesized that by limiting the screening time, only the most reactive peptides in the library would react to form the hydroxypyrazole product. The strategy proved beneficial in identifying a series of hits from our first generation libraries (Section iv). However, employment of the method uncovered a few inherit limitations. The library composition had to be restricted to peptide sequences with a molecular weight range no greater than 178 mass units, the mass of the hydroxypyrazole adduct, to avoid overlap of the tagged and untagged peptides in the mass spectrum. In addition, signal intensity is known to be dependent on the gas phase protonation affinities of each amino acid, requiring careful interpretation of library hits containing basic residues like lysine or arginine.[37]
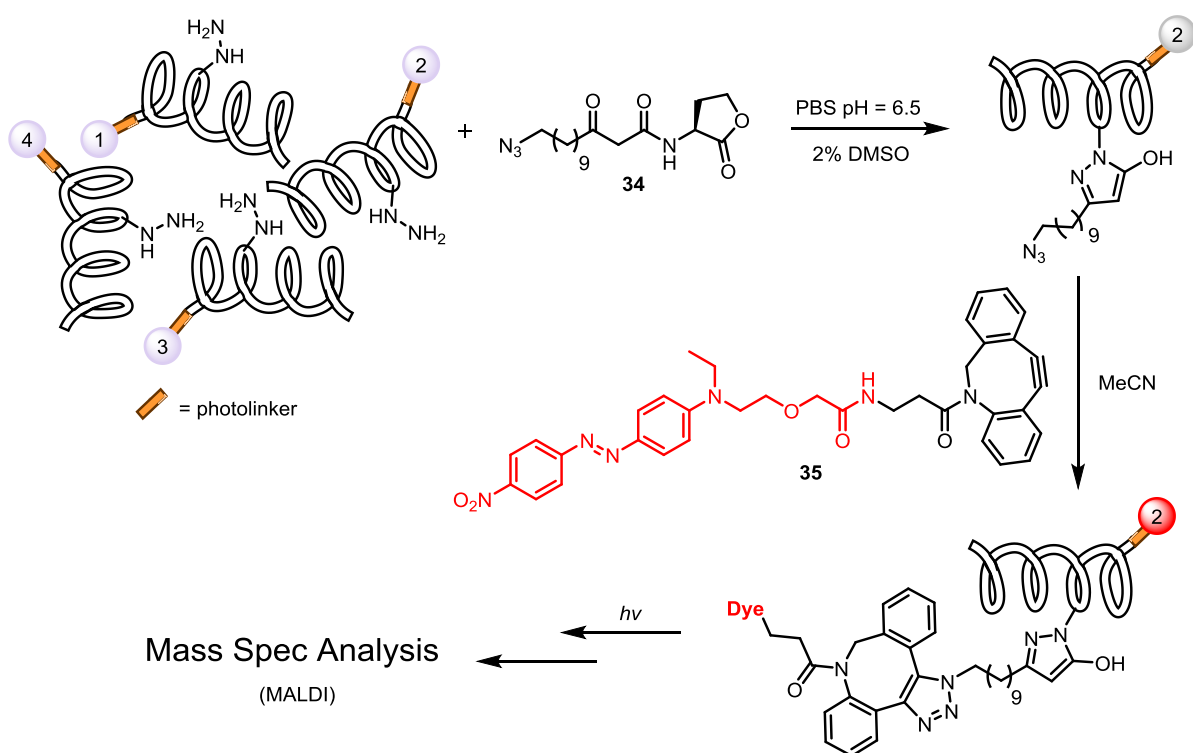
Figure 4.8. Revised screening protocol for hydrazine-containing peptide libraries via strain-promoted Huisgen cycloaddition.

To obviate these drawbacks, we considered a third modification to our screening protocol that would expose the library to a functionalized-AHL derivative under aqueous conditions followed by a chemoselective reaction of the AHL analog to develop the screen in organic media (Figure 4.8). This revised two-step assay would remove the non-specific interactions observed between the dye and the peptide library members while also allowing the synthesis of larger and more diverse libraries. Considering chemical processes orthogonal to hydrazone formation, the Huisgen cycloaddition presented a viable and efficient method for selectively linking the dye to the peptide-bound AHL. Consequently, an azido-functionalized 3-oxo-AHL (**34**) was prepared in addition to a complementary strained-cyclooctyne disperse red derivative (**35**). The azido-AHL was prepared to structurally mimic the native 3-oxo autoinducer in *P. aeruginosa*, the 3-oxo-C$_{12}$ AHL (**1**). Disperse red was

98

selected due to its frequent use in screening peptide catalyst libraries in organic solvents, including its previous uses in the Gagné Lab.[24,25,38] Modification of the dye with a dibenzocyclooctyne moiety, originally developed by the Boons group,[39] allows for rapid conversion to the desired cycloadduct without the use of a copper catalyst, an additive which would inherently discolor the resin. As a control reaction, **34** and **35** were combined in equimolar amounts in acetonitrile. Maximum conversion to the desired triazole-containing product **36** was observed by mass after 4 hours (Scheme 4.5). Further, when the two-step screen was performed with unmodified resin, the dye washed cleanly from the solid support proving that the non-specific interactions observed in our initial screening method had been avoided. This protocol was used to validate the hits in **L3** and will be used to screen all subsequent generations of peptide libraries.
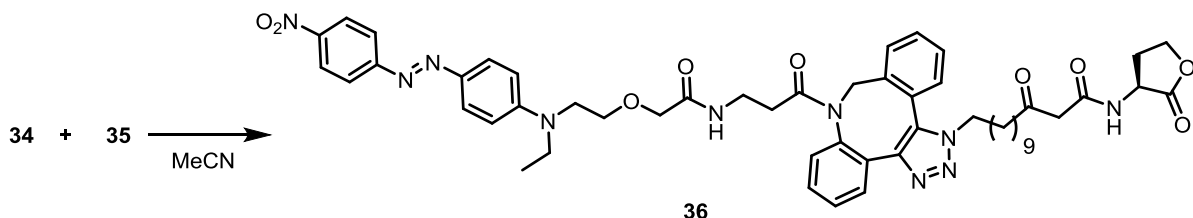
Scheme 4.5. Formation of the AHL-dye conjugate, Solution phase control reaction of the azido-AHL (2.0 mM) and dye-functionalized cyclooctyne (2.0 mM) for chemoselective formation of **36**.

iv. Library Hits and Solution Phase Screening

During the iterative redesign of our colorimetric assay, the first generation libraries were tested to identify sequences capable of rapid 3-oxo-AHL transamidation. Each library was screened in buffer at two pH values (4.5, 6.5) with two autoinducers (3-oxo-C_8-AHL, 3-oxo-C_{12}-AHL). Each screen displayed only mild differentiation amongst library members, resulting in a large collection of pyrazole-tagged sequences. The peptides selected as hits displayed the highest relative intensities by MALDI-MS across multiple screens (Table 4.2).

Table 4.2. Hit sequences from the first generation libraries.
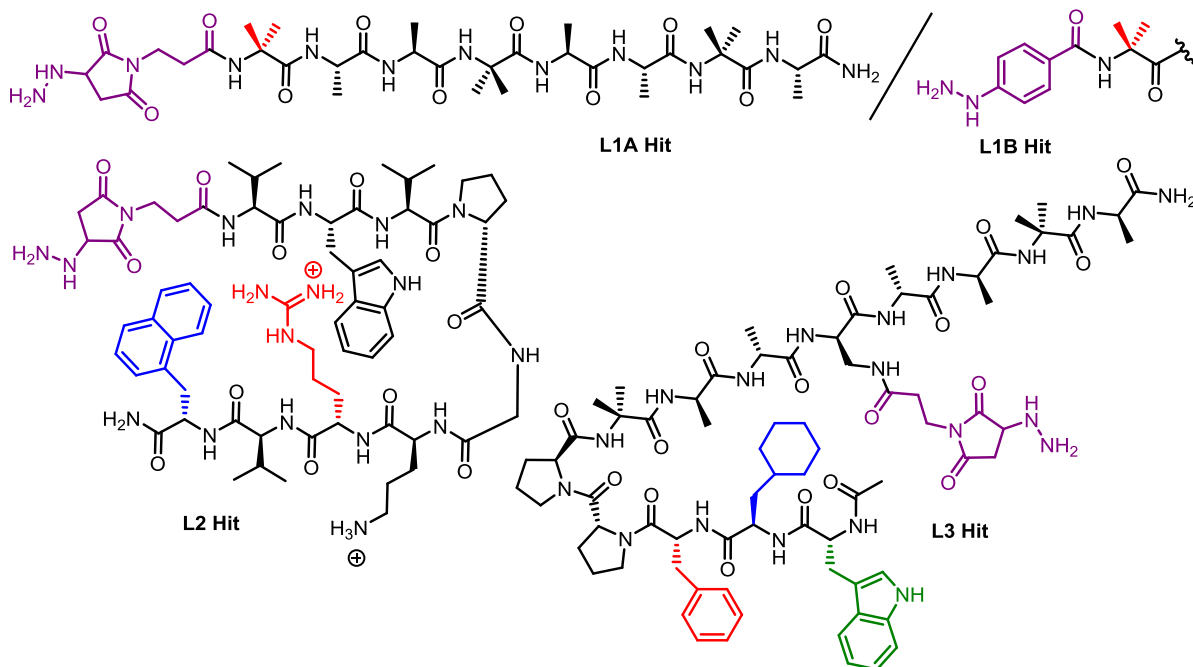
Library	Library Hits[a]
L1A	**ShU**AAUAAUA-NH$_2$
L1B	**PhHU**AAUAAUA-NH$_2$
L2	**Sh**VWVdPGO**R**V**(2-Nal)**-NH$_2$
L3	Ac-**W(Cha)(Phg)**PdPUAA**Sh**AAUA-NH$_2$

[a]Sh = succinimoyl-hydrazine; PhH = phenylhydrazine

As AIB is known to increase helix propensity in water, the selection of the amino acid in **L1** suggests that inducing greater conformational stability in the peptide may enhance its reactivity. The hits from **L2** and **L3** contain both lipophilic and aromatic residues, perhaps leading to more rapid AHL transamidation through hydrophobic interactions between the autoinducer and the peptide.

After identification in solid-phase screen, the hits from each library were resynthesized for solution phase screening with the 3-oxo-AHL. Solution phase screens were completed to determine the ability of each peptide to promote AHL derivatization in the absence of the resin and to compare the relative transamidation rates of peptides from

different libraries. As controls to validate hit selection, an additional non-hit peptide from

each library was synthesized and tested. The peptides were combined with the 3-oxo-C_8-

AHL in pH 6.5 buffer and the disappearance of the AHL was monitored by analytical HPLC

(Table 4.3). All the sequences tested were capable of AHL transamidation as the mass of

peptide-hydroxypyrazole adduct was detected by LC-MS in each experiment. Supporting

our proposed reaction pathway, the putative hydrazone product was observed to form and

dissipate as the reaction progressed to yield the hydroxypyrazole product (Figure 4.9). The

phenylhydrazine-functionalized peptide most efficiently decreased the concentration of AHL

in solution, consistent with our previously conducted small molecule screens (Chapter III).

However, the relative rates of AHL consumption achieved by each peptide did not display a

significant improvement in the rates provided by hydrazine alone, suggesting the presence of

the peptide in our initial design does not largely influence the transamidation reaction. The

selected variable residues also proved to be only mildly influential to reaction rates as

demonstrated by the similarity in k_{rel} between the peptides selected as hits and the non-hit

sequences synthesized.

Table 4.3. Relative rates of AHL consumption of hits and non-hits resynthesized from the
first generation libraries.
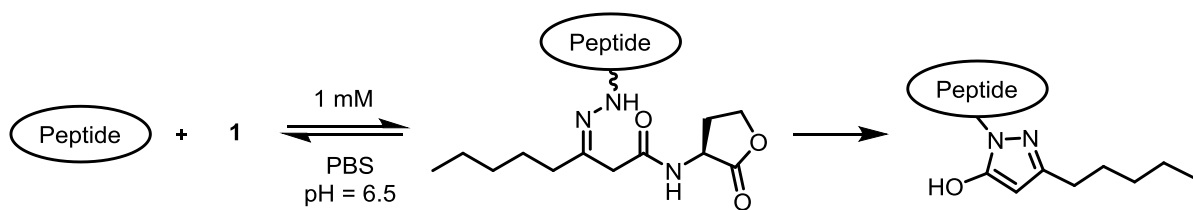
Library	Peptide	Sequence	k_{rel}(hydrazine)[a]
L1A	**40**	**ShU**AAUAAUA-NH$_2$	1.3
L1B	**41**	**PhHU**AAUAAUA-NH$_2$	5.2
	42	*HaaUAAUAAUA-NH$_2$*	1.2
L2	**43**	**Sh**VWVdPGO**R**V**(2-Nal)**-NH$_2$	1.0
	44	*ShVWVdPGOHV(2-Nal)-NH$_2$*	1.1
L3	**45**	Ac-**W**(**Cha**)(**Phg**)PdPUAA**Sh**AAUA-NH$_2$	0.7
	46	*Ac-FOYPdPUAAShAAUA-NH$_2$*	1.3

Screened non-hits are italicized; [a]relative rates in reference to the reaction of hydrazine (1.0 mM) with the 3-oxo-C8 AHL (1.0 mM) at pH 6.5.
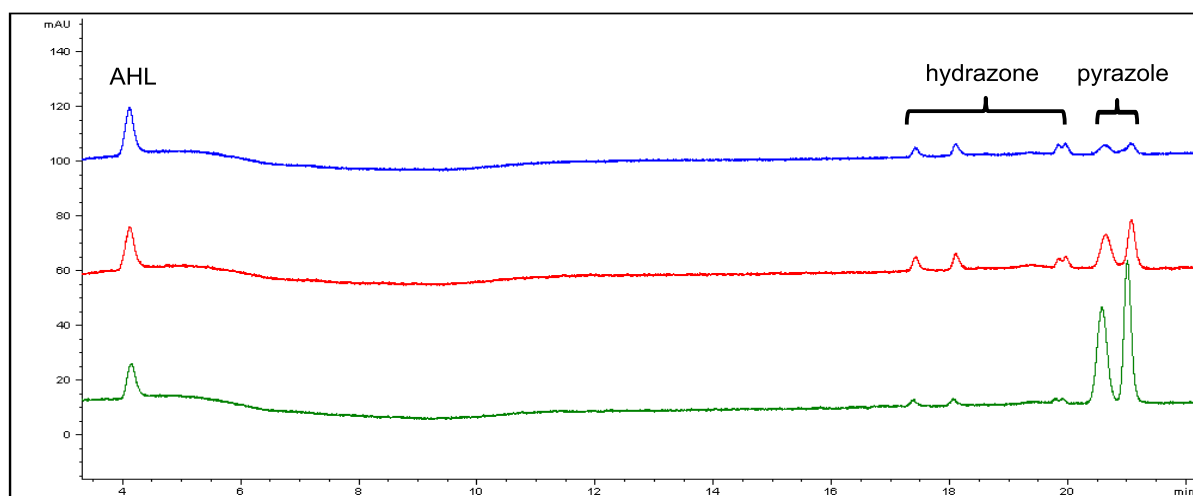
Figure 4.9. Representative HPLC trace for determining rates of AHL consumption in solution phase. In the above trace, the hit from L1A is combined with **40** and monitored from 0 to 14 h. The hydrazone and its isomers are initially visible before being consumed to produce the corresponding pyrazole product.

The minimal differentiation observed in the relative rates of our first generation libraries reflects the minimal differentiation observed during the solid-phase screens. The reactivity of the peptides also parallels the transamidation rates without the peptide. These results suggest that our initial libraries simply do not provide the necessary network of non-

covalent interactions to generate a pseudo-enzymatic environment for promoting AHL derivatization. Strategies to enhance the influence of the peptide on rate could include designing sequence with more well-folded and characterized secondary structures, such as introducing structurally reinforcing covalent crosslinks (i.e. – disulfide bonds, lactam formation) or conducting site-specific mutagenesis of miniature proteins. This would enable a more focused selection of variable sites and residues with a greater probability of those residues engaging at the active site of AHL transamidation. Based on the interpretation of our preliminary results above, the design of new generations of hydrazine-containing peptide libraries is currently ongoing.

v. Biofilm and Quorum Sensing Inhibition Screening

Despite the sluggish rates of our first generation library hits, we sought to advance our peptides to screening in cell-based assays to assess the potential of the 3-oxo-AHL transamidation for both biofilm and quorum sensing inhibition. Standard conditions for bacterial culture require the addition of amino acid and carbon sources to buffer in order to support bacterial growth and proliferation. To determine if our reaction would be sustained in bacterial growth media, peptide **47** was screened with the 3-oxo-C_8 AHL (**22**) in the presence of increasing concentrations of Luria-Bertani (LB) broth. (Figure 4.10). In all instances, conversion to the corresponding hydrazone and hydroxypyrazole products was observed by HPLC. The reaction proved equally robust when screened in PBS buffer containing 0.3 mg/mL tryptic soy broth and 0.01% w/v glucose, a potentially competitive electrophile for the hydrazine-containing peptide. Establishing the ability of the transamidation reaction to proceed in the presence of bacterial growth sources was a necessary precursor to conducting cell-based assays. With the variety of media tested, these

103

experiments also showcase the selectivity of the peptide for the 3-oxo AHL in an environment of diverse biomolecular functionality, a critical parameter for quorum sensing probes and inhibitors.
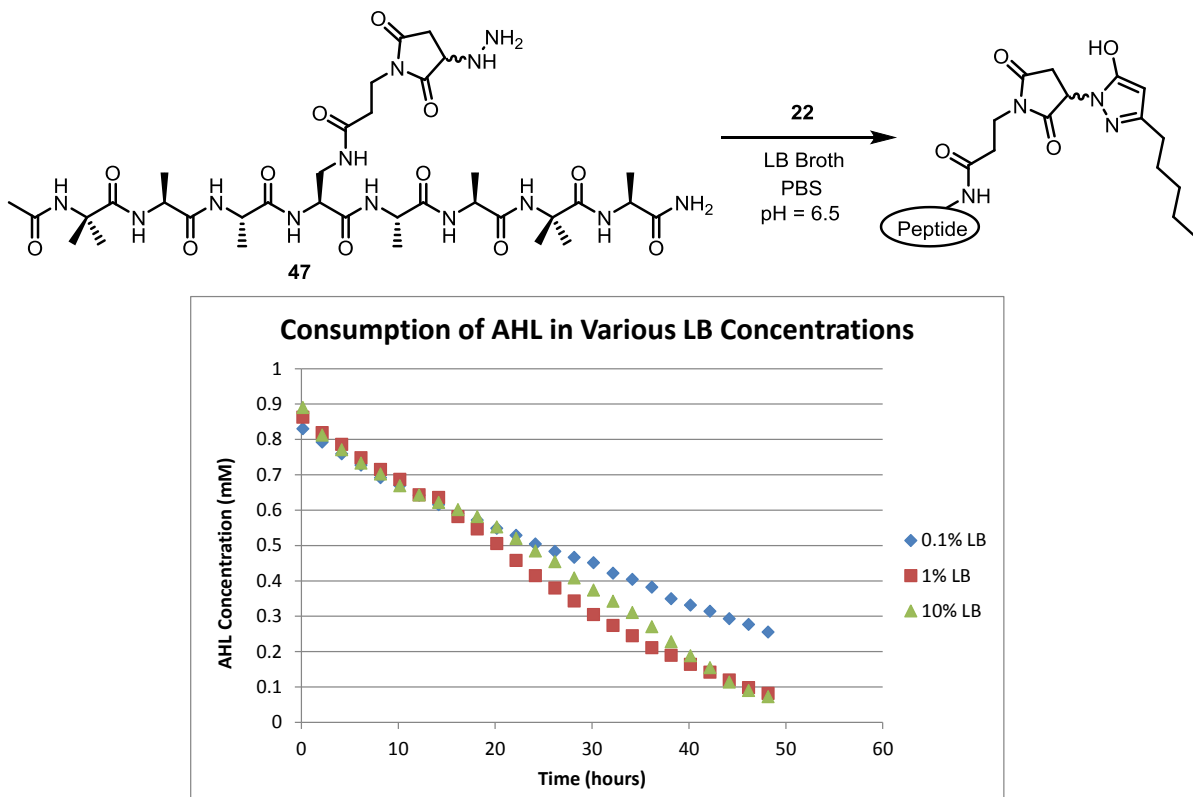
Figure 4.10. AHL transamidation in bacterial growth media. The disappearance of **1** (1.0 mM) is monitored upon the addition of peptide **47** (1.0 mM) in varied concentrations of LB broth. Conversion to the pyrazole product was confirmed by LC-MS.

As discussed in Chapter I, quorum sensing has been demonstrated to regulate biofilm production, the most prevalent mechanism for pathogenicity in *P.aeruginosa*. The sustained reactivity of peptide **47** in bacterial growth media encouraged screening of the first generation of libraries for biofilm inhibition. Effective derivitization of the primary autoinducer in *P.aeruginosa*, the 3-oxo-C_{12} AHL, would impede the bacteria's ability to reach the required quorate to regulate biofilm formation.[40] Peptides **40**, **41**, **43**, and **44** from the first generation library screens were prepared by serial dilution in 25% LB broth. Stock

solutions of diphenylsulfide (DPS), a known inhibitor of biofilm formation were also prepared as a positive control for comparison to the peptide-containing wells.[41] The peptides and DPS were added to a 24-well plate containing *P.aeruginosa* PAK and incubated for 18 - 24h. As expected, DPS prevented biofilm growth at both 1 mM and 100 μM, validating our conditions for the screen. Both peptides **40** and **41** inhibited biofilm formation at 1 mM, while peptides **43** and **44** inhibited at a reduced concentration of 100 uM. Peptide concentrations above 1 mM prohibited all cell growth, establishing an upper limit for the use of hydrazine-containing peptides in biofilm inhibition due to their cytotoxicity. Control experiments were also completed with **30** and **31** without the Boc-protection to determine if the hydrazine alone was causing reduction in the biofilm. Notably, the hydrazines prevented all planktonic growth at concentrations as low as 100 μM, proving more cytotoxic alone than when attached to the peptide. The reduced toxicity is valuable when considering the hydrazine-containing peptides as future candidates for *in vivo* testing.

a)
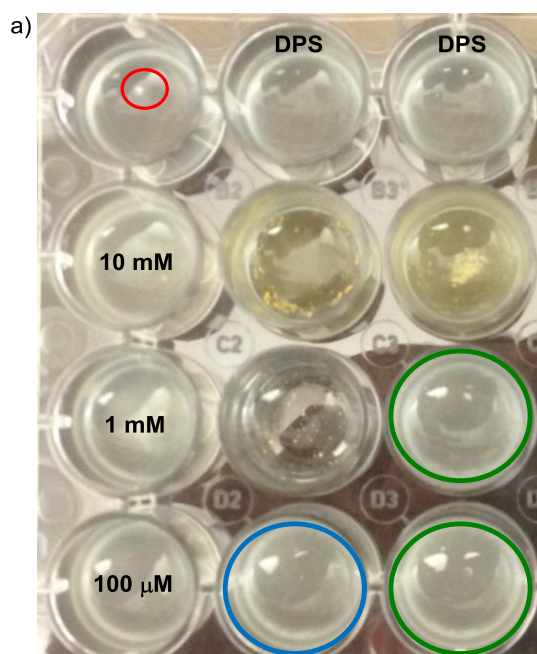
b)

Peptide	MICs
40	1 mM
41	1 mM
43	100 μM
44	100 μM

Figure 4.11. Biofilm inhibition assay with hydrazine-containing peptides. a) Well-plate displaying the biofilm reduction in the wells containing **43** and **44** compared to the control without a peptide (circled red); a clear well indicates concentrations at which all planktonic growth was inhibited. b) The corresponding minimum inhibitory concentrations (MICs) for biofilm formation of the screened peptides.

To confirm that the biofilm inhibition observed was a direct consequence of QS inhibition, the peptides were screened using a wild-type reporter strain of *P.aeruginosa* PAO1. The strain is transfected with a plasmid encoding for the production of green fluorescent protein (GFP) upon initiation of the QS mechanism. The mutant was cultured in full-strength LB broth and subjected to peptides **40-46** at a final concentration of 1.0 mM. By comparing the relative activity of the wild-type alone, no peptide succeeded in significantly inhibiting the quorum sensing mechanism. Consequently, a correlation between the observed potency of the peptides in biofilm inhibition with their ability to inhibit the QS mechanism cannot be made from our initial results.
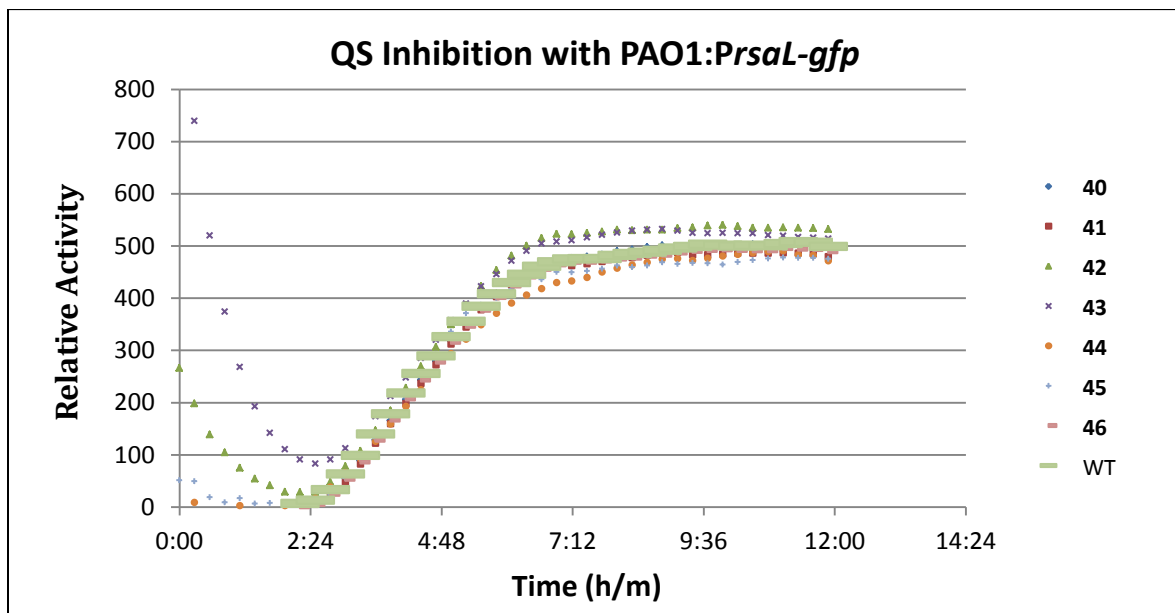
Figure 4.12 – Quorum sensing inhibition with hydrazine-containing peptides. Incubation of the first generation of hydrazine-containing peptides with a *P.aeruginosa* PAO1 reporter strain displayed no decrease in relative activity over the 12 h assay.

As determined by the initial spike in relative activity of the wild-type, quorum sensing was initiated in the mutant in less than two hours. Considering the rates of AHL transamidation observed in the solution phase screens of the peptide hits, derivatization of the 3-oxo-C_{12}-AHL is likely to be occurring too slowly to impact the quorum sensing pathway. Developing peptides capable of derivatizing the AHL on a similar time scale as quorum sensing initiation would increase the probability of inhibiting the pathway. Optimization of the growth conditions, including reducing the concentration of the growth media or decreasing the initial optical density of the bacteria, would also be beneficial for observing peptide-based quorum quenching in future screens.

C. Conclusions

The immense diversity and functional flexibility provided by synthetic peptides make them a powerful class of molecules for designing enzyme mimics. In this work, the utility of peptides as a scaffold for promoting our unique hydrazine-mediated AHL transamidation reaction was explored. Through the use of combinatorial chemistry and the power of split and pool peptide synthesis, 127 peptides in four independent OBOC libraries were screened. Library synthesis was facilitated by the employment of Boc-protected hydrazines in conjunction with the use of an orthogonally protected DAP(ivDde) residue for site-selective introduction of the nucleophile along the peptide sequence. Through a series of design modifications, a novel colorimetric reactive tagging assay was developed for high-throughput screening of the hydrazine-containing libraries while eliminating the propensity for non-specific peptide-dye interactions.

Both on solid-support and in solution, the selected peptide hits unequivocally displayed the capability of derivatizing 3-oxo-AHLs. Resynthesis and screening of selected

sequences demonstrated that the reactivity of the peptides was sustained in solution, even in the presence of bacterial carbon sources such as LB broth and glucose. The primary sequence proved to only mildly influence transamidation reaction rates in the first generation libraries, as relative rates similar to hydrazine alone were obtained. The efficiency of hydroxypyrazole formation was largely determined by the hydrazine incorporated, evidenced by comparing **41** (phenylhydrazine peptide) to the other sequences screened. We hypothesize that the modest reactivity of the peptides led to their inability to induce quorum sensing inhibition in *P.aeruginosa* PAO1. The key to increasing these reaction rates comes in identifying sequences in which the non-covalent interactions of the peptide variable residues participate at the site of AHL transamidation. We are confident that introducing a greater element of rational design in the selection of our libraries while continuing to increase the diversity of variable residues in each sequence will enable the identification of an authentic enzyme-like hit for AHL derivatization.

Interestingly, peptides **40, 41, 43** and **44** were qualitatively observed to inhibit biofilm formation at minimum concentrations of 100 μM. Our results encourage further screens of hydrazine-containing peptides to discover greater potencies for *P.aeruginosa* biofilm inhibition and determine sequence and structure-activity relationships. However, the mechanism of observed biofilm reduction is undetermined and cannot yet be correlated with QS inhibition without corroborating evidence for the *gfp*-reporter strain assay.
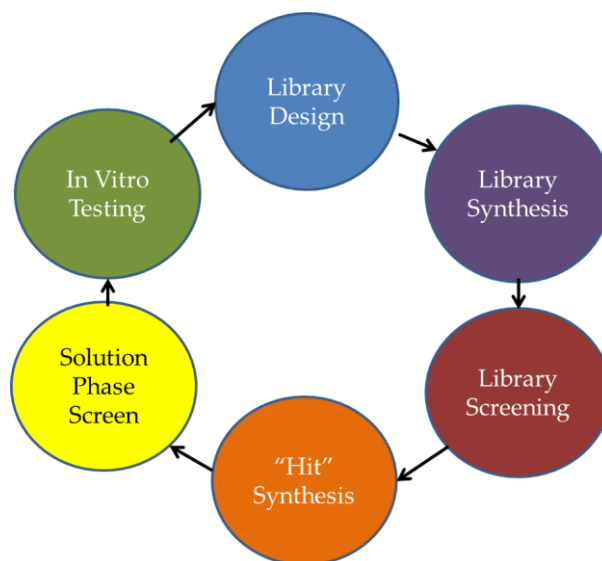
Figure 4.13. Developed protocol for peptide library design and screening. The above schematic depicts our developed procedure for the stepwise discovery of hydrazine-containing peptides for QS and biofilm inhibition through combinatorial peptide library design and colorimetric screening.

In summary, a functional protocol for screening hydrazine-containing peptides for quorum sensing and biofilm inhibition through a high-throughput reactive tagging assay has been established (Figure 4.12). Through iterations of library design, synthesis, and screening, the libraries can be sequentially modified to approach the most efficient scaffolds supporting AHL transamidation. Noting the relatively small number of peptides that were investigated in our first generation libraries, the sequence space remaining to be explored is vast and efforts in developing new generations of hydrazine-containing peptide libraries are currently underway.

D. Experimental

i. General Reagents and Synthesis

Commercial reagents and solvents were purchased from Sigma-Aldrich and Fisher Scientific. Resins for peptide synthesis were purchased from Peptides International and the Fmoc-photolabile linker was obtained from Advanced Chemtech. LB broth for the bacterial

cell assays was obtained from BD Biosciences. *P.aeruginosa* PAK was donated by the

Schoenfisch Lab at the University of North Carolina at Chapel Hill, while *P.aeruginosa*

PAO1 and the corresponding plasmid for *gfp* production (pGJB5 in *E.*coli DH5α) was

obtained from the Whiteley Lab at the University of Texas at Austin. Peptide libraries were

analyzed for hits by MALDI-FT on IonSpec spectrometer using 2,5-dihydroxybenzoic acid

as the matrix. Resynthesized peptides were purified using a Waters semi-prep HPLC/UV-

Vis with a Waters 4.2μM C$_{18}$ column. Relative rates of peptide transamidation were

obtained on an HP 1100 Series analytical HPLC/UV-Vis using a 2.7μM HALO C$_{18}$ column

at 210 nm with products confirmed by mass on an Agilent 1200 Series LC-MS using a

2.7μM HALO C$_{18}$ column. Small molecule product characterization (^{1}H and ^{13}C) was

completed on a 400 or 600 MHz Bruker NMR spectrometer. All related coupling constants

are reported in Hertz and shifts in ppm. NMR solvents were purchased from Cambridge

Isotopes Laboratories. High resolution mass spectra were obtained on an Agilent Accurate

LC-TOF Mass Spectrometer (Agilent Series 6220) operating in positive ion mode with an

electrospray ionization source (fragmentor = 175 V). The data was analyzed using an Agilent

MassHunter Workstation Software, Qualitative Analysis (V. B.02.00).

Synthesis of Boc-Protected Hydrazines

Boc-protected hydrazine **32** was purchased commercially and hydrazine **31** is a known

compounds and was synthesized following previously published procedures.[42] For the

synthesis of Boc-protected hydrazine **30**, 3-maleimidopropionic acid (1.69 g, 0.0100 mol)

was dissolved in 20 mL of EtOH. With stirring, *tert*-butyl carbazate (1.32 g, 0.0100 mol)

was dissolved in 5 mL of EtOH and added dropwise to the reaction mixture. The reaction

mixture was allowed to heat at 60°C for 8 h. The reaction mixture was concentrated under vacuum to yield **30**.

4-(2-(tert-butoxycarbonyl)hydrazinyl)benzoic acid (31)
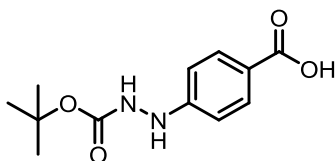
99.0% yield; δ_H (DMSO-d$_6$, 400 MHz) 12.2 (1H, s), 8.92 (1H, s), 8.24 (1H, s), 7.72 (2H, d, J = 8.8 Hz), 6.63 (2H, d, J = 8.8 Hz), 1.41 (9H, s); MS (ESI) calcd for $C_{12}H_{16}N_2O_4$: 253.11, found: 253.12 (M + H).

4-(2-(tert-butoxycarbonyl)hydrazinyl)benzoic acid (30)
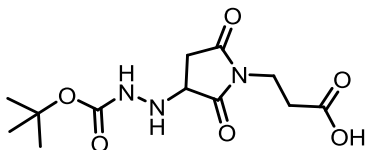
72.0% yield; δ_H (DMSO-d$_6$, 600 MHz) 12.4 (1H, s), 8.36 (1H, s), 5.09 (1H, s), 3.95 (1H, m), 3.55 (1H, m), 2.81 (1H, dd, J_1 = 8.4 Hz, J_2 = 9.6 Hz), 2.51 – 2.46 (3H, m), 1.39 (9H, s); δ_C (DMSO-d$_6$, 150 MHz) 176.5, 175.9, 172.4, 156.8, 79.3, 57.6, 34.4, 34.3, 32.0, 28.6; MS (ESI) calcd for $C_{12}H_{19}N_3O_6$: 302.1347, found: 302.1343 (M + H).

Synthesis of Fluorescein-AHL
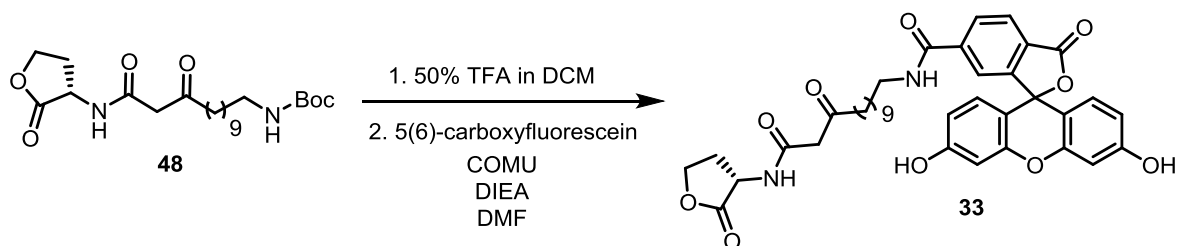
In a 20-mL scintillation vial, **48** (150 mg, 0.352 mmol) was dissolved in 2 mL of DCM and combined with 2 mL of TFA. After 20 min, the solvent and acid were removed under a stream of N_2 gas to yield the free amine. The deprotected AHL, 5(6)-carboxyfluorescein (139 mg, 0.369 mmol), and DIEA (0.121 mL, 0.739 mmol) were all combined and dissolved in DMF (4 mL). COMU (158 mg, 0.369 mmol) was then added and the reaction mixture was allowed to stir at 0°C for 1h. The reaction mixture was then warmed to room temperature and allowed to stir for an additional 3h. The contents of the flask was then diluted in EtOAc (50 mL) and extracted with 1M HCl (2 x 10 mL), 1M NaHCO$_3$ (2 x 10 mL), and washed with brine (1 x 15 mL). The organic layer was collected, dried over NaSO$_4$, filtered, and concentrated. The concentrated organic layer was redissolved in 40% MeCN in water and purified by reverse-phase HPLC to isolate the 5-carboxyfluorescein regioisomer (**33**). The Boc-protected AHL **48** was prepared according to previous published procedures.[43]

(S)-N-(11,13-dioxo-13-((2-oxotetrahydrofuran-3-yl)amino)tridecyl)-3',6'-dihydroxy-3-oxo-3H-spiro[isobenzofuran-1,9'-xanthene]-6-carboxamide (33)
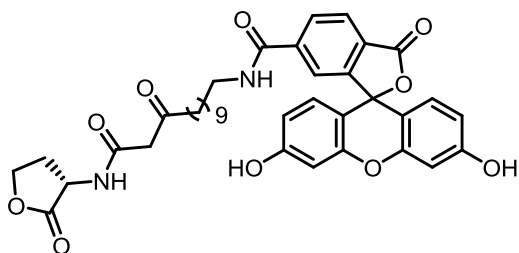
2.1% Yield; δ_H (CDCl$_3$, 600 MHz) 8.06 (2H, m), 7.54 (1H, s), 7.25 (1H, br s), 7.15 (1H, s)

6.77 (2H, d, J = 2.4 Hz), 6.73 (2H, d, J = 8.4 Hz), 6.62 (2H, dd, J_1 = 2.4 Hz, J_2 = 8.4 Hz),

4.53 (1H, m), 4.40 (1H, td, J_1 = 7.2 Hz, J_2 = 1.8 Hz), 4.24 (1H, m), 3.38 (2H, s), 3.29 (2H,

m), 2.53 (3H, m), 2.26 (1H, m), 1.51 (4H, m), 1.53 – 1.25 (13H, m); δ_C (CD$_3$CN, 150 MHz);

MS (ESI) calcd for C$_{38}$H$_{40}$N$_2$O$_{10}$: 685.2759, found: 685.2756 (M + H).

Synthesis of Azido-AHL

Azido-AHL **34** is a known compounds and was synthesized following previously published

procedures.[43]

(S)-13-azido-3-oxo-N-(2-oxotetrahydrofuran-3-yl)tridecanamide (34)
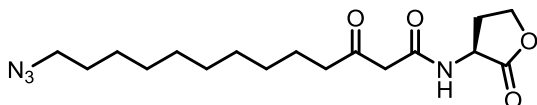
17.7% Overall Yield (3 steps); δ_H (CDCl$_3$, 600 MHz) 7.29 (1H, s), 4.60 (1H, m), 4.47 (1H,

td, J_1 = 7.6 Hz, J_2 = 1.6 Hz), 4.29 (1H, m), 3.48 (2H, s), 3.26 (2H, t, J = 6.8 Hz), 2.75 (1H,

m), 2.54 (2H, t, J = 7.2 Hz), 2.26 (1H, m), 2.22 (1H, m), 1.60 (4H, m), 1.39-1.21 (12H, m);

MS (ESI) calcd for C$_{17}$H$_{28}$N$_4$O$_4$: 353.21, found: 353.25 (M + H).

Synthesis of Strained-Cyclooctyne Disperse-Red Dye
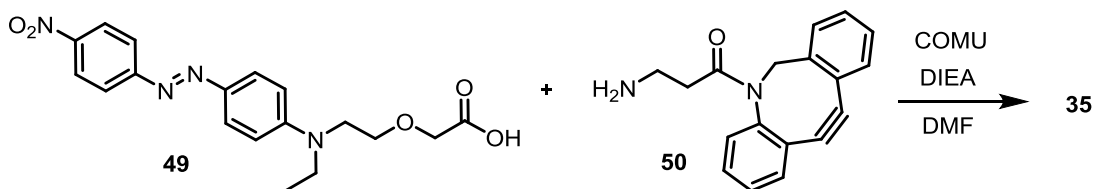
In a 10-mL RB flask, **49** (70.8 mg, 0.190 mmol), **50** (50.0 mg, 0.181 mmol), and DIEA (0.066 mL, 0.3801 mmol) were all combined and dissolved in DMF (2 mL). COMU (81.4 mg, 0.190 mmol) was then added and the reaction mixture was allowed to stir at 0°C for 1h. The reaction mixture was then warmed to room temperature and allowed to stir for an additional 3h. The contents of the flask was then diluted in EtOAc (25 mL) and extracted with 1M HCl (2 x 5 mL), 1M $NaHCO_3$ (2 x 5 mL), and washed with brine (1 x 5 mL). The organic layer was collected, dried over $NaSO_4$, filtered, and concentrated. The concentrated organic layer was redissolved in DCM and purified by column chromatography. Compound **38** was synthesized by previously reported procedure[25] and **39** was purchased commercially.
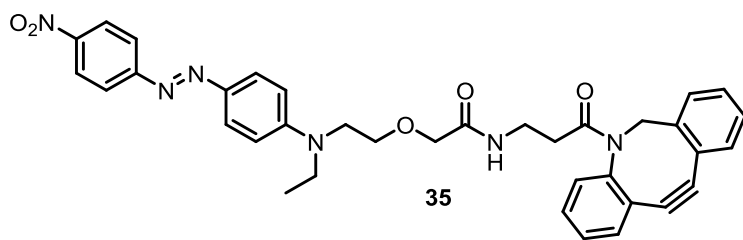
73.7% Yield; δ_H (CDCl$_3$, 600 MHz) 8.32 (2H, d, J = 9 Hz), 7.92 (3H, m), 7.69 (1H, d, J = 7.6 Hz), 7.42 – 7.27 (7H, m), 7.03 (1H, t, J = 5.6 Hz), 6.76 (2H, d, J = 9 Hz), 5.15 (1H, d, J = 13.8 Hz), 3.86 (2H, q, J = 18.6 Hz), 3.69 (1H, d, J = 14.0 Hz), 3.65 – 3.52 (6H, m), 3.39 (1H, m), 3.21 (1H, m), 2.48 (1H, m), 1.95 (1H, m), 1.26 (3H, t, J = 7.1 Hz); MS (ESI) calcd for $C_{36}H_{34}N_6O_5$: 631.2663, found: 631.2666 (M + H).

ii. Peptide Library Synthesis and Screening

General Procedure for Synthesis of Peptide Libraries

Peptides were synthesized by hand using standard Fmoc-SPPS on TentaGel S NH$_2$ resin

(0.29 meq/g loading). As the first coupling in each library synthesis, the Fmoc-photolabile

linker (2 eq) was attached to the resin by agitation with N$_2$ in a 0.2 M solution of

HBTU/HOBt in DMF (2 eq) and DIEA (4 eq) for 2 h. All subsequent couplings were

completed with a 4:4:8-fold excess of amino acid:0.2 M HBTU/HOBt:DIEA in DMF with a

coupling time of 1.5 h. After coupling, the resin was washed sequentially with DMF (3x),

DCM (3x), and DMF (2x). Fmoc-deprotection was completed by subjecting the resin to a

20% piperdine/DMF solution (3 x 30 min) followed by the same washing sequence as the

coupling reaction. Completed sequences were acetyl capped at the N-terminus with a

solution of 5% acetic anhydride and 6% lutidine in DMF (2 x 30 min) followed by the same

washing sequence. *For peptides containing DAP(ivDde)*, the resin was agitated in a 2%

hydrazine/DMF solution (6 x 2 min) with a DMF wash (5x) in between each cycle to remove

the ivDde protecting group. The desired Boc-protected hydrazine was then coupled onto the

resin using the same ratios of HBTU/HOBt and DIEA as previous. The peptides were then

dried under N$_2$ and stored in the freezer until screening.

General Procedure for Screening of Peptide Libraries

The protected peptide library (25 mg, 0.0070 mmol) was added to a 25-mL plastic fritted

syringe and deprotected by shaking on an orbital shaker with 95:2.5:2.5 trifluoroacetic

acid:triisopropylsilane:water for 2 h. The deprotected resin was washed thoroughly with

water (3x), MeOH (3x), DMF (3x), and DCM (3x). *For non-colorimetric screens of* **L1***,* **L2***,*

and **L3**, the 3-oxo-C$_{12}$ AHL (2.08 mg, 0.0070 mmol) was dissolved in a 2% solution of

DMSO in PBS buffer and added to the resin. The resin was allowed to shake in buffer for 1

h, with reaction times varying in subsequent screens based on the intensity of the tagged products observed mass spectrometry. The resin was then washed and transferred to a 2-mL Eppendorf tube containing MeOH (0.5 – 1.0 mL). The Eppendorf tube was placed under a UV light (365 nm) for at least 3 h with stirring to cleave the photolinker and solubilize the peptide library. The peptide solution was then analyzed by MALDI-MS. *For colorimetric screens of* **L3**, *etc.* the azido-AHL **34** (1.97 mg, 0.0070 mmol) was dissolved in a 2% solution of DMSO in PBS buffer and added to the resin. The resin was shaken, washed, and then combined with dye **35** (4.4 mg, 0.007 mmol) in 3.5 mL of MeCN. The resin was again shaken in the present of the dye for 4 h, washed with MeCN (2x), DMF (3x), and DCM (3x) and plated on a plastic petri dish. The resin was inspected under a confocal microscope and the darkest colored beads were manually picked for cleavage. The "hits" were transferred to a MeOH containing Eppendorf tube, placed under UV-light, and then analyzed by MALDI-MS.

Synthesis of Peptides for Solution Phase Screening

The peptides were synthesized by the same procedure utilized for peptide library synthesis but on CLEAR Amide resin (0.35 meq/g). The completed sequences were cleaved from the resin by shaking with 95:2.5:2.5 trifluoroacetic acid:triisopropylsilane:water for 2 h. The solution was then flushed from the resin into a 50 mL Falcon tube and concentrated under N_2. The concentrated acid solution was then precipitated in 50 mL of diethyl ether and centrifuged to pellet the peptide. The ether was decanted and the crude peptide was again dried under N_2. The peptide was then purified by semi-prep HPLC in an MeCN:H_2O mobile phase with 0.1% trifluoroacetic acid and lyophilized to dryness.

Solution Phase Peptide Screening

The purified peptide (0.0010 mmol) was added to a solution of the 3-oxo-C_8-AHL (0.24 mg, 0.0010 mmol) in PBS at pH = 6.5. The reagents were combined at time = 0 ± 5 min and placed on an analytical HPLC autosampler for injection every 135 minutes. Separations were performed in a mobile phase of 25 to 50% B over 25 minutes. Relative rates were obtained calculating the decrease in AHL concentration over time.

iii. QS and Biofilm Inhibition Assays

Biofilm Inhibition Assay

An overnight culture of *P. aeruginosa* PAK was grown in 100% LB broth in PBS at 37°C on a rotary shaker. The bacteria was then reinoculated in 25% LB at pH 6.5 and grown to an OD_{600} = 0.25. The peptides (0.015 mmol) were dissolved in DMSO (15 μL) followed by the addition of 25% LB PBS at pH = 6.5 to a final reach a final peptide concentration of 100 mM. Serial dilutions to 10 mM and 1.0 μM were prepared from a stock of 5% DMSO/95% LB PBS solution. In a 24-well plate, 900 μL of the bacterial culture was combined with 100 μL of the peptide solutions and incubated for 18 h. Biofilm inhibition was qualitatively assessed by visual inspection to determine the presence of a pellicle biofilm.

QS Inhibition Assay

Tested peptides (0.010 mmol) were dissolved in DMSO (5 μL) and followed by the addition of 100% LB PBS at pH 6.5 to reach a final concentration of 20 mM. An overnight culture of *P.aeruginosa* PAO1 (P*rsaL-gfp*) was diluted to an OD_{600} of 0.05 in the same broth containing

buffer. The culture (190 µL) was then transferred to a Greiner 96-well flat bottom plate followed by the addition of the peptide (10 µL) to their corresponding wells. The resultant GFP expression was monitored by fluorescence plate reader over 12 h. The fluorescence intensities recorded were normalized for cell density to obtain the reported relative activity of each peptide.

REFERENCES

1. Wolfenden, R. & Snider, M. J. The Depth of Chemical Time and the Power of Enzymes as Catalysts. *Accounts of Chemical Research* **34**, 938–945 (2001).

2. Kirby, A. J. Enzyme Mechanisms, Models, and Mimics. *Angewandte Chemie International Edition in English* **35**, 706–724 (1996).

3. Suh, J. Synthetic Artificial Peptidases and Nucleases Using Macromolecular Catalytic Systems. *Accounts of Chemical Research* **36**, 562–570 (2003).

4. Wentworth, Paul, J. & Janda, K. Catalytic antibodies. *Cell Biochemistry and Biophysics* **35**, 63–87 (2001).

5. Breslow, R. Biomimetic Chemistry and Artificial Enzymes: Catalysis by Design. *Accounts of Chemical Research* **28**, 146–153 (1995).

6. Davie, E. A. C., Mennen, S. M., Xu, Y. & Miller, S. J. Asymmetric Catalysis Mediated by Synthetic Peptides. *Chemical Reviews* **107**, 5759–5812 (2007).

7. Wennemers, H. Asymmetric catalysis with peptides. *Chemical Communications* **47**, 12036-12041 (2011).

8. Jarvo, E. R., Copeland, G. T., Papaioannou, N., Bonitatebus, P. J. & Miller, S. J. A Biomimetic Approach to Asymmetric Acyl Transfer Catalysis. *Journal of the American Chemical Society* **121**, 11638–11643 (1999).

9. Vasbinder, M. M., Jarvo, E. R. & Miller, S. J. Incorporation of Peptide Isosteres into Enantioselective Peptide-Based Catalysts as Mechanistic Probes. *Angewandte Chemie International Edition* **40**, 2824–2827 (2001).

10. Lewis, C. A. & Miller, S. J. Site-Selective Derivatization and Remodeling of Erythromycin A by Using Simple Peptide-Based Chiral Catalysts. *Angewandte Chemie International Edition* **45**, 5616–5619 (2006).

11. Lewis, C. A. *et al.* Remote Desymmetrization at Near-Nanometer Group Separation Catalyzed by a Miniaturized Enzyme Mimic. *Journal of the American Chemical Society* **128**, 16454–16455 (2006).

12. Lewis, C. A., Longcore, K. E., Miller, S. J. & Wender, P. A. An Approach to the Site-Selective Diversification of Apoptolidin A with Peptide-Based Catalysts. *Journal of Natural Products* **72**, 1864–1869 (2009).

13. Tanaka, F., Fuller, R. & Barbas, C. F. Development of Small Designer Aldolase Enzymes: Catalytic Activity, Folding, and Substrate Specificity. *Biochemistry* **44**, 7583–7592 (2005).

14. Tanaka, F. & Barbas, C. F. A Modular Assembly Strategy for Improving the Substrate Specificity of Small Catalytic Peptides. *Journal of the American Chemical Society* **124**, 3510–3511 (2002).

15. Broo, K. S., Brive, L., Ahlberg, P. & Baltzer, L. Catalysis of Hydrolysis and Transesterification Reactions of *p* -Nitrophenyl Esters by a Designed Helix−Loop−Helix Dimer. *Journal of the American Chemical Society* **119**, 11362–11372 (1997).

16. Broo, K. S., Nilsson, H., Nilsson, J., Flodberg, A. & Baltzer, L. Cooperative Nucleophilic and General-Acid Catalysis by the HisH $^+$ −His Pair and Arginine Transition State Binding in Catalysis of Ester Hydrolysis Reactions by Designed Helix−Loop−Helix Motifs. *Journal of the American Chemical Society* **120**, 4063–4068 (1998).

17. Johnsson, K., Allemann, R. K., Widmer, H. & Benner, S. A. Synthesis, structure and activity of artificial, rationally designed catalytic polypeptides. *Nature* **365**, 530–532 (1993).

18. Nicoll, A. J. & Allemann, R. K. Nucleophilic and general acid catalysis at physiological pH by a designed miniature esterase. *Organic & Biomolecular Chemistry* **2**, 2175 (2004).

19. Lam, K. S. *et al.* A new type of synthetic peptide library for identifying ligand-binding activity. *Nature* **354**, 82–84 (1991).

20. Furka, A., Sebestyén, F., Asgedom, M. & Dibó, G. General method for rapid synthesis of multicomponent peptide mixtures. *International Journal of Peptide and Protein Research* **37**, 487–493 (2009).

21. Merrifield, R. B. Solid Phase Peptide Synthesis. I. The Synthesis of a Tetrapeptide. *Journal of the American Chemical Society* **85**, 2149–2154 (1963).

22. Merrifield, R. B. Solid Phase Synthesis. *Angewandte Chemie International Edition in English* **24**, 799–810 (1985).

23. Lam, K. S., Lebl, M. & Krchňák, V. The 'One-Bead-One-Compound' Combinatorial Library Method. *Chemical Reviews* **97**, 411–448 (1997).

24. Bezer, S. *et al.* Identification and optimization of short helical peptides with novel reactive functionality as catalysts for acyl transfer by reactive tagging. *Organic & Biomolecular Chemistry* **12**, 1488-1494 (2014).

25. Madder, A. *et al.* A Novel Sensitive Colorimetric Assay for Visual Detection of Solid-Phase Bound Amines. *European Journal of Organic Chemistry* **1999**, 2787–2791 (1999).

26. De Muynck, H. *et al.* Application of Combinatorial Procedures in the Search for Serine-Protease-Like Activity with Focus on the Acyl Transfer Step. *Angewandte Chemie International Edition* **39**, 145–148 (2000).

27. Madder, A. *et al.* Evaluation of a Two-Stage Screening Procedure in the Combinatorial Search for Serine Protease-Like Activity. *Journal of Combinatorial Chemistry* **4**, 552–562 (2002).

28. Krattiger, P., McCarthy, C., Pfaltz, A. & Wennemers, H. Catalyst–Substrate Coimmobilization: A Strategy for Catalysts Discovery in Split-and-Mix Libraries. *Angewandte Chemie International Edition* **42**, 1722–1724 (2003).

29. Witus, L. S. *et al.* Identification of Highly Reactive Sequences For PLP-Mediated Bioconjugation Using a Combinatorial Peptide Library. *Journal of the American Chemical Society* **132**, 16812–16817 (2010).

30. Sletten, E. M. & Bertozzi, C. R. Bioorthogonal Chemistry: Fishing for Selectivity in a Sea of Functionality. *Angewandte Chemie International Edition* **48**, 6974–6998 (2009).

31. Nair, D. P. *et al.* The Thiol-Michael Addition Click Reaction: A Powerful and Widely Used Tool in Materials Chemistry. *Chemistry of Materials* **26**, 724–744 (2014).

32. Kalia, J. & Raines, R. Advances in Bioconjugation. *Current Organic Chemistry* **14**, 138–147 (2010).

33. Banerjee, R., Chattopadhyay, S. & Basu, G. Conformational preferences of a short Aib/Ala-based water-soluble peptide as a function of temperature. *Proteins: Structure, Function, and Bioinformatics* **76**, 184–200 (2009).

34. Riemen, A. J. & Waters, M. L. Design of Highly Stabilized β-Hairpin Peptides through Cation−π Interactions of Lysine and *N*-Methyllysine with an Aromatic Pocket [†]. *Biochemistry* **48**, 1525–1531 (2009).

35. Wennemers, H. & Still, W. C. Peptide complexation in water : Sequence-Selective binding with simple dye molecules. *Tetrahedron Letters* **35**, 6413 – 6416 (1994).

36. Marani, M. M. *et al.* Screening of One-Bead-One-Peptide Combinatorial Library Using Red Fluorescent Dyes. Presence of Positive and False Positive Beads. *Journal of Combinatorial Chemistry* **11**, 146–150 (2009).

37. Cole, R.B. *Electrospray and MALDI mass spectrometry: fundamentals, instrumentation, practicalities, and biological applications*. (Wiley, 2010).

38. Revell, J. D. & Wennemers, H. Peptidic catalysts developed by combinatorial screening methods. *Current Opinion in Chemical Biology* **11**, 269–278 (2007).

39. Ning, X., Guo, J., Wolfert, M. A. & Boons, G.-J. Visualizing Metabolically Labeled Glycoconjugates of Living Cells by Copper-Free and Fast Huisgen Cycloadditions. *Angewandte Chemie International Edition* **47**, 2253–2255 (2008).

40. Geske, G. D., Wezeman, R. J., Siegel, A. P. & Blackwell, H. E. Small Molecule Inhibitors of Bacterial Quorum Sensing and Biofilm Formation. *Journal of the American Chemical Society* **127**, 12762–12763 (2005).

41. Cady, N. C. *et al.* Inhibition of Biofilm Formation, Quorum Sensing and Infection in Pseudomonas aeruginosa by Natural Products-Inspired Organosulfur Compounds. *PLoS ONE* **7**, e38492 (2012).

42. Paris, J. *Novel azapeptide or azapeptidomimetic compounds inhibiting bcrp and/or p-gp*. US Patent 20120010161 A1, January 12, 2012 (Google Patents, 2012) at <https://www.google.com/patents/US20120010161>

43. Amara, N. *et al.* Covalent Inhibition of Bacterial Quorum Sensing. *Journal of the American Chemical Society* **131**, 10610–10619 (2009).